Masters Dissertation

Light Quark Masses from QCD Finite Energy Sum Rules

Alexes K. Mes

Department of Physics
University of Cape Town

Dissertation presented for the degree of Master of Science in the Department of Physics, University of Cape Town

February, 2019

Abstract

Due to quark-gluon confinement in QCD, the quark masses entering the QCD Lagrangian cannot be measured with the same techniques one would use to determine the mass of non-confined particles. They must be determined either numerically from Lattice QCD, or analytically using QCD sum rules. The latter makes use of the complex squared energy plane, and Cauchy's theorem for the correlator of axial-vector divergences. This procedure relates a QCD expression containing the quark masses, with an hadronic expression in terms of known hadron masses, couplings, and lifetimes/widths. Thus, the quark masses become a function of known hadronic information.

In this dissertation, the light quark masses are determined from a QCD finite energy sum rule, using the pseudoscalar correlator to six-loop order in perturbative QCD, with the leading vacuum condensates and higher order quark mass corrections included. The systematic uncertainties stemming from the hadronic resonance sector are reduced, by introducing an integration kernel in the Cauchy integral in the complex squared energy plane. Additionally, the issue of convergence of the perturbative QCD expression for the pseudoscalar correlator is examined. Both the fixed order perturbation theory (FOPT) method and contour improved perturbation theory (CIPT) method are explored. Our results from the latter exhibit good convergence and stability in the window $s_0 = 3.0 - 5.0$ GeV^2 for the strange quark and $s_0 = 1.5 - 4.0$ GeV^2 for the up and down quarks; where s_0 is the radius of the integration contour in the complex s-plane. The results are: $\overline{\mathrm{m}}_s(2\ \mathrm{GeV}) = 91.8 \pm 9.9$ MeV, $\overline{\mathrm{m}}_u(2\ \mathrm{GeV}) = 2.6 \pm 0.4$ MeV, $\overline{\mathrm{m}}_d(2\ \mathrm{GeV}) = 5.3 \pm 0.4$ MeV, and the sum $\overline{\mathrm{m}}_{ud} \equiv (\overline{\mathrm{m}}_u + \overline{\mathrm{m}}_d)/2$, is $\overline{\mathrm{m}}_{ud}(2\ \mathrm{GeV}) = 3.9 \pm 0.3$ MeV. They compare favourably to the PDG and FLAG world averages.

Further in this dissertation the updated series expansion of the quark mass renormalization group equation (RGE) to five-loop order is derived. The series provides the relation between a light quark mass in the modified minimal subtraction ($\overline{\mathrm{MS}}$) scheme defined at some given scale, e.g. at the tau-lepton mass scale, and another chosen energy scale, s. This relation explicitly depicts the renormalization scheme dependence of the running quark mass on the scale parameter, s, and is important in accurately determining a light quark mass at a chosen scale. The five-loop QCD $\beta(a_s)$ and $\gamma(a_s)$ functions are used in this determination.

Contents

List of Figures

List of Tables

Abbreviations

OPE: **O**perator **P**roduct **E**xpansion

FESR: **F**inite **E**nergy **S**um **R**ules

QCD: **Q**uantum **C**hromo**d**ynamics

LQCD: **L**attice **Q**uantum **C**hromo**d**ynamics

PQCD: **P**erturbative **Q**uantum **C**hromo**d**ynamics

FOPT: **F**ixed **O**rder **P**erturbation **T**heory

CIPT: **C**ontour **I**mproved **P**erturbation **T**heory

CPT: **C**hiral **P**erturbation **T**heory

Publications

The following publications resulted from the work in this dissertation:

- C. A. Dominguez, A. Mes, and K. Schilcher, *Up- and down-quark masses from QCD sum rules,* Journal of High Energy Physics, 2019(2):57, `arXiv:1809.07042 [hep-ph]`.

- A. Mes, *Precision Determination of the Light Quark Masses from QCD Finite Energy Sum Rules,* Conference proceedings: Kruger 2018 - Discovery Physics at the LHC, submitted for publication in the Open Access Journal of Physics: Conference Series.

- A. Mes, and J. Stephens, *An Application of Rubi: Series Expansion of the Quark Mass Renormalization Group Equation,* `arXiv:1811.04892 [hep-ph]`.

The White Rabbit put on his spectacles. “Where shall I begin, please your Majesty?” he asked.

“Begin at the beginning,” the King said gravely, “and go on till you come to the end: then stop.”

Alice in Wonderland

1 Introduction

Physics rises and falls by the ability to accurately know its fundamental parameters. Within different theories the importance placed on various parameters differs. In the field of Quantum Chromodynamics, the strong coupling, vacuum condensate densities and the masses of the six known quarks are the fundamental parameters of the theory. This dissertation aims to accurately determine the light quark masses. A precise determination of the up and down quark masses is of critical importance as they will affect the proton-neutron mass difference. Further, the masses of the up and down quarks establish the magnitude of flavour SU(2) and chiral SU(2) $\bigotimes$ SU(2) symmetry breaking. The strange quark mass is equally as important, since it has a strong impact in a variety of Standard Model tests, and determines the magnitude of flavour SU(3) and chiral SU(3) $\bigotimes$ SU(3) symmetry breaking.

There are two major approaches in Quantum Chromodynamics that can be used to calculate the quark masses at some given energy scale. Broadly this divides into a numerical approach (lattice QCD [1], [2]) and an analytical approach (QCD sum rules [3–5]). Lattice QCD discretizes space and time to reduce the infinite number of field variables in QCD to a finite countable number within the path-integral formulation of Quantum Field Theory [6]. QCD sum rules separate the perturbative and non-perturbative contributions in QCD, where the latter are described by quark and gluon condensates which are present. The sum rule method relates low energy hadronic quantities (which are measurable) to high energy expressions in QCD, such that unmeasurable QCD parameters become a function of known hadronic information. Lattice QCD and QCD sum rules are two approaches which, in many respects, are complementary; and the rivalry that exists between them, beneficial in incentivizing a deeper understanding of Quantum Chromodynamics and the strong interaction. While lattice QCD achieves high precision; QCD sum rules provide vital insight into the origins of different parameters.

QCD sum rules were first formulated by Shifman, Vainshtein, and Zakharov in 1979 [7], within the framework of Laplace integral transforms. Currently, there are numerous sum rule frameworks. Various physicists advocate for performing QCD sum rule calculations using integral transform frameworks (Laplace, Borel or Hilbert); finite energy sum rules, or the relatively new method of Light-cone sum rules. The finite energy sum rule method, in which QCD sum rules are placed within the complex squared energy plane, is the approach taken in this dissertation. This method (first proposed in [8]) can offer precision determinations of QCD and hadronic parameters that currently rival the numerical Quantum Chromodynamic lattice simulations.

A further deterrent from using integral transform sum rules is that these sum rules tend to exponentially suppress the dependence of relevant quantities (such as the quark masses) on the energy parameter s_0. This is in favour of using a new scale parameter M^2, that lacks a direct physical interpretation. On the other hand, s_0 does have a clear physical interpretation since it is related to finite temperature quark-gluon deconfinement. Recently, a possible relationship between s_0 and the Polyakov loop which signals deconfinement in lattice QCD has been found [9]. Finite energy sum rules enhance this important parameter, with s_0^2 appearing in the sum rule expression. Additionally, finite energy sum rules allow for the easy use of integration kernels: polynomial expressions which are used to quench the unknown hadronic resonances in the model, thereby reducing systematic uncertainties.

It is here that we have landed; firmly, in using the analytical QCD finite energy sum rule (FESR) approach to calculate the mass of the light quarks. There are two major approaches to performing the contour integral in FESR: fixed order perturbation theory (FOPT) and contour improved perturbation theory (CIPT). Fixed order keeps – as its name suggests – the strong coupling, $\alpha_s(s)$, frozen on the integration contour, and performs the renormalization group improvement after integration. On the other hand, in contour improved perturbation theory the strong coupling is running and the renormalization group improvement is implemented before integration. The obvious question arises: *Do the results agree?*. This leads to a more crucial matter: *Which method is superior?*. A question which is difficult to answer, since it is application dependent. In most cases, FOPT and CIPT are either in agreement, or CIPT presents more reliable results in terms of stability and convergence considerations. The latter scenario occurs in this determination.

By now, new readers in this field might have wondered why QCD practitioners turn towards theoretical sum rules or numerical simulations in order to predict the quark masses. *Where is the role of standard experimental physics? Why cannot the masses of the quarks be measured using methods similar to those used to detect other high energy particles?*
The answer lies in a curious concept called confinement.

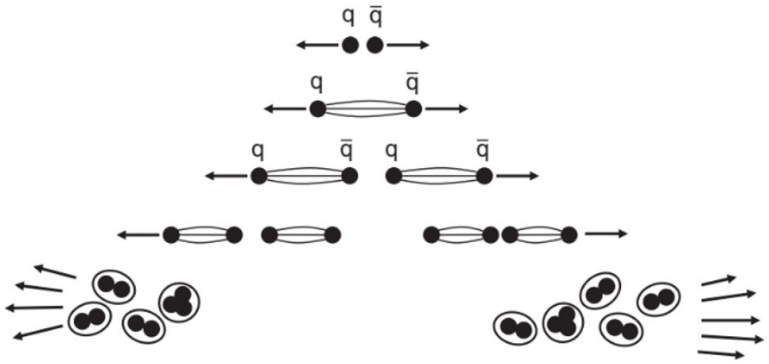

Figure 1: Qualitative diagram of quark confinement and the steps in the hadronisation process [10].

Quantum Chromodynamics is a confining theory, meaning that quarks do not exist in nature as single, free particles; but, are rather found in hadronic bound states. Due to this quark and gluon confinement it is impossible to determine the quark masses with the same techniques as one would use to determine the mass of non-confined particles. Hence, the need for QCD sum rules becomes evident.

QCD sum rules have been successful in extracting an assortment of fundamental parameters and analyzing a wide range of phenomena in strong-interaction physics. For example, the sum rule method can calculate the lowest-mass hadronic bound states, the lowest-order hadronic contribution to the muon anomalous magnetic moment, effective coupling constants, and quark masses; and can yield interesting insights into the internal wave functions of nucleons and pions [6]. For recent reviews of the method and it's applications, see [3, 4, 11, 12].

This dissertation provides a determination of the up, down and strange quark masses which represent a substantial improvement on previous FESR results. The determination of these light quark masses is done within both the CIPT and FOPT framework. In 2018, The Particle Data Group [13] considered two phenomenological determinations [14, 15] when determining the world average of the up and down quark masses. The latest calculation of $\overline{m}_{ud}$ [14], published in 2017, determines the up and down quark masses in the I = 0 scalar channel within the Borel transform framework. It further differs from our determination since it includes an instanton contribution as a non-perturbative effect in the theoretical representation of the correlation function. The previous determination [15] – published in 2009 and also included in the Particle Data Group world average of $\overline{m}_{ud}$ – is a FESR determination of the up and down quark masses. At this point, the question naturally emerges: *How does our current determination differ from the previous calculation of $\overline{m}_{ud}$ in [15]?*

The determination presented in this dissertation offers considerable improvements in terms of (i) the analysis of different kernels, (ii) examining the issue of the convergence of the perturbative QCD expansion, (iii) a different implementation of the running QCD coupling, (iv) a more careful error analysis, and (v) the high numerical precision achieved in this calculation.

The previous determination [15] performed the calculation of the quark masses in the framework of CIPT and restricted the choice of kernels to vanish at the resonance peaks, eventually preferring the kernel $P_5(s) = 1 - a_0\, s - a_1\, s^2$, with $a_0 = 0.897$ GeV^{-2} and $a_1 = -0.1806$ GeV^{-4}. In the current determination, different integration kernels are considered and the calculations are done in the framework of both FOPT and CIPT.

Further, the issue of the convergence of the perturbative QCD expansion and its effect on the up and down quark masses was not addressed in [15], but will be considered in the present determination.

In the previous determination [15], the strong coupling was expressed in terms of the QCD scale $\Lambda_{\rm QCD}$, as in $\alpha_s(s) \propto 1/\ln(s/\Lambda^2_{\rm QCD})$, a procedure that will not be followed here as it leads to unnecessary larger uncertainties. Instead, the renormalization group equation for the strong coupling will be used in order to express the coupling in terms of some well known value at a given scale, e.g. at the tau-lepton mass scale.

Additionally, the error analysis in [15] did not include the error due the dependence of the up and down quark masses on the value of s_0; calculated the uncertainty due to the gluon condensate by gauging the effect of multiplying the gluon condensate by a factor of two; and assumed, somewhat arbitrarily, a 30% uncertainty in the hadronic sector. A more robust error analysis is given in this determination.

A final remark is the comparative high numerical precision of the present determination: the calculations have been computed in Mathematica (see the supplementary material), a modern 64-bit computer language with natural support for precision real and complex numbers. At a minimum, using the machine precision corresponds to 16 digits of mantissa, although higher multiples of the machine precision can be used. In comparison, the determination in [15] was performed using Fortran 90 with code edited and updated from Fortran 77; respectively these are 1991 and 1977 computer languages. Typically the early

standard Fortran versions only contain single precision (numbers accurate to 7 digits of mantissa), while double precision (typically 14 digits of mantissa) can be specified for real numbers. Complex numbers present more of an issue, as the double precision must be split between the real and imaginary components. Notwithstanding this, it is the confluence of these different working numerical precisions in earlier Fortran languages that can typically result in an accumulated error. The issue of numerical precision can make a notable impact on the results. For example, in CIPT where the renormalization group equations must be solved at 10 000 points around the circular contour, with each point relying on the previous value of the strong coupling as an initial condition, the opportunity for numerical carried error is pronounced. In Mathematica the numerical underflow in such a situation can be managed with greater care. The determination present in this dissertation therefore represents a significant advancement in achieved numerical precision of FESR determinations of the up and down quark masses.

Similarly, in 2018 the Particle Data Group [13] considered three phenomenological determinations [16–18] when determining the world average of the strange quark mass. The latest publication [16], published in 2016, uses a renormalization group summed perturbation theory and relates this to τ-decay spectral function data in order to extract the strange quark mass. This is not a FESR sum rule determination of $\overline{m}_s$, and as such will not be examined further here. The previous determination [17], published in 2013, is a FESR determination of the strange quark mass. The determination is performed in Mathematica and the convergence of the perturbative QCD expansion is examined. However, the calculations in [17] are only performed in the framework of FOPT. Here, in this dissertation, both FOPT and CIPT are considered, leading to a different conclusion about the preferred framework in which to calculate the strange quark mass (in terms of stability and convergence) being made. The 2008 determination [18], was calculated by the same collaboration and around the same time as the determination in [15]. Consequently it suffers from all the issues pertaining to the determination in [15] discussed previously.

A final comment is that the fully annotated Mathematica notebooks supporting this determination of the up, down and strange quark masses are openly available. This is one of the first determinations within the field of QCD sum rules to make its code available with the paper for publication, since the author strongly believes in the importance of modern research and open collaboration. See Appendix (A.4) for details about accessing the code on the Github repository. Further, the annotated Mathematica notebooks are provided in the supplementary material.

1.1 Dissertation Structure

This dissertation is organized in two parts. The first part details the determination of the up, down and strange quark mass. Part II describes regularization and renormalization in QCD, and how these tools are used in the light quark mass determinations that appear in Part I. Part I and Part II do not have to be read consecutively.

In Part I:

First, quark-hadron duality and Cauchy's Theorem, the cornerstone of finite energy sum rules, will be reviewed in section (2).

Section (3) discusses the operator product expansion and its ability to describe higher dimensional non-perturbative effects. The expressions for the pseudoscalar correlator are given.

In section (4) the calculation of the contour integral in the FESR is developed. The two major approaches used this dissertation: fixed order perturbation theory and contour improved perturbation theory are described in detail.

Section (5) explores the spectral function of the correlator $\Psi_5(q^2)$ in the hadronic sector. The spectral function beyond the chiral limit is compared to the spectral function in the chiral limit. The full hadronic spectral function beyond the chiral limit is modelled for both $\overline{m}_{ud}$ and $\overline{m}_s$.

Several different kernels can be used in order to quench the hadronic resonances. These integration kernels are explored in section (6).

The perturbative QCD expansion is only known up to the $\mathcal{O}(\alpha_s^4)$ term and does not appear to converge. Section (7) examines how this affects the light quark masses calculated using fixed order perturbation theory.

In section (8) the results for the up, down and strange quark masses in the CIPT and FOPT framework are presented. Further, the effect of different integration kernels on the stability of the light quark masses is explored. This section includes an analysis of the contributing uncertainties in the quark mass determinations and a review of the previous results.

In Part II:

To begin Part II, section (9) reviews the derivation of the QCD renormalized coupling constant g_R to lowest order and the first β coefficient, β_0.

The renormalization group equations are given in section (10).

In section (11) we calculate the updated series expansion of the quark mass renormalization group equation (RGE) to five-loop order using Rule-based Integration (Rubi) [19], a new Mathematica package that provides a method of symbolic integration.

Section (12) concludes the dissertation.

There are a number of appendices to this dissertation. Appendix (A.1) derives, through the use of Cauchy's theorem, the finite energy sum rule which forms the basis of the light quark mass calculation. Appendix (A.2) derives the perturbative contribution of the pseudoscalar correlator to lowest order of α_s. The quark mass definitions pertaining to this dissertation are described in appendix (A.3). Appendix (A.4) provides details for accessing the GitHub repository where the latest annotated Mathematica code notebooks supporting the determination of the light quark masses presented here, can be found.

Part I
Up, Down and Strange Quark Mass Determinations

2 Quark-Hadron Duality and Cauchy's Theorem

The relationship between Quantum Chromodynamics (the strong-interaction theory between quarks and gluons) and hadronic physics (the theory of strongly interactive bound states of quarks) is known as the quark-hadron duality [20]. The notion was first formulated in 1976 by Poggio, Quinn and Weinberg [21] who explored the idea that cross-sections calculable in quark-gluon perturbation theory should approximately coincide with inclusive high energy hadronic cross sections averaged over an energy range. Unfortunately, the idea has remained vague for many decades – with physicists still being unable to answer fundamental questions as to the energy scale relevant in invoking quark-hadron duality; if non-perturbative effects should be included in the QCD predictions; or if we are able to quantify the effects of potential duality violations. Despite this, there are numerous applications in which the notion of the quark-hadron duality has been beneficially implemented, for example: deep inelastic scattering, e^+e^- annihilation, hadronic τ decays and Z peak physics [20].

The basic structure of all QCD sum rules relies on invoking the notion of quark-hadron duality to relate fundamental Quantum Chromodynamic parameters which cannot be measured, to experimentally measurable hadronic spectral densities. This is done by considering a QCD correlation function of currents within the framework of the operator product expansion (OPE). This framework enables one to separate the short-distance/large-momentum and the large-distance/small-momentum interactions. Asymptotic freedom allows the first type of quark-gluon interactions to be calculated using perturbative QCD, while the second type are described as non-perturbative vacuum condensates which enter as higher dimensional power corrections in the OPE [4, 5, 22]. The sum rule approach then matches this QCD calculation to a sum over hadronic states using dispersion relations. Through this method one is able to isolate a particular parameter and theoretically determine its value.

The starting point in calculating the light quark masses, then, is to consider the correlator of two pseudoscalar densities in momentum space. The pseudoscalar density $j_5(x)$ with quantum number $J^{PC} = 1^{++}$ [23], is the divergence of the flavour i, j axial-vector current given by the Ward Identity

$$j_5(x) \equiv \partial^\mu A_\mu(x)|_{\rm QCD} = (\overline{m}_i + \overline{m}_j)\, {\rm N}\{\overline{q}_j(x)\, i\,\gamma_5\, q_i(x)\}\,, \tag{2.1}$$

where N{ } is the standard normal-ordering operator, $\overline{m}_{i,j}$ are the running quark masses in QCD, and i, j denotes the quark flavour.

The correlator of $j_5(x)$ is particularly useful in the calculation of the light quark masses, since it involves these quark masses as overall multiplicative factors. It is defined as

$$\Psi_5(s \equiv -q^2) = i \int d^4x\, e^{iqx}\, \langle\Omega|\, T\{j_5(x)\, j_5^\dagger(0)\}\, |\Omega\rangle\,, \tag{2.2}$$

where Ω represents the physical vacuum and the Mandelstam variable $s \equiv -q^2$ used.

To determine the masses of the up and down quarks, we consider $\Psi_5(q^2)$ where $j_5(x) = (\overline{m}_d + \overline{m}_u)\,\mathrm{N}\{\overline{d}(x)\,i\,\gamma_5\,u(x)\}$. In the strange quark case we consider $\Psi_5(q^2)$ where $j_5(x) = (\overline{m}_s + \overline{m}_{ud})\,\mathrm{N}\{\overline{s}(x)\,i\,\gamma_5\,u(x)\}$ and $\overline{m}_{ud} \equiv (\overline{m}_u + \overline{m}_d)/2$.

In this dissertation there will be different correlators depending on the currents in their definition. However, the flavour indices i, j have been omitted when referring to $j_5(x)$ and $\Psi_5(q^2)$. This simplified notation is used throughout the dissertation to keep the formulas readable. In context it will always be made clear if the correlator for the case of the up and down quark mass determination, or the correlator for the case of the strange quark mass determination, is being considered.

The two-point correlation function $\Pi_5(q^2)$ is defined to differ from $\Psi_5(q^2)$ by a normalization factor,

$$\Psi_5(q^2) \;\equiv\; (\overline{m}_i + \overline{m}_j)^2\,\Pi_5(q^2)\,. \tag{2.3}$$

This normalization factor is motivated by the perturbative result for $\Psi_5(q^2)$ which, to lowest order of α_s, is derived in appendix (A.2). $\Pi_5(q^2)$ has an analyticity property that is important in developing the QCD sum rule methods.

Theorem 2.1 (Analyticity of the correlator) *Barring a branch-cut along the positive real axis,* $\Pi_5(q^2)$ *is an analytic function in the entire complex s-plane.*

Theorem (2.1) does not only hold in QCD perturbation theory, but is a general property of local quantum field theories [24, 25].

The QCD representation of the correlator, Eq.(2.2), is clearly the Fourier transform of the vacuum expectation value of the time-ordered product of a local current operator and its hermitian conjugate. This pseudoscalar correlator can also be represented in terms of hadronic currents and fields. When one is faced with two different representations of the same object, the natural question arises as to how to relate them. Finite energy sum rules approach this question through applying the renowned Cauchy's theorem within the framework of the complex squared energy plane. Due to the analyticity of the correlator $\Pi_5(q^2)$, the Quantum Chromodynamic singularities in the complex plane belong on the positive real axis in the form of poles along the branch-cut corresponding to hadrons which do not decay in terms of the strong-interaction, and resonances on the second Riemann sheet corresponding to excitations (π', π'', K etc.). These resonances, each with a particular width Γ (relating to their lifetime, $\Gamma \propto 1/\tau$) are located a distance $\sqrt{\Gamma}$ from the real axis.

Consider an integration contour in the complex energy plane, figure (2). Due to the aforementioned singularities, the perturbative QCD approximation is not valid on the real axis. However, if the radius of the circle $|s_0|$ is sufficiently large (i.e. $|s_0| \geq 1\,\mathrm{GeV}^2$), perturbative QCD is expected to hold elsewhere on the contour [5]. The hadronic physics on the real axis is then related to the QCD physics on the circle through the use of Cauchy's Theorem.

In full generality, Cauchy's Residue Theorem states

$$\oint ds\,\Pi(s) = 2\pi i\;\mathrm{Res}[\,\Pi(s), s = 0\,]\,, \tag{2.4}$$

with $\Pi(s)$ an analytic function in the complex energy plane, and $\mathrm{Res}[\,\Psi_5(s)P_5(s), s=0\,]$ the residues at the pole(s) inside the integration contour.

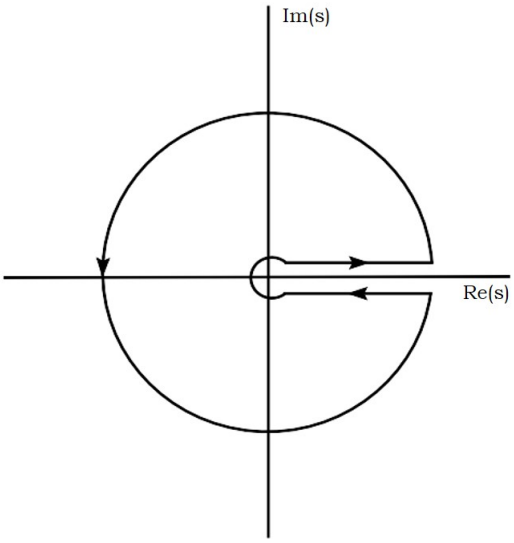

Figure 2: The integration contour in the complex s-plane involves the QCD correlator; while the branch cut across the real axis brings in the hadronic spectral function. The radius of the circular contour $|s_0|$ represents the onset of pQCD.

Following a short derivation (see appendix (A.1)), Cauchy's theorem for the pseudoscalar correlation function, Eq.(2.2), becomes

$$\frac{1}{2\,\pi\,i}\oint_{C(|s_0|)} ds\,\Psi_5(s)|_{\mathrm{QCD}}\,P_5(s) + \int_{s_{th}}^{s_0} ds\,\frac{1}{\pi}\,\mathrm{Im}\,\Psi_5(s)|_{\mathrm{HAD}}\,P_5(s) = \mathrm{Res}[\,\Psi_5(s)P_5(s), s=0\,]\,, \tag{2.5}$$

where s_{th} is the quark-pair production threshold, $P_5(s)$ is some meromorphic function, and $\mathrm{Res}[\,\Psi_5(s)P_5(s), s=0\,]$ are the residues at the pole(s). A meromorphic function of s, $P_5(s)$, is introduced in order to quench the contribution from the hadronic resonance sector which would otherwise result in a major source of systematic uncertainties in the calculation.

For the up and down quark mass determination, the hadronic spectrum consists primarily of the pion pole (whose characteristics are known from direct experimental measurement) and two radial excitations of the pion (which are the resonances with known masses and widths). In calculating the strange quark mass, the hadronic spectrum consists of the kaon pole, the narrow width resonant sub-channel $K^*(892)$, and two radial excitations of the kaon. However, in both the up and down quark and the strange quark case, the knowledge of a pole and radial excitations is not enough to fully construct the hadronic spectral function due to inelasticity, non-resonant background noise and interference [18]. It is for these reasons that $P_5(s)$, a quenching kernel, is used.

3 The Operator Product Expansion in QCD

In 1969, K.G. Wilson suggested that a linear combination of local operators could be used to calculate the effect of multiple products of operators [26, 27]. This is known as the operator product expansion (OPE) in quantum field theory. The OPE provides us with an approximate means of calculating $\Psi_5(q^2)|_{\rm QCD}$ which enters the left-hand side of our FESR Eq.(2.5). $\Psi_5(q^2)|_{\rm QCD}$ consists firstly, of a perturbative contribution calculated in pQCD (see appendix (A.2) for the derivation of $\Psi_5(q^2)|_{\rm pQCD}$ to lowest order); and secondly, of non-perturbative effects due to the soft gluon and quark fields in the QCD vacuum. The nonlinear nature of the QCD Lagrangian is responsible for these vacuum fluctuations [7].

In this section, we briefly describe the fundamental ideas around the OPE, before giving the explicit expressions of the perturbative and non-perturbative contributions of $\Psi_5(q^2)|_{\rm QCD}$.

Let $\mathcal{O}_1$ and $\mathcal{O}_2$ be two operators in QFT separated by a small distance x'. Consider a general product of these operators at $x = x'$ and $x = 0$, i.e. $\mathcal{O}_1(x)\,\mathcal{O}_2(0)$. The product has the potential to create a general disturbance locally around $x = 0$. However, the OPE suggests that this product of operators can be replaced by a local operator $\mathcal{O}_3(0)$, with the same global symmetry quantum numbers as $\mathcal{O}_1(x)\,\mathcal{O}_2(0)$ [28]. The local operator $\mathcal{O}_3(0)$, can then be re-expressed as a linear sum of standard basis operators

$$\mathcal{O}_1(x)\,\mathcal{O}_2(0) \;\to\; \sum_n \mathrm{C}_{12\,d}(x)\,\mathcal{O}_d(0)\;, \tag{3.1}$$

where $\mathcal{O}_d(0)$ are local operators and $\mathrm{C}_{12\,d}(x)$ are singular distributions.

Using Eq.(3.1) we are able to write the two-point correlation function (Eqs.(2.2-2.3)) in terms of an operator product expansion

$$\Pi_5(q^2)|_{\rm QCD} = \mathrm{C}_0\,I + \sum_{n=1} \mathrm{C}_{2\,n}(q^2,\mu^2)\,\langle 0|\,\mathcal{O}_{2\,n}(\mu^2)\,|0\rangle\;, \tag{3.2}$$

where $\mathrm{C}_{2\,n}(q^2,\mu^2)$ are known as the Wilson coefficients, and the operators are ordered in terms of their dimension d, where $d \equiv 2n$.

The term $\mathrm{C}_0\,I$ has dimensionality $d = 0$ and is the purely perturbative contribution of $\Psi_5(q^2)|_{\rm QCD}$, i.e. $\mathrm{C}_0\,I = \Pi_5(q^2)|_{\rm PQCD}$. The terms $\langle 0|\,\mathcal{O}_{2\,n}(\mu^2)\,|0\rangle$ are vacuum expectation values of the product of gauge invariant gluon and quark fields. These QCD vacuum fields are known as vacuum condensates. The vacuum condensates represent the higher order non-perturbative corrections to the OPE, and are in fact properties of the QCD vacuum [29].

Through our representation of $\Pi_5(q^2)|_{\rm QCD}$ in the framework of an operator product expansion (Eq.(3.2)) we introduced a scale μ. This scale is responsible for the separation of short and long distance effects. The Wilson coefficients $\mathrm{C}_{2\,n}(q^2,\mu^2)$ absorb interactions at momenta $q^2 > \mu^2$, while interactions at momenta $q^2 < \mu^2$ are absorbed into the vacuum condensates [4].

There are no dimension $d = 2$ operators, formed from the quark and gluon fields of QCD, that are invariant under gauge transformations [4,30]. Hence, it is usually assumed that the OPE starts at dimension $d = 4$. Here, $\langle 0| G^a_{\mu\nu} G^{a\,\mu\nu} |0\rangle$ and $\langle 0| m\,\overline{q}\,q\,|0\rangle$ are the relevant vacuum condensates, which are depicted in diagrams 4 and 5 (figure 3) respectively.

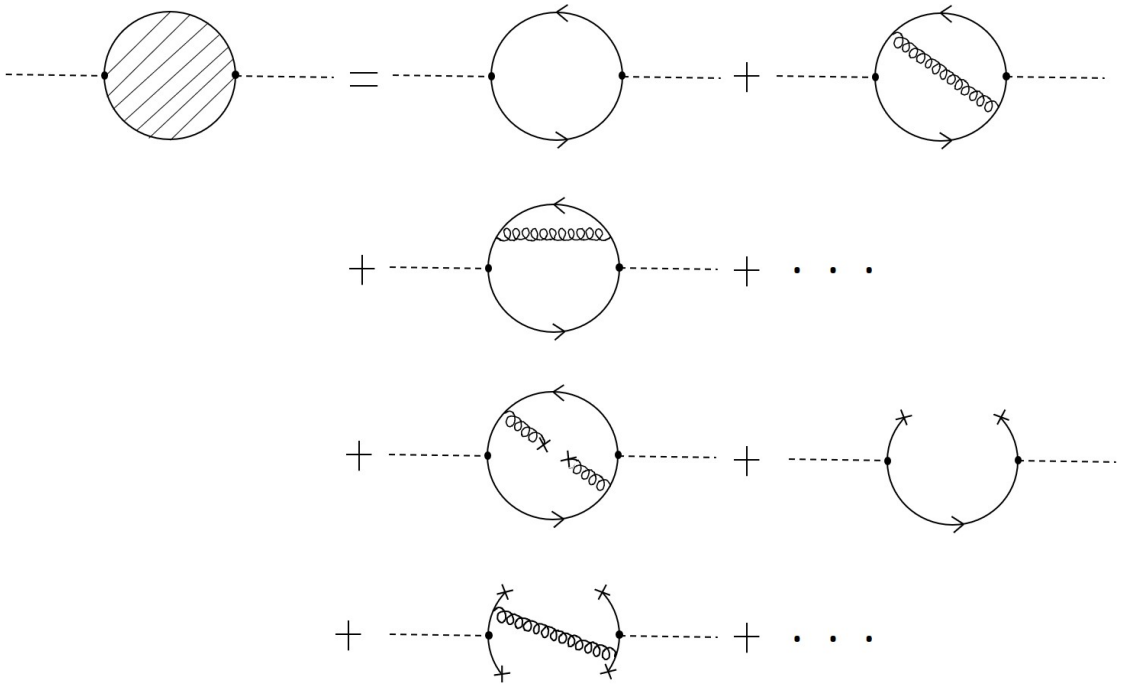

Figure 3: Feynman Diagrams representing the operator product expansion for $\Pi_5(q^2)$ [23]. The first three diagrams represent one- and two- loop peturbative contributions in the OPE, while the last three diagrams represent the non-perturbative contributions due to the vacuum condensates: the gluon condensate, quark condensate and a typical six-dimension condensate respectively.

Both the gluon condensate and quark condensate are renormalization group invariant. For example, in the $d = 4$ quark case, the dependence of the quark masses on the scale μ^2 cancels with the corresponding quark condensate in OPE. Therefore, once the vacuum condensates in a specific channel are determined, their same values can be used throughout the calculation [3].

While the Wilson coefficients can be calculated in perturbative QCD, the values of the vacuum condensates cannot be obtained analytically from first principles as this would essentially be solving QCD analytically and exactly. Thus, these values need to be solved either through finite energy sum rule applications involving theory and data, or through Lattice QCD. The simplest condensate to determine is the quark condensate, which can be related to the pion decay constant through the Gell-Mann-Oakes-Renner (GMOR) relation [31]

$$(\overline{m}_u + \overline{m}_d)\,\langle 0|\,\bar{u}\,u + \bar{d}\,d\,|0\rangle = -\,2\,f_\pi^2\,m_\pi^2\,(1-\delta_\pi)\,, \tag{3.3}$$

where $f_\pi = 92.07 \pm 1.20\,\text{MeV}$ is the experimentally measured pion decay constant [13].

In current applications we use the fact that due to isospin symmetry, $\langle \bar{q}q \rangle = \langle \bar{u}u \rangle = \langle \bar{d}d \rangle$. Further, due to spontaneous symmetry breaking, $\langle \bar{q}q \rangle \neq 0$. Higher order corrections to the GMOR relation which stem from the hadronic sector are encoded by δ_π and are at the level of a few percent in SU(2) $\bigotimes$ SU(2) (6.5% using fixed order perturbation theory and 7.0% using contour improved perturbation theory [32]), and approximately 55% in SU(3) $\bigotimes$ SU(3) [33].

Regarding $d = 6$ dimension contributions such as $\langle 0|\, \overline{q}\, \Gamma_1\, q\, \overline{q}\, \Gamma_2\, q\, |0\rangle$ (diagram 6, figure (3)) they are, at the present time, reliant on the assumption of vacuum saturation. As such, they are not well known and shall not be included in these calculations. Higher order condensates entering the OPE for $d > 6$ are not known with good accuracy.

We expect these higher dimensional condensates to be suppressed by large powers of Λ_{vac}^2/Q^2, where Λ_{vac} dictates the long-distance scale at which the quark and gluon fields fluctuate in the QCD vacuum [4]. However, a question remains: *Is there still a significant impact from not knowing the value of the higher dimensional condensates ($d \geq 6$) on our results for the light quark masses?* This is an open question which depends on how quickly the OPE series in Eq.(3.2) converges. Techniques, such as performing a Taylor expansion of this series, seem to reduce the dependence of the calculations on the higher order unknown condensates. This is explored in more detail in section (7).

3.1 Pseudoscalar Correlator

Expanding the pseudoscalar correlator $\Psi_5(q^2)|_{\text{QCD}}$ within the OPE framework, Eq.(3.2), gives

$$\Psi_5(q^2)|_{\text{QCD}} \;=\; (\overline{m}_i + \overline{m}_j)^2 \Bigg\{ -\, q^2\, \Pi_5^0(q^2) \;+\; (\overline{m}_i + \overline{m}_j)^2\, \Pi_5^2(q^2) \\ \pm\, \frac{C_q(L,a_s)}{-q^2}\, (\overline{m}_i + \overline{m}_j)\, \langle \bar{q}\, q \rangle + \sum_{j=1}^{3} \frac{C_j(L,a_s)}{-q^2}\, \langle O_j \rangle + \mathcal{O}\left(\frac{1}{q^4}\right) \Bigg\}, \tag{3.4}$$

where $\overline{m}_{i,j}$ stands for the quark masses with i, j flavour in the $\overline{\text{MS}}$ renormalization scheme, and the upper indices appearing on the two-point correlator $\Pi_5(q^2)$ denote the $d = 0$ peturbative function and the $d = 2$ perturbative mass correction term respectively. The third term in Eq.(3.4) takes on a specific sign depending on the type of correlator: $-\frac{C_q(L,a_s)}{-q^2}\, (\overline{m}_i + \overline{m}_j)\, \langle \bar{q}\, q \rangle$ is used in the case of the pseudoscalar correlator and $+\frac{C_q(L,a_s)}{-q^2}\, (\overline{m}_i + \overline{m}_j)\, \langle \bar{q}\, q \rangle$ is used in the case of the scalar correlator.

For the case of the correlator Eq.(3.4) determining the mass of the up and down quark, we have

$$(\overline{m}_i \,+\, \overline{m}_j) \,\rightarrow\, (\overline{m}_d \,+\, \overline{m}_u)\,, \tag{3.5}$$

and for the case of the correlator Eq.(3.4) determining the strange quark mass, we have

$$(\overline{m}_i \,+\, \overline{m}_j) \,\rightarrow\, (\overline{m}_s \,+\, \overline{m}_{ud})\,, \tag{3.6}$$

where $\overline{m}_{ud} \equiv (\overline{m}_u \,+\, \overline{m}_d)/2$. The definitions in Eqs.(3.5 - 3.6) are used throughout this dissertation.

The perturbative QCD function $\Pi_5^0(q^2)$ can be found in [22, 34], whilst the $\mathcal{O}(\alpha_s^4)$ result can be obtained from [35] through twice integrating[1] $\Pi_5^{0\,\prime\prime}(q^2)$ with respect to $-q^2$. To $\mathcal{O}(\alpha_s^4)$ it is given by

$$\Pi_5^0(q^2) \,=\, \frac{1}{16\,\pi^2}\Big[\,-\,12 + 6\,L \,+\, a_s A_1(q^2) \,+\, a_s^2 A_2(q^2) \,+\, a_s^3 A_3(q^2) \,+\, a_s^4 A_4(q^2)\,\Big]\,, \tag{3.7}$$

where the variables L and a_s used throughout this dissertation are defined as

$$L \equiv \ln(-q^2/\mu^2)\ \ ,\ \ a_s \equiv \alpha_s(-q^2)/\pi\ \ , \tag{3.8}$$

and the $A_i(q^2)$ are

$$A_1(q^2) \,=\, -\frac{131}{2} \,+\, 34\,L \,-\, 6\,L^2 \,+\, 24\,\zeta_3$$

$$\begin{aligned} A_2(q^2) \,=\, & -\frac{17645}{24} \,+\, 353\,\zeta_3 \,-\, 8\,n_f\,\zeta_3 \,+\, \frac{511}{18}\,n_f \,+\, \frac{3}{2}\,\zeta_4 \,-\, 50\,\zeta_5 \\ & +\, \left(4\,n_f\,\zeta_3 \,-\, \frac{65}{4}n_f \,-\, 117\,\zeta_3 \,+\, \frac{10801}{24}\right)L \,+\, \left(\frac{11}{3}n_f \,-\, 106\right)L^2 \\ & +\, \left(-\frac{n_f}{3} + \frac{19}{2}\right)L^3 \end{aligned}$$

$$\begin{aligned} A_3(q^2) \,=\, & \left(\frac{4748953}{864} \,-\, \frac{\pi^4}{6} \,-\, \frac{91519}{36}\,\zeta_3 \,+\, \frac{715}{2}\,\zeta_5\right)L \,-\, 6\left(\frac{4781}{18} \,-\, \frac{475}{8}\,\zeta_3\right)L^2 \\ & +\, 229\,L^3 \,-\, \frac{221}{16}\,L^4 \end{aligned}$$

[1]The process of integrating a function twice introduces two integration constants. Hence, the $\mathcal{O}(\alpha_s^4)$ result for the correlator, Eq.(3.7), is only correct up to some constant. However, these unfixed integration constants are unimportant since $\Pi_5^0(q^2)$ only appears in the contour integral. Any analytic function added to $\Pi_5^0(q^2)$ will not change the contour integral.

$$A_4(q^2) \,=\, \sum_{i=1}^{5} H_i \, L^i \,, \tag{3.9}$$

with ζ_n the Riemann zeta-function, $n_f = 3$ in the light quark sector, and the coefficients H_i involving long expressions obtained from [35], numerically reducing to $H_1 = 33532.3$, $H_2 = -15230.645111$, $H_3 = 3962.454926$, $H_4 = -534.0520833$, and $H_5 = 24.17187500$. The perturbative contribution of the pseudoscalar correlator, Eq.(3.7), to lowest order of α_s is derived in appendix (A.2).

The $d = 2$ perturbative mass correction term in Eq.(3.4) is obtained from [35]

$$\begin{aligned} \Pi_5^2(q^2) \,=\, \frac{1}{16\,\pi^2}\Big[&-12 \,+\, 12\,L \,+\, a_s\,\big(-100 \,+\, 64\,L \,-\, 24\,L^2 \,+\, 48\,\zeta_3\big) \\ &+\, a_s^2\,\big(5065 \,-\, 1848\zeta_3 \,-\, 1746\,L \,+\, 300\,L^2\big)\Big] \,. \end{aligned} \tag{3.10}$$

The mass correction term Eq.(3.10) is negligible when determining the mass of the up and down quark. It must, however, be taken into consideration when determining the mass of the strange quark.

Next, we have the $d = 4$ perturbative mass correction term in the OPE Eq.(3.4)

$$\begin{aligned} \frac{C_3(L,a_s)}{-q^2}\,\langle O_3\rangle \,=\, \frac{1}{-q^2}\,\frac{3}{16\,\pi^2}\,\Bigg[1 \,+\, 2\,L \,+\, a_s\,\bigg(-\frac{6520}{567} \,+\, \frac{346}{63}\,L\bigg) \\ +\, a_s^2\,\bigg(-\frac{67}{324} \,+\, \frac{16}{7}\,L\bigg)\Bigg]\,(\overline{m}_i + \overline{m}_j)^4 \,. \end{aligned} \tag{3.11}$$

As with the $d = 2$ mass correction term, the $d = 4$ term Eq.(3.11) is only taken into consideration when determining the mass of the strange quark, and is negligible in the up and down quark case.

The leading order non-perturbative terms in $\Psi_5(q^2)|_{\rm QCD}$ are the light quark condensate contribution, the gluon condensate contribution and the strange quark condensate contribution, respectively.

The light quark condensate contribution in the OPE Eq.(3.4) is

$$-\,\frac{C_q(L,a_s)}{-q^2}\,(\overline{m}_i + \overline{m}_j)\,\langle\bar{q}\,q\rangle \,=\, -\,\frac{1}{-q^2}\bigg[1 \,+\, a_s\,\bigg(\frac{14}{3} \,-\, 2\,L\bigg)\bigg]\,(\overline{m}_i + \overline{m}_j)\,\langle\bar{q}\,q\rangle \,, \tag{3.12}$$

where there is a minus sign in front of the coefficient $C_q(L,a_s)$ since we are considering the pseudoscalar correlator. When determining the up and down quark mass it is safe to ignore here the light quark condensate contribution [22, 36]. For the case of the correlator

determining the strange quark mass, Eq.(3.6) and the light quark condensate contribution Eq.(3.12) are taken into account.

The gluon condensate contribution in the OPE Eq.(3.4) is

$$\frac{C_1(L,a_s)}{-q^2}\,\langle O_1\rangle \;=\; \frac{1}{-q^2}\,\frac{1}{8}\left[1\,+\,a_s\left(\frac{11}{2}\,-\,2\,L\right)\right]\left\langle a_s\,G^a_{\mu\nu}\,G^{a\,\mu\nu}\right\rangle . \tag{3.13}$$

In theory, there is an issue related to the removal of logarithmic quark-mass singularities [22] present in the gluon condensate contribution. However, due to the magnitude of uncertainties from other sources this turns out to be numerically negligible. Hence, Eq.(3.13) may be safely used. The gluon condensate contribution is important in both cases – in determining the up and down quark mass, and in determining the strange quark mass. In the up and down quark case Eq.(3.5) is relevant, while in the strange quark case we take Eq.(3.6) into account.

Finally, the strange quark condensate contribution in the OPE Eq.(3.4) is given by

$$\frac{C_2(L,a_s)}{-q^2}\,\langle O_2\rangle \;=\; \frac{1}{-q^2}\,\frac{1}{2}\left[1\,+\,a_s\left(\frac{11}{3}\,-\,2\,L\right)\right](\overline{m}_i+\overline{m}_j)\left\langle \bar{s}\,s\right\rangle . \tag{3.14}$$

The strange quark condensate Eq.(3.14) only contributes, as its name suggests, in the case of the correlator determining the strange quark mass.

4 Integration in the Complex Energy Plane

Section (3) described how to calculate the pseudoscalar correlator $\Psi_5(q^2)|_{\rm QCD}$ in the framework of an operator product expansion. Through the use of renormalization group equations we can simplify the pseudoscalar correlator. Sections (10) and (11) provide details on the renormalization group equations. In this section, we focus on performing the contour integral of $\Psi_5(q^2)|_{\rm QCD}$ that appears in our finite energy sum rule Eq.(2.5). This contour integral is usually performed in two ways: viz. fixed order perturbation theory (FOPT), and contour improved perturbation theory (CIPT) [37, 38]. The two methods differ depending on the order in which the operations are performed – the renormalization group improvement before integration or vice versa [39].

In a variety of applications either both methods (CIPT or FOPT) give similar results, or CIPT leads to better behaved predictions [37]. The latter will turn out to be the case in this determination. Both approaches are described below.

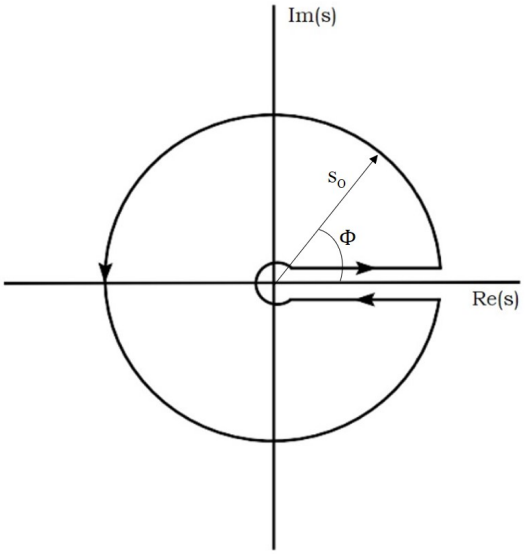

Figure 4: Circular contour in the complex energy plane, clearly marking the contour radius $|s_0|$ and the integration angle ϕ. The contour integral can be performed using fixed order perturbation theory or contour improved perturbation theory

4.1 Fixed Order Perturbation Theory

In FOPT the strong coupling, $\alpha_s(s)$, is frozen on the integration contour (i.e. at a given energy scale $s = s_0$, when integrating in ϕ. All contributions to the pseudoscalar correlator $\Psi_5(q^2)|_{\rm QCD}$ (Eqs.(3.4) – (3.11)), including the logarithmic terms ($\ln(-q^2/\mu^2)$), are present in the integral.

The renormalization group (RG) improvement (the re-summation over leading log terms) of the QCD correlator is implemented after integration by setting the renormalization scale $\mu^2 = -q^2$.

4.2 Contour Improved Perturbation Theory

In CIPT, the renormalization group (RG) improvement of the QCD correlator is performed before integration. The setting of $\mu^2 = -q^2$ eliminates all the logarithmic terms $(\ln(-q^2/\mu^2))$.

The strong coupling $\alpha_s(s)$ and quark mass $\overline{m}_q(s)$ are running, and as such must be obtained by numerically solving the renormalization group equations at each point around the circular contour (i.e. at each value of the integration angle ϕ) during integration (see figure (4)).

To describe the running of the strong coupling, $\alpha_s(s)$ is expressed in terms of a chosen scale $s = s^*$ where its value is known with high precision. As an initial value for the strong coupling, we use the world average of the strong coupling constant $\alpha_s(M_Z^2) = 0.1181 \pm 0.0011$ [13]. This is run to our chosen scale $s^* = M_\tau^2$ using RunDec (version 3) [40] to decouple over flavour thresholds, which yields

$$\alpha_s(s^* \equiv M_\tau^2) = 0.3205 \pm 0.0183\,. \tag{4.1}$$

The series expansion of the renormalization group equation (Eq.(11.6)) is then used to determine $\alpha_s(s)$ at each point around the circular contour. Similarly, by Taylor expanding the renormalization group equation for $\overline{m}_q(s)$, the quark mass can also be expressed at each point around the circular contour in terms of its value at some scale $s = s^*$ (see Eq.(11.8)).

It is worth noting the asymptotic behaviour of perturbative part of the correlator $\Psi_5^0(q^2)$: it diverges quadratically as $-q^2 \to \infty$

$$\lim|_{-q^2\to\infty}\ \Psi_5^0(q^2) \;=\; \lim|_{-q^2\to\infty}\ \Big(-q^2\,(\overline{m}_i+\overline{m}_j)\,\Pi_5^0(q^2)\Big) \;\sim\; q^2\,. \tag{4.2}$$

From Eq.(4.2) we infer that the dispersion relations for $\Psi_5(q^2)$ will involve two subtractions. Normally this not a major concern in finite energy sum rules, as the integrals are over a finite range. The alternative is to consider the second derivative, $\Psi_5''(q^2)$. In FOPT one can either use the correlator $\Psi_5(q^2)|_{\rm QCD}$ (Eq.(3.4)), or its second derivative[2]. However, in CIPT it is far more convenient to use the second derivative, $\Psi_5''(q^2)|_{\rm QCD}$. In the remainder of this section we give the expressions for the second derivative of the correlator with respect to $-q^2$, and the corresponding FESR.

The expansion of $\Psi_5''(q^2)|_{\rm QCD}$ within the OPE framework Eq.(3.2) is given by

$$\Psi_5''(q^2)|_{\rm QCD} \;=\; (\overline{m}_i+\overline{m}_j)^2\left\{-\frac{1}{q^2}\,\Pi_5^{0\,\prime\prime}(q^2) \;-\; \frac{1}{q^4}(\overline{m}_i+\overline{m}_j)^2\,\Pi_5^{2\,\prime\prime}(q^2)\right.$$
$$\left.\pm\,\frac{I_q(L,a_s)}{-q^6}\,(\overline{m}_i+\overline{m}_j)\,\langle\bar{q}\,q\rangle + \sum_{j=1}^{3}\frac{I_j(L,a_s)}{-q^6}\,\langle O_j\rangle + \mathcal{O}\left(\frac{1}{q^8}\right)\right\}, \tag{4.3}$$

[2] $\Psi_5(q^2)|_{\rm QCD}$ only appears in the contour integral. Hence, the information contained in the two constants which are lost when taking the second derivative of $\Psi_5(q^2)|_{\rm QCD}$ are unimportant.

where $\overline{m}_{i,j}$ are the quark masses in the $\overline{\rm MS}$ renormalization scheme, Eq.(3.5) is relevant in the up and down quark mass determination, and Eq.(3.6) is taken into account in the strange quark mass determination. The lower sign in front of the third term in Eq.(4.3) corresponds to the case of the pseudoscalar correlator and the upper sign corresponds to the case of the scalar correlator.

The second derivative of the perturbative QCD function, $\Pi_5^{0\,\prime\prime}(q^2)$, can be found in [36,41], and the $\mathcal{O}(\alpha_s^4)$ result is given in [35]

$$\Pi_5^{0\,\prime\prime}(q^2) \,=\, \frac{3}{8\,\pi^2}\Big[1 \,+\, a_s K_1(q^2) \,+\, a_s^2 K_2(q^2) \,+\, a_s^3 K_3(q^2) \,+\, a_s^4 K_4(q^2)\Big]\,, \tag{4.4}$$

where the variables L and a_s are defined in Eq.(3.8), and the $K_i(q^2)$

$$\begin{aligned}
K_1(q^2) \,&=\, \frac{11}{3} \,+\, 2\,L \\
K_2(q^2) \,&=\, \frac{5071}{144} \,-\, \frac{35}{2}\,\zeta_3 \,+\, \frac{139}{6}\,L \,+\, \frac{17}{4}\,L^2 \\
K_3(q^2) \,&=\, \frac{1995097}{5184} \,-\, \frac{1}{36}\,\pi^4 \,-\, \frac{65869}{219}\,\zeta_3 \,+\, \frac{715}{12}\,\zeta_5 \,+\, \left(\frac{2720}{9} \,-\, \frac{475}{4}\,\zeta_3\right) L \\
&\quad +\, \frac{695}{8}\,L^2 \,+\, \frac{221}{24}\,L^3 \\
K_4(q^2) \,&=\, \frac{2361295759}{497664} \,-\, \frac{2915}{10368}\,\pi^4 \,-\, \frac{25214831}{5184}\,\zeta_3 \,+\, \frac{192155}{216}\,\zeta_3^2 \,+\, \frac{59875}{108}\,\zeta_5 \,-\, \frac{625}{48}\,\zeta_6 \\
&\quad -\, \frac{52255}{256}\,\zeta_7 \,+\, \left(\frac{43647875}{10368} \,-\, \frac{1}{18}\,\pi^4 \,-\, \frac{864685}{288}\,\zeta_3 \,+\, \frac{24025}{48}\,\zeta_5\right) L \\
&\quad +\, \left(\frac{1778273}{1152} \,-\, \frac{16785}{32}\,\zeta_3\right) L^2 \,+\, \frac{79333}{288}\,L^3 \,+\, \frac{7735}{384}\,L^4\,,
\end{aligned} \tag{4.5}$$

are the second derivatives of the $A_i(q^2)$ (defined in Eq.(3.9)) with respect to $-q^2$, with ζ_n the Riemann zeta-function and $n_f = 3$ in the light quark sector.

The second derivative of the $d = 2$ perturbative mass correction term in Eq.(4.3) is found in [35]

$$\Pi_5^{2\,\prime\prime}(q^2) \,=\, \frac{6}{8\,\pi^2}\left[1 \,+\, a_s\left(\frac{28}{3} \,+\, 4\,L\right) \,+\, a_s^2\left(\frac{8557}{72} \,-\, \frac{77}{3}\,\zeta_3 \,+\, \frac{147}{2}\,L \,+\, \frac{25}{2}\,L^2\right)\right]. \tag{4.6}$$

The mass correction term Eq.(4.6) is considered important in the case of the strange quark mass determination, but can safely be ignored in the determination of the up and down quark mass.

Next, we have the second derivative of the $d = 4$ perturbative mass correction term in the OPE Eq.(4.3)

$$\begin{aligned}\frac{I_3(L,a_s)}{-q^6}\,\langle O_3\rangle \;=\; \frac{1}{-q^6}\,\Bigg\{ &-\frac{3}{36\,\pi^2}\left[1+\frac{4}{3}\,a_s\right]\left[1+a_s\left(\frac{121}{18}+2\,L\right)\right]\\ &+\frac{3}{7\,\pi^2}\left[\frac{1}{a_s}-\frac{53}{24}\right]\left[1+a_s\left(\frac{64}{9}+2\,L\right)\right]\\ &-\frac{3}{7\,\pi^2}\left[\frac{1}{a_s}+\frac{155}{24}+\frac{15}{4}\,L\right]\Bigg\}\,(\overline{m}_i+\overline{m}_j)^4\,.\end{aligned} \tag{4.7}$$

As with the $d = 2$ mass correction term, the $d = 4$ term Eq.(4.7) is negligible in the up and down quark case, and is taken into consideration when determining the mass of the strange quark.

The second derivative of leading order non-perturbative terms in $\Psi_5''(q^2)|_{\rm QCD}$ – the light quark condensate contribution, the gluon condensate contribution and the strange quark condensate contribution – are given in Eqs.(4.8 - 4.10), respectively.

The light quark condensate contribution in the OPE Eq.(4.3) is

$$-\;\frac{I_q(L,a_s)}{-q^6}\,(\overline{m}_i+\overline{m}_j)\,\langle\bar{q}\,q\rangle \;=\; -\,\frac{2}{-q^6}\left[1+a_s\left(\frac{23}{3}+2\,L\right)\right](\overline{m}_i+\overline{m}_j)\,\langle\bar{q}\,q\rangle\;, \tag{4.8}$$

where there is a minus sign in front of the coefficient $I_q(L,a_s)$ since we are considering the pseudoscalar correlator. For the case of the correlator determining the up and down quark mass, it is safe to ignore the light quark condensate contribution [22, 36].

The gluon condensate contribution in the OPE Eq.(4.3) is

$$\frac{I_1(L,a_s)}{-q^6}\,\langle O_1\rangle \;=\; \frac{1}{-q^6}\,\frac{1}{4}\left[1+\frac{16}{9}\,a_s\right]\left[1+a_s\left(\frac{121}{18}+2\,L\right)\right]\langle a_s\,G^a_{\mu\nu}\,G^{a\,\mu\nu}\rangle\,. \tag{4.9}$$

The gluon condensate contribution is important in both cases – in determining the up and down quark mass, and in determining the strange quark mass.

Finally, the strange quark condensate contribution in the OPE Eq.(4.3) is given by

$$\frac{I_2(L,a_s)}{-q^6}\,\langle O_2\rangle \;=\; \frac{1}{-q^6}\Bigg\{ -\frac{4}{9}\,a_s\left[1+\frac{91}{24}\,a_s\right]\left[1+a_s\left(\frac{121}{18}+2\,L\right)\right] + \left[1+a_s\left(\frac{64}{9}+2\,L\right)\right]\Bigg\}\,(\overline{m}_i+\overline{m}_j)\,\langle\,\bar{s}\,s\,\rangle\;. \tag{4.10}$$

The strange quark condensate Eq.(4.10) only contributes in the case of the correlator determining the strange quark mass.

In the framework of CIPT, the QCD finite energy sum rule is given by

$$\frac{1}{2\,\pi\,i}\oint_{C(|s_0|)} ds\,\Psi_5^{''}(s)|_{\rm QCD}\,\big[F(s)\,-\,F(s_0)\big]\,+\,\int_{s_{th}}^{s_0} ds\,\frac{1}{\pi}\,{\rm Im}\,\Psi_5(s)|_{\rm HAD}\,P_5(s) \;=\; {\rm Res}[\,\Psi_5(s)P_5(s),s=0\,]\,, \tag{4.11}$$

where, as in Eq.(2.5), s_{th} is the the quark-pair production threshold, $P_5(s)$ is an integration kernel chosen to quench the uncertainty in the hadronic resonance sector, $F(s)$ is the form of this kernel accompanying the second derivative of the correlator $\Psi_5^{''}(s)|_{\rm QCD}$, and ${\rm Res}[\,\Psi_5(s)P_5(s),s=0\,]$ are the residues at the pole(s).

$F(s)$ depends on the explicit form of the kernel $P_5(s)$ and on the energy scale s_0 which corresponds to the radius in the complex energy plane. Specifically

$$\oint ds\;\frac{d^2\,\Psi_5(s)}{d\,s^2}\;\big[F(s)\,-\,F(s_0)\big]\;=\;\oint ds\;\Psi_5(s)\;P_5(s)\;, \tag{4.12}$$

with

$$F(s)\;=\;\int_0^s\;\big[G(s^{'})\,-\,G(s_0)\big]\,ds^{'}\;=\;\int_0^s\,\Big[\int_0^{s^{'}}\;P_5(s^{''})\,ds^{''}\;-\;\int_0^{s_0}\;P_5(s^{''})\,ds^{''}\Big]\,ds^{'}\;, \tag{4.13}$$

where we have made use of the Fundamental Theorem of Calculus. Various different integration kernels are discussed in section (6).

5 The Hadronic Spectrum

Now we turn towards the hadronic sector. For the case of the the up and down quark mass determination, the spectral function of the correlator $\Psi_5(q^2)$, Eq.(2.2), involves the pion pole followed by the three-pion resonance contribution

$$\frac{1}{\pi}\,\mathrm{Im}\,\Psi_5(s\equiv -q^2)|_{\mathrm{HAD}} \,=\, 2\,f_\pi^2\,m_\pi^4\,\delta(s-m_\pi^2) \,+\, \frac{1}{\pi}\,\mathrm{Im}\,\Psi_5(s)|_{\mathrm{RES}} \tag{5.1}$$

where $f_\pi = (92.07 \pm 1.20)$ MeV [13], $m_\pi = (134.9770 \pm 0.0005)$ MeV [13], and the three-pion resonance contribution is due to the $\pi(1300)$ followed by the $\pi(1800)$ excitations [13].

In the chiral limit the threshold behaviour of the three-pion state, first obtained in [42], is

$$\frac{1}{\pi}\,\mathrm{Im}\,\Psi_5(s)|_{\pi\pi\pi} \,=\, \theta(s)\,\frac{1}{3}\,\frac{m_\pi^4}{f_\pi^2}\,\frac{1}{2^8\,\pi^4}\,s\,. \tag{5.2}$$

Beyond the chiral limit the threshold behaviour, first obtained correctly in [43], is given by

$$\frac{1}{\pi}\,\mathrm{Im}\,\Psi_5(s)|_{\pi\pi\pi} \,=\, \theta\big(s-9\,m_\pi^2\big)\,\frac{1}{9}\,\frac{m_\pi^4}{f_\pi^2}\,\frac{1}{2^8\,\pi^4}\,I_{PS}(s)\,, \tag{5.3}$$

where the phase-space integral $I_{PS}(s)$ is

$$\begin{aligned} I_{PS}(s) \,=\, \int_{4\,m_\pi^2}^{(\sqrt{s}-m_\pi)^2} du\,\sqrt{1\,-\,\frac{4\,m_\pi^2}{u}}\,\lambda^{1/2}(1,\,u/s,\,m_\pi^2/s)\,\Bigg\{5\,+\,\frac{1}{2}\,\frac{1}{(s\,-\,m_\pi^2)^2} \\ \times\,\Bigg[(s\,-\,3\,u\,+\,3\,m_\pi^2)^2+\,3\,\lambda(s,\,u,\,m_\pi^2)\,\Bigg(1\,-\,\frac{4\,m_\pi^2}{u}\Bigg)\,+\,20\,m_\pi^4\Bigg] \\ +\,\frac{1}{(s\,-\,m_\pi^2)}\,\Big[3(u\,-\,m_\pi^2)\,-\,s\,+\,9\,m_\pi^2\Big]\Bigg\}\,, \end{aligned} \tag{5.4}$$

where

$$\lambda(1,\,u/s,\,m_\pi^2/s) \,\equiv\, \Bigg[1\,-\,\frac{(\sqrt{u}\,+\,m_\pi)^2}{s}\Bigg]\,\Bigg[1\,-\,\frac{(\sqrt{u}\,-\,m_\pi)^2}{s}\Bigg]\,, \tag{5.5}$$

and

$$\lambda(s,\,u,\,m_\pi^2) \,\equiv\, \Big[s\,-\,(\sqrt{u}\,+\,m_\pi)^2\Big]\,\Big[s\,-\,(\sqrt{u}\,-\,m_\pi)^2\Big]\,, \tag{5.6}$$

which in the chiral limit reduces to $I_{PS} \,=\, 3\,s$.

The threshold expression Eq.(5.3) normalizes the hadronic resonance spectral function, modelled as a combination of Breit-Wigner forms $BW_i(s)$

$$\frac{1}{\pi}\,\mathrm{Im}\,\Psi_5(s)|_{\mathrm{RES}} \;=\; \frac{1}{\pi}\,\mathrm{Im}\,\Psi_5(s)|_{\pi\pi\pi}\,\frac{[BW_1(s)\,+\,\kappa\,BW_2(s)]}{(1\,+\,\kappa)}\,, \tag{5.7}$$

where $s_{th} \,=\, 9\,m_\pi^2$ is the threshold energy, and $BW_1(s_{th}) \,=\, BW_2(s_{th}) \,=\, 1$, with

$$BW_i(s) \,=\, \frac{(m_i^2\,-\,s_{th})^2\,+\,m_i^2\,\Gamma_i^2}{(s\,-\,m_i^2)^2\,+\,m_i^2\,\Gamma_i^2}\;\;(i\,=\,1,2)\,, \tag{5.8}$$

and κ an unknown parameter controlling the relative weight of the resonances.

In considering the value of κ we follow [15]. The requirement that the first resonance should be the leading resonance restricts the parameter κ within the range $\kappa = 0.1 - 0.2$. Varying κ within this range produces only a 1% change in $\overline{m}_{ud}$, which is included in the overall uncertainty analysis. The value $\kappa \,=\, 0.1$ comfortably ensures a smaller contribution of the second resonance compared to the first, and it will be used in the sequel.

The widths of these radial excitations of the pion are affected by large uncertainties [13]. For the first resonance, $\pi(1300)$, we shall use the determination from the two-photon process $\gamma\,\gamma \,\to\, \pi^+\,\pi^-\,\pi^0$, as it is the most reliable [44]. The width is $\Gamma_1 \,=\, (260 \,\pm\, 36)$ MeV. The second resonance is the $\pi(1800)$ with a width $\Gamma_2 \,=\, (208 \,\pm\, 12)$ MeV [13].

Figure (5) displays the hadronic spectral function in the resonance region (Eqs.(5.3 – 5.8)).

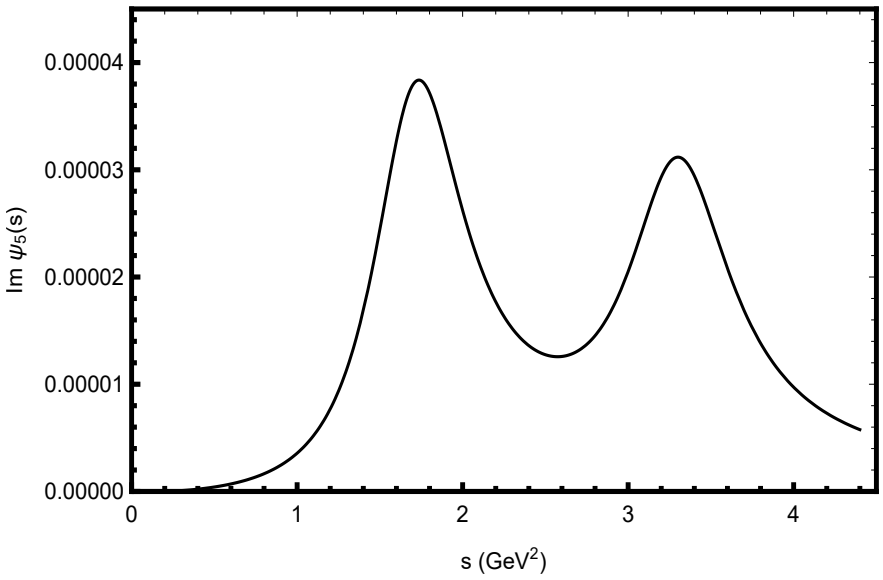

Figure 5: Hadronic spectral function in the resonance region for the case of the up and down quark mass determination (Eqs.(5.3 – 5.8)) with $\kappa = 0.1$ and involving two radial excitations of the pion, $\pi(1300)$ and $\pi(1800)$.

Before moving onto the spectral function of the correlator determining the strange quark mass, we pause to examine how the threshold behaviour in the chiral limit Eq.(5.2) compares to the threshold behaviour beyond the chiral limit Eqs.(5.3 – 5.6). In the past determinations [15,18] the threshold behaviour in the chiral limit is used for simplicity and it is assumed that this makes little or no impact on the final light quark mass determinations. This assumption requires critical examination.

First we study the behaviour in the limit as $m_\pi \to 0$ with fixed $s = 2\,\mathrm{GeV}^2$. The chiral limit is reached very quickly and the phase-space integral $I_{PS}(s)$ (Eq.(5.4)), agrees with $I_{chiral}(s) = 3\,s$ (Eq.(5.2)) already for $m_\pi = 10\,\mathrm{MeV}$ to high precision. This is seen in figure (6).

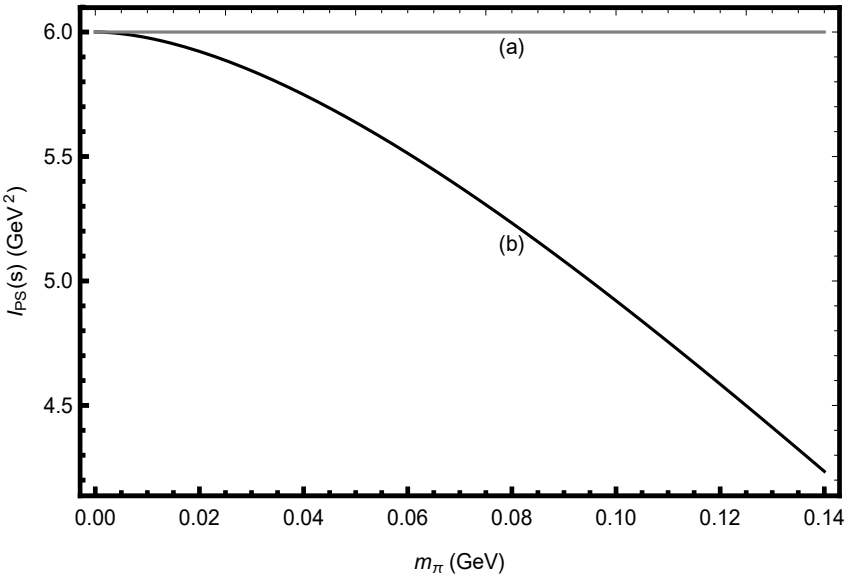

Figure 6: The behaviour of (a) the chiral threshold $I_{chiral}(s) = 3\,s$ (Eq.(5.2)), and (b) the phase-space integral $I_{PS}(s)$ (Eq.(5.4)), in the limit $m_\pi \to 0$ with fixed $s = 2\,\mathrm{GeV}^2$.

Plotting the behaviour in the limit as $s \to \infty$ with fixed $m_\pi = 140\,\mathrm{MeV}$, one finds that the function $I_{PS}(s)$ differs from $I_{chiral}(s)$ even at comparatively large values of s. In figure (7), we see that at the first resonance $\pi(1300)$ the difference between $I_{PS}(s)$ and its chiral limit $I_{chiral}(s)$ amounts to almost 50 percent: $I_{PS}(s = 1.69\,\mathrm{GeV}^2) = 3.4$ and $I_{chiral}(s = 1.69\,\mathrm{GeV}^2) = 5.1$.

In order to find agreement between $I_{PS}(s)$ and $I_{chiral}(s)$ at the level of half a percent, one has to increase s to $1000\,\mathrm{GeV}^2$ for fixed $m_\pi = 140\,\mathrm{MeV}$, i.e. four orders of magnitude larger than m_π^2 and far larger than the order of magnitude of the up and down quark mass determination (where $s \sim 10\,\mathrm{GeV}^2$). This is suprising since the naïve expectation is that the limits of large s and small m_π are equivalent.

In conclusion, the threshold behaviour in the chiral limit containing $I_{chiral}(s)$ (Eq.(5.2)) is only a rough approximation of the threshold behaviour beyond the chiral limit containing the phase-space integral $I_{PS}(s)$ (Eqs.(5.3 – 5.6)). In the interest of accuracy, the hadronic spectrum in the up and down quark mass determination presented here, in this dissertation, uses the full threshold behaviour, Eqs.(5.3 – 5.6).

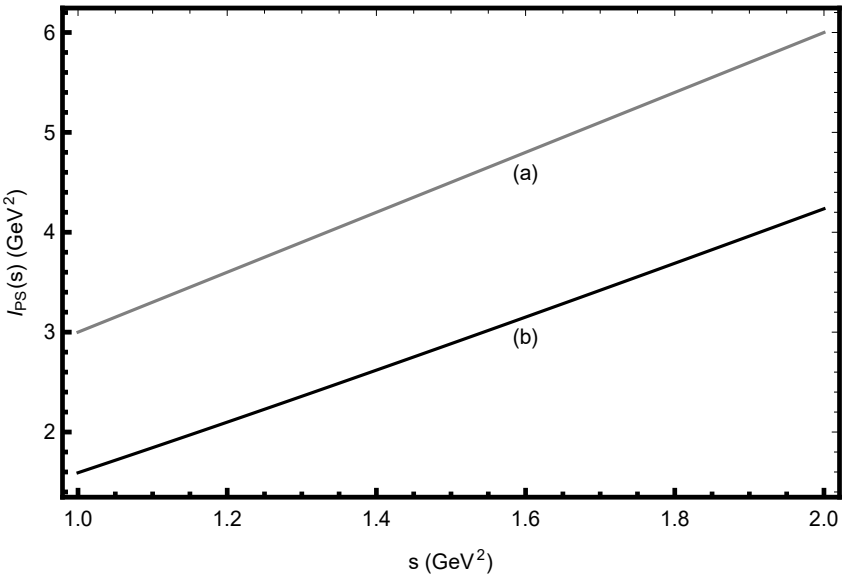

Figure 7: The behaviour of (a) the chiral threshold $I_{chiral}(s) = 3\,s$ (Eq.(5.2)), and (b) the phase-space integral $I_{PS}(s)$ (Eq.(5.4)), between $s = (1.0 - 2.0)\,\mathrm{GeV}^2$ with fixed $m_\pi = 140\,\mathrm{MeV}$.

Now turning to the case of the strange quark mass determination. The spectral function of the correlator $\Psi_5(q^2)$, Eq.(2.2), involves the kaon pole followed by the $K\pi\pi$ resonance contribution

$$\frac{1}{\pi}\,\mathrm{Im}\,\Psi_5(s \equiv -q^2)|_{\mathrm{HAD}} \,=\, 2\,f_K^2\,m_K^4\,\delta(s - m_K^2) \,+\, \frac{1}{\pi}\,\mathrm{Im}\,\Psi_5(s)|_{\mathrm{RES}} \tag{5.9}$$

where $f_K = (110.03 \pm 0.28)$ MeV [13], $m_K = (493.677 \pm 0.016)$ MeV [13], and the $K\pi\pi$ resonance contribution is dominated by the $K(1460)$ followed by the $K(1830)$ excitations [13]. This makes modeling the hadronic spectrum much simpler in the pseudoscalar channel compared to in the scalar channel where the strong $K\pi$ scattering in S-wave ($J^P = 0^+$) requires special analysis [45, 46].

The full threshold behaviour of the $K\pi\pi$ resonance contribution is given in [47]

$$\frac{1}{\pi}\,\mathrm{Im}\,\Psi_5(s)|_{K\pi\pi} \,=\, \theta\big(s \,-\, m_K^2\big)\,\frac{m_K^4}{2\,f_\pi^2}\,\frac{3}{2^8\,\pi^4}\,\frac{I_{PS}(s)}{s\,(m_K^2 \,-\, s)^2}\,, \tag{5.10}$$

where the phase-space integral $I_{PS}(s)$ is

$$\begin{aligned} I_{PS}(s) \,=\, \int_{m_K^2}^{s} \frac{du}{u}\,\big(u \,-\, m_K^2\big)\,\big(s \,-\, u\big)\bigg[\big(m_K^2 \,-\, s\big)\,\bigg(u \,-\, \frac{s \,+\, m_k^2}{2}\bigg) \\ -\, \frac{1}{8\,u}\,\big(u^2 \,-\, m_k^4\big)\,\big(s \,-\, u\big) \,+\, \frac{3}{4}\,\big(u \,-\, m_K^2\big)^2\,|F_K(u)|^2\bigg]\,, \end{aligned} \tag{5.11}$$

where

$$|F_K(u)|^2 \;=\; \frac{\left(m_{K^*}^2 \,-\, m_K^2\right)^2 \,+\, m_{K^*}^2\;\Gamma_{K^*}^2}{\left(m_{K^*}^2 \,-\, u\right)^2 \,+\, m_{K^*}^2\;\Gamma_{K^*}^2}\,, \tag{5.12}$$

and K^* refers to the $K^*(892) - \pi$ sub-channel, with $m_{K^*} = 891.76 \pm 0.25$ MeV [13] and $\Gamma_{K^*} = 50.3 \pm 0.3$ MeV [13]. The $K^*(892) - \pi$ sub-channel is numerically important due to its narrow width [47].

The threshold expression Eq.(5.10) normalizes the hadronic resonance spectral function, modelled as a combination of Breit-Wigner forms $BW_i(s)$

$$\frac{1}{\pi}\,\mathrm{Im}\,\Psi_5(s)|_{\mathrm{RES}} \;=\; \frac{1}{\pi}\,\mathrm{Im}\,\Psi_5(s)|_{K\pi\pi}\,\frac{[BW_1(s) \,+\, \lambda\, BW_2(s)]}{(1 \,+\, \lambda)}\,, \tag{5.13}$$

where $s_{th} = (m_\pi + m_K)^2$ is the threshold energy, and $BW_1(s_{th}) = BW_2(s_{th}) = 1$, with

$$BW_i(s) \;=\; \frac{(m_i^2 \,-\, m_K^2)^2 \,+\, m_i^2\;\Gamma_i^2}{(s \,-\, m_i^2)^2 \,+\, m_i^2\;\Gamma_i^2} \quad (i \,=\, 1, 2)\,, \tag{5.14}$$

and λ a unknown parameter controlling the relative weight of the resonances.

Figure (8) displays the hadronic spectral function in the resonance region given Eqs.(5.10 – 5.14).

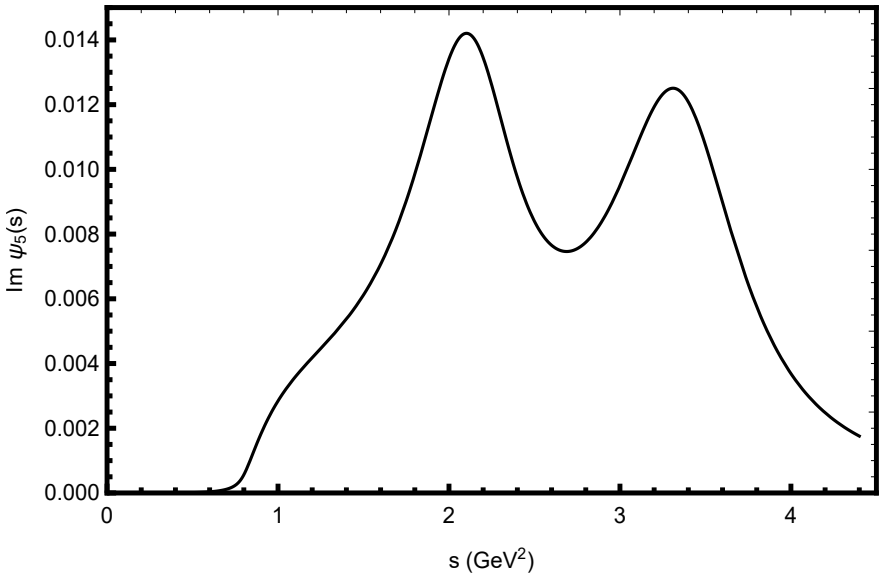

Figure 8: Hadronic spectral function in the resonance region for the case of the strange quark mass determination (Eqs.(5.10 – 5.14)) with $\lambda = 1$ and involving two radial excitations of the kaon, $K(1460)$ and $K(1830)$.

Previous determinations [17,47] have set $\lambda = 1$ as it comfortably ensures a smaller contribution of the second resonance compared to the first resonance. This determination does so too. However, the variation of λ in the range $\lambda = (0.7 - 1.1)$ only produces a change in $\overline{m}_s$ of the order of a couple of percent. This range satisfies the requirement that the first resonance should be the leading resonance.

The widths of the radial excitations of the kaon are not very well established and are affected by large uncertainties [13]. The width of the first resonance, $K(1460)$ is given approximately as $\Gamma_1 \sim 250$ MeV [48] and $\Gamma_1 \sim 260$ MeV [49]. While, the width of the second resonance $K(1830)$ is given as $\Gamma_2 \sim 250$ MeV [50] and $\Gamma_2 = (168 \pm 90\,^{+280}_{-104})$ MeV [51], with the latter being the most recent determination. These results for the kaon resonance widths are the only ones currently recognized by the Particle Data Group [13]. In this determination, we consider the resonances to have equal widths and use $\Gamma_1 \sim 250$ MeV and $\Gamma_2 \sim 250$ MeV, while considering a variation of ± 25 MeV in the uncertainty analysis.

Besides the model we use here (presented in figure (8)), other hadronic models of the resonance region exist, such as the model proposed in [35,52]. These models rely on unmeasured decay constants f_{K_1} and f_{K_2} of the $K_1 = K(1460)$ and $K_2 = K(1830)$ kaonic resonances. The effect on the strange quark mass from a change in hadronic model is not examined in this dissertation. However, from previous determinations, it is expected to be small [17].

6 The Choice of Kernel

In many respects modelling the complex hadronic information present in our FESR Eq.(2.5), is unsatisfactory. Inelasticity, non-resonant background noise and interference means that our hadronic model – which takes the form of a primary pole and the sum of two predominant radial excitations represented as Breit-Wigner functions – does not provide enough information to fully reconstruct the hadronic spectral function [18]. Further, from our discussions in section (5) we see that the masses and widths of these radial excitations ($\pi(1300)$ and $\pi(1800)$ for the up and down quark mass determination, and $K(1460)$ and $K(1830)$ for the strange quark mass determination) are not always precisely known [13].

The systematic errors introduced from our hadronic model severely impact the accuracy of our final quark mass determination. It is for this reason that we introduce a meromorphic function $P_5(s)$ which multiples through all the terms in our FESR Eq.(2.5). It is expected that by the introduction of this quenching kernel $P_5(s)$ the importance of the hadronic resonances in the determination of the light quark masses is considerably reduced [3].

Several functional forms for the hadronic quenching integration kernel are considered in this work. A simple kernel mentioned in the Introduction and originally proposed in [15,18] takes the form of a second degree polynomial

$$P_{5\,1}(s) \,=\, 1 \,-\, a_0\, s \,-\, a_1\, s^2\,, \tag{6.1}$$

where a_0 and a_1 are free parameters which are determined by requiring that the kernel vanishes at the peak of the two predominant radial excitations with masses m_1 and m_2 respectively. Requiring that $P_{5\,1}(m_1^2) \,=\, P_{5\,1}(m_2^2) \,=\, 0$, yields $a_0 \,=\, 0.8962\,\mathrm{GeV}^{-2}$ and $a_1 \,=\, -0.1802\,\mathrm{GeV}^{-4}$ in the case of the up and down quark mass; and $a_0 \,=\, 0.768\,\mathrm{GeV}^{-2}$ and $a_1 \,=\, -0.140\,\mathrm{GeV}^{-4}$ in the case of the strange quark mass. An equivalent form of this kernel is $P_5(s) \,=\, (s - m_1^2)\,(s - m_2^2)$.

We can also consider higher dimensional kernels, such as

$$P_{5\,2}(s) \,=\, (s \,-\, m_1^2)\,(s \,-\, m_2^2)\,(s \,-\, s_0)\,, \tag{6.2}$$

where $P_{5\,2}(s)$ suppresses the contribution from the hadronic resonances by vanishing at the peaks of the two predominant radial excitations and at s_0. The radius in the complex energy plane, $|s_0|$, represents the onset of pQCD, although, it remains unclear what the exact value of $|s_0|$ should be.

The third kernel quenches the hadronic resonance contribution at $s = s_0$, as well as in the region between the two resonances. It takes the form

$$P_{5\,3}(s) \,=\, (s \,-\, c)\,(s \,-\, s_0)\,, \tag{6.3}$$

where $c = 2.4\,\mathrm{GeV}^{-2}$ lies halfway between the two resonances in the case of the up and down quark, and $c = 2.7\,\mathrm{GeV}^{-2}$ lies halfway between the two resonances in the case of the strange quark.

Pinching kernels, such as Eq.(6.2), have been suggested since they reduce the sensitivity of our FESR on the value of $|s_0|$ and counteract potential duality violations [17]. However these potential, in principle unknown [53, 54], duality violations are expected to be quenched above $s_0 \approx 3.0\,\mathrm{GeV}^2$, the region where our final light quark mass results are obtained (see section (8)). Therefore, there exists no pressing reason why the kernel $P_{\bar{5}\,2}(s)$ should be preferred over the kernels $P_{\bar{5}\,1}(s)$ and $P_{\bar{5}\,3}(s)$. In fact, we are lead to disfavour the kernel given in Eq.(6.2), since it requires the dimension $d = 8$ condensate (whose value is completely unknown) to be included in the FESR. Choosing the kernel $P_{\bar{5}\,2}(s)$ would bring in an unknown systematic uncertainty into the calculation.

In this dissertation, we will find Eq.(6.3) to be the optimal kernel. Several criteria were used in choosing the integration kernel Eq.(6.3). For instance, the kernel should not bring in higher dimensional condensates, as their values are poorly known. This constrains substantially the powers of s. Further, the relative contribution of the second resonance should not exceed that of the first one. The kernel Eq.(6.3) leads to the most stable result for the up and down quark masses in the wide region $s_0 \simeq (1.5 - 4.0)\,\mathrm{GeV}^2$, and for the strange quark mass in the region $s_0 \simeq (3.0 - 5.0)\,\mathrm{GeV}^2$. Results showing how the light quark masses vary over a given energy range depending on the choice of kernel are given in detail in section (8). However, it must be noted that the choice of kernel is likely dependent on the application. For example, a kernel which ensures maximum stability in the case of the up and down quark mass may not result in the same stability in the case of the strange quark mass, since these quarks possess a different underlying hadronic structure.

Eqs.(4.11 - 4.13) describe the FESR for the case of the second derivative of the correlator $\Psi_5^{''}(s)|_{\mathrm{QCD}}$. The function $F(s)$ is the form of the integration kernel $P_5(s)$ which accompanies $\Psi_5^{''}(s)|_{\mathrm{QCD}}$ in the FESR. The $F(s)$ corresponding to our optimal integration kernel $P_{\bar{5}\,3}(s)$, is given by

$$F(s) \,=\, \frac{1}{12}\,s^4 \,-\, \frac{1}{6}\,\big(c \,+\, s_0\big)\,s^3 + \frac{1}{2}\,c\,s_0\,s^2 + \left(\frac{s_0^3}{6} \,-\, \frac{1}{2}\,c\,s_0^2\right)s\,, \tag{6.4}$$

and $F(s_0)$ becomes

$$F(s_0) \,=\, \frac{s_0^3}{12}\,\big(-\,2\,c \,+\, s_0\big)\,, \tag{6.5}$$

where the value of c is defined after Eq.(6.3).

7 The Convergence of the Perturbative QCD Series

In this section we address the issue of the convergence of the perturbative QCD expansion and its effect on the light quark masses. The starting point is the analysis of the convergence of the correlator function's PQCD expansion using fixed order perturbation theory. In FOPT, the strong coupling is fixed for a given radius s_0 in the complex s-plane. After the contour integration is performed one finds a series in terms of $\alpha_s(s)$ (Eq.(7.4)) the convergence of which can be analysed.

A remark must be made that this is not the case in CIPT where the strong coupling is running, i.e. its value must be found by solving the relevant renormalization group equation at each point along the contour. As such, the contour integration in CIPT must be performed numerically and no symbolic series in terms of $\alpha_s(s)$ can be found. Hence, the convergence of PQCD expansion of the correlator function can not be analysed using analytical expressions in CIPT.

This does not, however, preclude one from analyzing the convergence of the quark mass in both FOPT and CIPT by successively including higher order terms of α_s in the correlator function, which is addressed later in this paper (see figures (10) and (14)).

The sum of the quark masses $(\overline{m}_i(s_0) + \overline{m}_j(s_0))$ is determined in FOPT from the FESR, Eq.(2.5), as

$$(\overline{m}_i + \overline{m}_j)^2 = \frac{\delta_5(s_0)|_{\rm HAD}}{\delta_5(s_0)|_{\rm QCD}}\,, \tag{7.1}$$

$$\delta_5(s_0)|_{\rm HAD} = \int_{s_{th}}^{s_0} ds\,\frac{1}{\pi}\,{\rm Im}\,\Psi_5(s)|_{\rm HAD}\,P_5(s)\,, \tag{7.2}$$

$$\delta_5(s_0)|_{\rm QCD} = -\frac{1}{2\pi i}\oint_{C(|s_0|)} ds\,\Pi_5(s)|_{\rm QCD}\,P_5(s)\,, \tag{7.3}$$

where $\Pi_5(s)|_{\rm QCD}$ stands for the correlator with the overall quark mass squared factor removed (Eq.(2.3)), and $P_5(s)$ is an analytic integration kernel (discussed in section (6)). Notice that the dimension d of $\delta_5(s_0)|_{\rm HAD}$ is $d = 6$, while that of $\delta_5(s_0)|_{\rm QCD}$ is $d = 4$.

7.1 Padé Approximants

For the case of the correlator determining the mass of the up and down quark, substituting the PQCD result, as given in Eqs.(3.4 - 3.7) at a typical scale of $s_0 = 3.3\,{\rm GeV}^2$, leads to

$$[\delta_5(s_0)|_{\rm PQCD}]^{-1/2} = 2.42\,\big[\,1 + 2.68\,\alpha_s + 8.63\,\alpha_s^2 + 25.77\,\alpha_s^3 + 71.63\,\alpha_s^4 + \mathcal{O}(\alpha_s^5)\,\big]^{-1/2}\,, \tag{7.4}$$

in units of ${\rm GeV}^{-2}$, and $\alpha_s \equiv \alpha_s(s_0)$.

Using Eqs.(4.1, 11.6) to obtain $\alpha_s(s_0)$, shows that all terms beyond the leading order are roughly of the same size

$$[\delta_5(s_0)|_{\rm PQCD}]^{-1/2} \,=\, 2.42\,\big[\,1 \,+\, 0.85 \,+\, 0.86 \,+\, 0.82 \,+\, 0.72\,\big]^{-1/2}\,. \qquad (7.5)$$

Since the quark mass actually depends on the square-root of δ_5, the relevant power series expansion is instead

$$[\delta_5(s_0)|_{\rm PQCD}]^{-1/2} \,=\, 2.42\,\big[\,1 \,-\, 1.34\,\alpha_s \,-\, 1.62\,\alpha_s^2 \,-\, 1.55\,\alpha_s^3 \,-\, 0.11\,\alpha_s^4 \,+\, \mathcal{O}(\alpha_s^5)\,\big]\,. \quad (7.6)$$

Substituting in $\alpha_s(s_0)$ (found from Eqs.(4.1, 11.6)), Eqs.(7.6) becomes

$$[\delta_5(s_0)|_{\rm PQCD}]^{-1/2} \,=\, 2.42\,\big[\,1 \,-\, 0.42 \,-0.16 \,-\, 0.05 \,-\, 0.001\,\big]\,. \qquad (7.7)$$

While it is not possible to draw conclusions about the convergence of a series by only studying its first four terms, it looks unlikely that the first series (Eq.(7.5)) will be convergent, while there is greater hope that the series will converge after being Taylor expanded (Eq.(7.7)).

In the strange quark case, substituting the PQCD result which includes the $d \,=\, 0$ and $d \,=\, 2$ contributions (Eqs.(3.4 - 3.10)), at a typical scale within the stability window of $s_0 \,=\, 4.2\,{\rm GeV}^2$, leads to

$$[\delta_5(s_0)|_{\rm PQCD}]^{-1/2} \,=\, 2.00\,\big[\,1 \,+\, 3.25\,\alpha_s \,+\, 11.22\,\alpha_s^2 \,+\, 35.93\,\alpha_s^3 \,+\, 106.59\,\alpha_s^4\,\big]^{-1/2}\,, \quad (7.8)$$

in units of ${\rm GeV}^{-2}$, and $\alpha_s \equiv \alpha_s(s_0)$.

The strong coupling $\alpha_s(s_0)$ is obtained using Eqs.(4.1, 11.6). Inserting the value of $\alpha_s(s_0)$ in Eq.(7.8) shows that all terms beyond the leading order are roughly of the same size

$$[\delta_5(s_0)|_{\rm PQCD}]^{-1/2} \,=\, 2.00\,\big[\,1 \,+\, 0.96 \,+\, 0.99 \,+\, 0.93 \,+\, 0.82\,\big]^{-1/2}\,. \qquad (7.9)$$

Expanding the square-root of δ_5 in Eq.(7.8) yields the relevant power series expansion

$$[\delta_5(s_0)|_{\rm PQCD}]^{-1/2} \,=\, 2.00\,\big[\,1 \,-\, 1.63\,\alpha_s \,-\, 1.65\,\alpha_s^2 \,-\, 1.34\,\alpha_s^3 \,+\, 0.88\,\alpha_s^4\,\big]\,. \qquad (7.10)$$

Substituting in $\alpha_s(s_0)$ (found from Eqs.(4.1, 11.6)), Eqs.(7.6) becomes

$$[\delta_5(s_0)|_{\rm PQCD}]^{-1/2} \,=\, 2.00\,\big[\,1 \,-\, 0.48 \,-0.14 \,-\, 0.12 \,+\, 0.01\,\big]\,, \qquad (7.11)$$

which shows a greater hope of being convergent than the first series Eq.(7.9).

Interestingly, the expansions, Eqs.(7.6, 7.10), are examples of a Padé approximant; in this case a [4/0] approximant.

A Padé approximant is defined as a rational function approximation of the form

$$f(z) \approx [m/n] \equiv \frac{a_0 + a_1 z + ... + a_m z^m}{1 + b_1 z + ... + b_n z^n} . \tag{7.12}$$

The order of the Padé approximant is given by k, where $k = m+n$. The simplest form of a Padé approximant, the [m/0] approximant, is the Taylor series expansion of $f(z)$ to the m^{th} order around zero. However, other types of Padé approximants do exist. For example, a third-order Padé approximant of a function $f(x)$ may take the form of the familiar Taylor expansion around zero $f(x) = a_0 + a_1 x + a_2 x^2$, $f(x) = (b_0 + b_1 x + b_2 x^2)^{-1}$ or $f(x) = (c_0 + c_1 x)/(1 + c_2 x)$. The expansion which provides the closest approximation to the function $f(x)$, or displays the best convergence, depends on the analytic properties of $f(x)$. An example depicting this is given in figure (9).

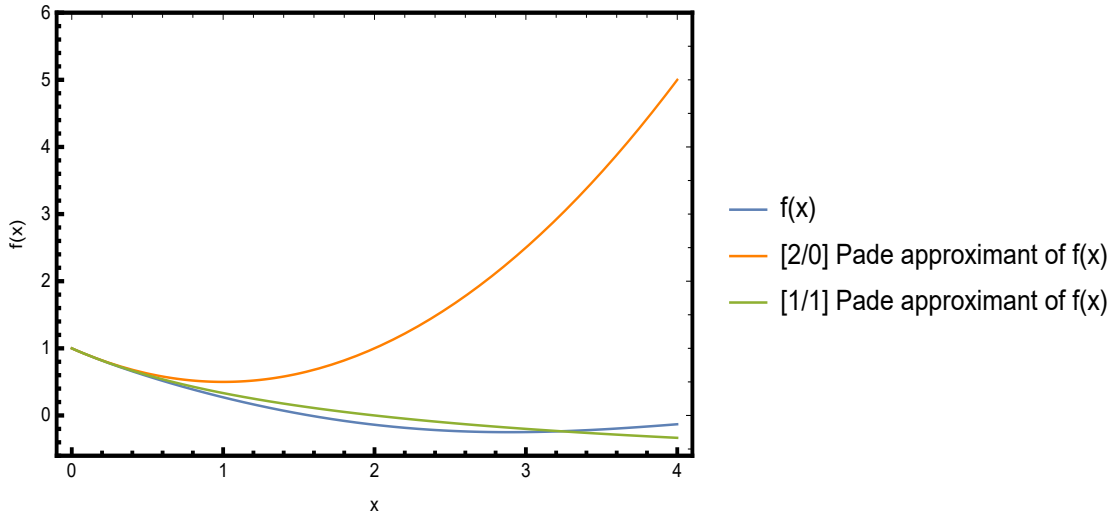

Figure 9: A plot of the function $f(x) = \frac{\cos(x)}{1+x}$, along with the [2/0] Padé approximant $f(x) \approx 1 - x + \frac{x^2}{2}$, and the [1/1] Padé approximant $f(x) \approx (1 - \frac{x}{2})/(1 + \frac{x}{2})$.

Evidently, it is important to choose a Padé approximant that agrees with the function within a given range. As a consequence of this, other types of Padé approximants in examining the convergence of the perturbative QCD series have been tried; but the simple [4/0] Padé approximant (Eqs.(7.6, 7.10)) provides the optimal expansion in this application. While this Padé improvement is unquestionably a positive feature, there remain other unwelcome issues with FOPT. These include a large unfavorable impact on the results for $\overline{m}_{ud}$ and $\overline{m}_s$ from (i) the dependence of the results on the value of s_0, (ii) the estimate of the unknown six-loop contribution, and (iii) the uncertainties in α_s when using Padé approximants. These issues are under much better control in CIPT.

8 Results

In this section the results for the up and down quark masses are presented first. Following this, the results for the strange quark mass are presented. In both cases the results are compared with recent determinations from the literature.

A number of inputs are required before discussing the final results. Firstly, the initial value of the strong coupling is obtained from Eqs.(4.1, 11.6). Next, in the non-perturbative sector a recent determination [55] (earlier determinations are discussed in detail in [5]) provides the value of the gluon condensate in Eq.(3.13)

$$\left\langle a_s \, G^a_{\mu\nu} \, G^{a\,\mu\nu} \right\rangle \, = \, (0.037 \, \pm \, 0.015) \, \mathrm{GeV}^4 \, . \tag{8.1}$$

As previously discussed, the value of the quark condensate $\left\langle \bar{q} \, q \right\rangle$ in Eq.(3.12) is found from the Gell-Mann-Oakes-Renner (GMOR) relation Eq.(3.3), taking note of the chiral corrections to this relation given in [32, 33]. Finally, the strange quark condensate in Eq.(3.14) requires the ratio of strange to non-strange quark condensates, found in [56]

$$\frac{\langle \bar{s} \, s \rangle}{\langle \bar{q} \, q \rangle} \, = \, (0.8 \, \pm \, 0.1) \, . \tag{8.2}$$

These inputs allow us to determine the up, down and strange quark mass. Now on to presenting the results in the case of the up and down quark. Figure (10) shows the convergence of $\overline{m}_{ud}$ in both CIPT and FOPT, plotted by successively including higher order terms of α_s in the peturbative QCD function $\Pi^0_5(q^2)$, Eq.(3.7).

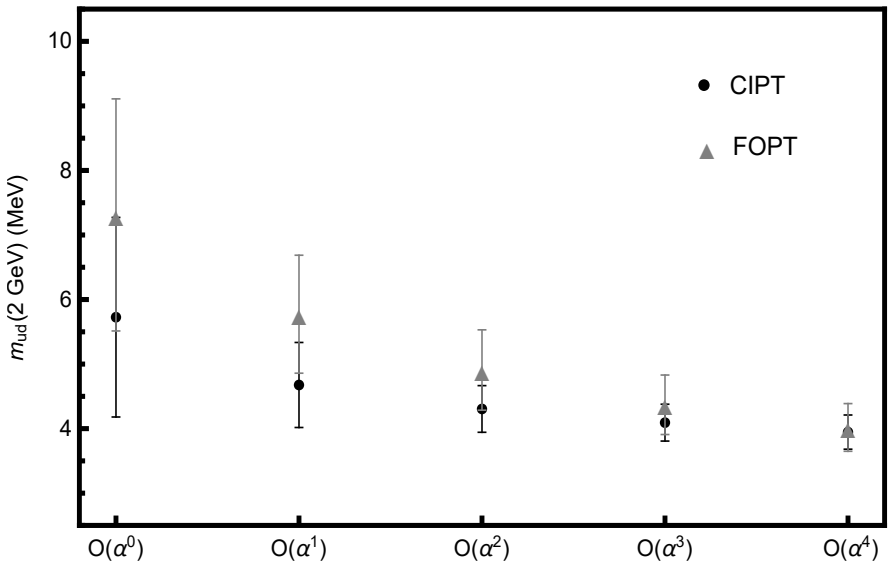

Figure 10: The quark mass $\overline{m}_{ud}(2 \text{ GeV})$ plotted by successively including higher order terms of α_s in the correlator function in both CIPT and FOPT.

The error bars in figure (10) give the total uncertainty of $\overline{m}_{ud}$ at each order in α_s. The various dominant sources of uncertainty are due to (i) the uncertainty in the strong coupling α_s, Eq.(4.1); (ii) the uncertainty in the value of the gluon condensate, Eq.(8.1); (iii)

the range $s_0 = (1.5 - 4.0)\,\mathrm{GeV}^2$; (iv) the uncertainty in the resonance widths and the parameter κ in the hadronic spectral function; and (v) the assumption that the next higher order term of α_s is equal to the previous term. This fifth source of uncertainty is a truncation uncertainty and stems from the terms of $\mathcal{O}(\alpha_s^5)$ and above in the peturbative QCD function $\Pi_5^0(q^2)$ being unknown. The uncertainty in the up and down quark mass from these various sources are added in quadrature, resulting in the total uncertainty for $\overline{m}_{ud}$.

Figure (10) shows that the up and down quark mass converges quicker within the CIPT framework. Therefore, for the up and down quark mass calculated by including all known terms in the correlator function (terms up to and including $\mathcal{O}(\alpha_s^4)$), CIPT places less importance on the unknown higher order terms ($\mathcal{O}(\alpha_s^5)$ and above). The uncertainty caused by the unknown higher order terms is thereby reduced.

Next, an examination of the stability of $\overline{m}_{ud}$ as a function of s_0 from the sum rule Eq.(2.5) (FOPT), and Eq.(4.11) (CIPT). The stability of $\overline{m}_{ud}$ in the region $s_0 \simeq (1.5 - 4.0)\,\mathrm{GeV}^2$ is very similar within the FOPT and CIPT framework. This is shown in figure (11).

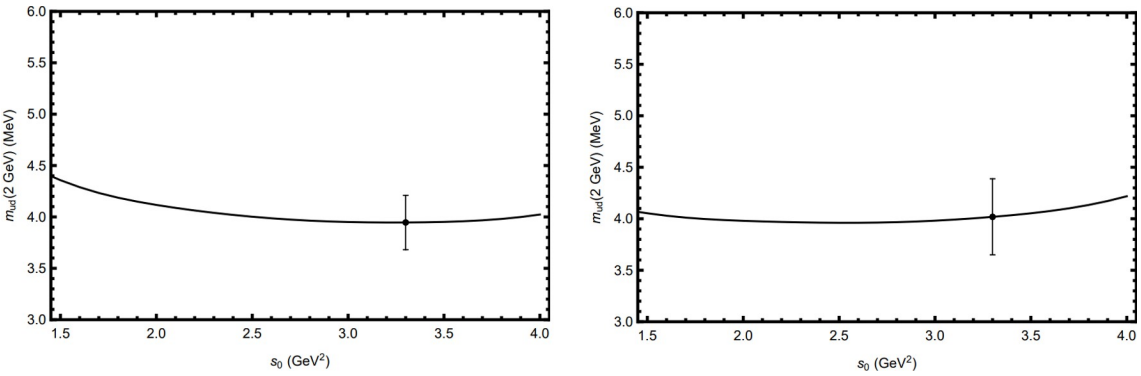

Figure 11: The quark mass $\overline{m}_{ud}(2\ \mathrm{GeV})$ as a function of s_0 within the framework of CIPT (left) and FOPT (right). At a typical point $s_0 = 3.3\,\mathrm{GeV}^2$, $\overline{m}_{ud}$ and its associated total uncertainty (represented as an error bar) is given.

The graphs in figure (11) each include a typical point, $s_0 = 3.3\,\mathrm{GeV}^2$, within the stability region where the error bar for $\overline{m}_{ud}$ is displayed. The error bars represent the total uncertainty of $\overline{m}_{ud}$ calculated from the various sources of uncertainty described after figure (10). Notice that the error bar is larger within the FOPT framework than within the CIPT framework. The quark masses are calculated with a lower overall uncertainty in CIPT – as can be seen from the magnitude of the error bars in figures (10) and (11). The higher uncertainty in FOPT is mainly caused by the importance FOPT places on the unknown higher order terms in the peturbative QCD function $\Pi_5^0(q^2)$.

From figures (10) and (11) one can see that in calculating $\overline{m}_{ud}$ the results from FOPT and CIPT are in agreement. However, based on the two central criteria - convergence and stability - CIPT is the preferred framework for determining $\overline{m}_{ud}$.

The form of the integration kernel $P_5(s)$ still remains to be chosen. The first consideration is the stability of the up and down quark mass under various different integration kernels. Figure (12) shows how $\overline{m}_{ud}(2\ \mathrm{GeV})$ varies over a given energy range depending on the choice of kernel (a) Eq.(6.1), (b) Eq.(6.2), or (c) Eq.(6.3).

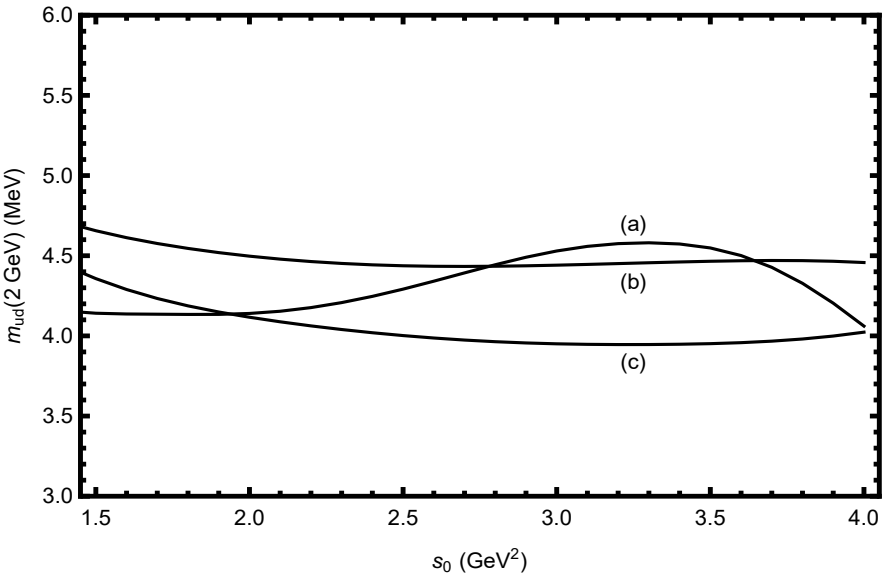

Figure 12: The quark mass $\overline{m}_{ud}(2\text{ GeV})$ as a function of s_0 in CIPT from the FESR Eq.(4.11), where the integration kernel has the form (a) $P_{5\,1}(s) = 1 - a_0\,s - a_1\,s^2$, (b) $P_{5\,2}(s) = (s - m_1^2)\,(s - m_2^2)\,(s - s_0)$ or (c) $P_{5\,3}(s) = (s - c)\,(s - s_0)$.

From figure (12), stability considerations give preference to kernels (b) and (c). Stability is, however, not the only criteria one would take into account when deciding on the optimal choice of kernel. As discussed in section (6), kernels which bring in higher dimensional condensates should be disfavoured since their values are poorly known. Hence, we are averse to kernel (b) since it requires the dimension $d = 8$ condensate to be included in the FESR, which would bring into the calculation an unknown systematic uncertainty. Therefore, this dissertation argues the preferred kernel is (c), which quenches the hadronic resonance contribution at $s = s_0$ as well as halfway between the two pionic resonances.

The final up and down quark mass determination uses the hadronic kernel (c) Eq.(6.3), within the framework of CIPT. Table (1) gives the numerical value and uncertainty break down for $\overline{m}_{ud}(2\,\text{GeV})$.

	$\bar{m}_{ud}(2\,\text{GeV})$ (MeV)	Δ_{α_s}	$\Delta_{\langle G^2\rangle}$	Δ_{s_0}	Δ_{HAD}	$\Delta_{\text{6-loop}}$	Δ_{T}
CIPT	3.946	0.207	0.052	0.017	0.084	0.132	0.265

Table 1: Results for the various uncertainties of $\overline{m}_{ud}(2\,\text{GeV})$ within the CIPT framework, together with the total uncertainty added in quadrature, Δ_T.

The various sources of uncertainty in table (1) have been described in detail after figure (10). Briefly, the uncertainty in the strong coupling (Δ_{α_s}), the uncertainty in the value of the gluon condensate ($\Delta_{\langle G^2\rangle}$), the range s_0 (Δ_{s_0}), the uncertainty in the hadronic spectral function (Δ_{HAD}), and the assumption that the unknown PQCD six-loop contribution is equal to the five-loop one ($\Delta_{\text{6-loop}}$), contribute to the total uncertainty of $\overline{m}_{ud}$.

The error analysis in this determination provides a significant improvement over the error

analysis in [15], the most recent FESR publication which determined the mass of the up and down quark. This previous determination does not consider the source of uncertainty due to the variation of $\overline{m}_{ud}$ in the range s_0. Further, the calculation of the uncertainty in [15] due to the gluon condensate and the hadronic sector are unmotivated – the former being calculated by gauging the effect of multiplying the gluon condensate by a factor of two, while in the latter case a 30% uncertainty is assumed.

Table (1) leads to the result

$$\overline{m}_{ud}|_{\text{CIPT}}(2\,\text{GeV}) \;=\; (3.9 \,\pm\, 0.3)\,\text{MeV}\,, \tag{8.3}$$

to compare with the PDG value [13] $\overline{m}_{ud}|_{\text{PDG}}(2\,\text{GeV}) = (3.5\,^{+0.5}_{-0.2})\,\text{MeV}$, and the FLAG Collaboration result [2] $\overline{m}_{ud}|_{\text{FLAG}}(2\,\text{GeV}) = (3.373 \,\pm\, 0.080)\,\text{MeV}$. A detailed comparison of this dissertation's result Eq.(8.3) compared to previous determinations in the field – both numerical (lattice QCD) and analytical (QCD sum rule) results – is given in figure (13).

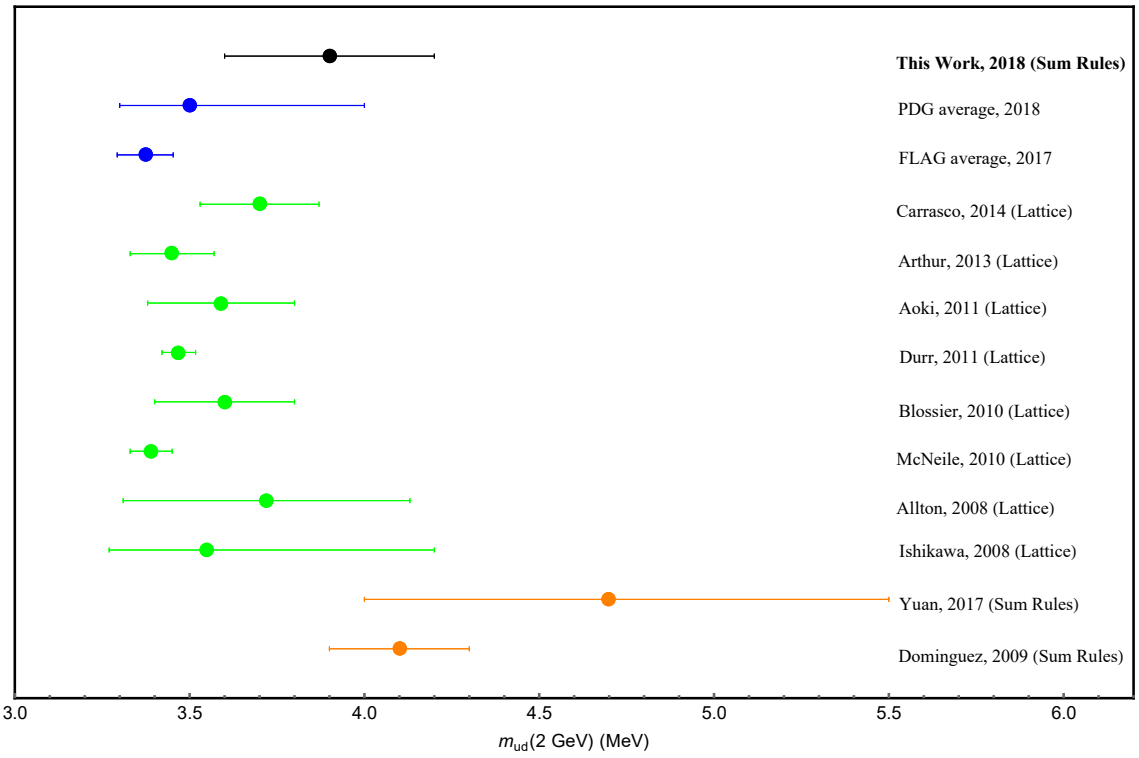

Figure 13: The up and down quark mass obtained in Eq.(8.3) compared to the PDG [13] and FLAG [2] averages, as well as the most recent sum rule results [14, 15] and lattice QCD results [57–64].

There is a trend for lattice QCD determinations to generally yield lower up and down quark mass values than sum rule determinations. Although this is observed, it is not apparent what the cause is. From figure (13) we can see that this determination (Eq.(8.3)) – through its original aspects and various improvements – is in good agreement with the

recent numerical determinations; thereby reducing the existing tension between QCD sum rules and lattice QCD determinations.

In order to disentangle the individual mass values to yield the mass of the up quark and the mass of the down quark separately, one requires as external input the quark mass ratio m_u/m_d. Using the recent PDG value [13]

$$\frac{m_u}{m_d} = 0.48^{+\,0.7}_{-\,0.8}\,, \tag{8.4}$$

results in

$$\overline{m}_u(2\,\mathrm{GeV}) \;=\; (2.6 \,\pm\, 0.4)\,\mathrm{MeV}\,, \tag{8.5}$$

and

$$\overline{m}_d(2\,\mathrm{GeV}) \;=\; (5.3 \,\pm\, 0.4)\,\mathrm{MeV}\,, \tag{8.6}$$

to be compared with the PDG values [13]: $\overline{m}_u\,(2\,\mathrm{GeV}) = (2.2^{+0.5}_{-0.4})$ MeV, and $\overline{m}_d\,(2\,\mathrm{GeV}) = (4.7^{+0.5}_{-0.3})$ MeV; and with the FLAG Collaboration results [2]: $\overline{m}_u\,(2\,\mathrm{GeV}) = (2.16 \pm 0.09 \pm 0.07)$ MeV, and $\overline{m}_d\,(2\,\mathrm{GeV}) = (4.68 \,\pm\, 0.14 \,\pm\, 0.07)$ MeV.

Next are the results for the strange quark mass determination. Similar to figure (10) is figure (14), where one can examine the convergence of $\overline{m}_s$ in the framework of both FOPT and CIPT by successively including higher order terms of α_s in the peturbative QCD function $\Pi^0_5(q^2)$, Eq.(3.7).

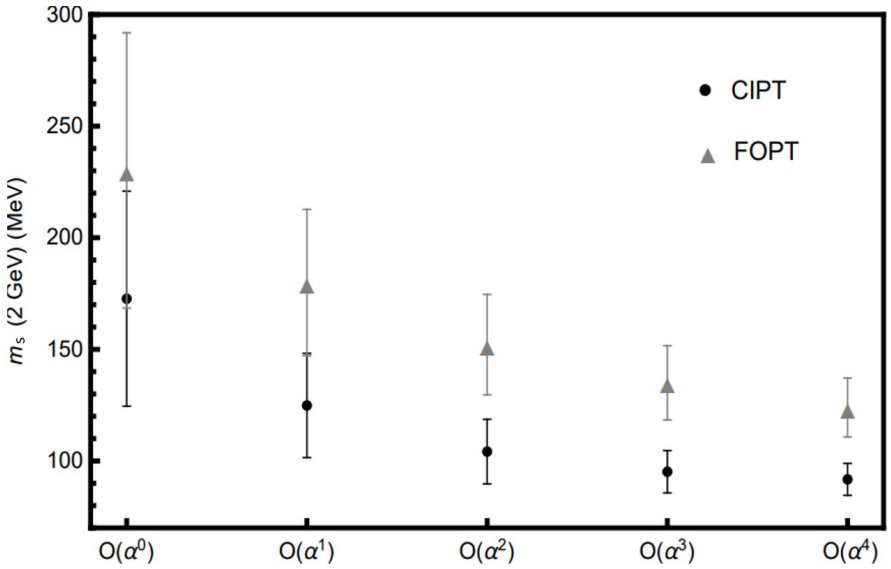

Figure 14: The quark mass $\overline{m}_s(2\ \mathrm{GeV})$ plotted by successively including higher order terms of α_s in the correlator function in both CIPT and FOPT.

The error bars in figure (14) give the total uncertainty of $\overline{m}_s$ at each order in α_s. As in the up and down quark mass uncertainty analysis, the various dominant sources of uncertainty

are due to (i) the uncertainty in the strong coupling α_s, Eq.(4.1); (ii) the uncertainty in the value of the gluon condensate, Eq.(8.1); (iii) the range $s_0 = (3.0 - 5.0)\,\mathrm{GeV}^2$; (iv) the uncertainty in the resonance widths and the parameter λ in the hadronic spectral function; and (v) the assumption that the next higher order term of α_s is equal to the previous term. These uncertainties are added in quadrature, resulting in the total uncertainty for $\overline{m}_s$. One can argue that there is an additional error in the strange quark determination stemming from the disagreement between the results in the frameworks of FOPT and CIPT. This uncertainty, however, has not been taken into account in this analysis since the final result for the strange quark mass is not the average $\overline{m}_s$ determined in both frameworks. The framework of FOPT or CIPT is chosen after considering how the strange quark mass behaves in terms of convergence and stability within each framework.

From figure (14) we see that, although the difference in convergence between the FOPT and CIPT framework is not as pronounced as in the case of $\overline{m}_{ud}$ (figure (10)), the strange quark mass converges quicker within the CIPT framework. In CIPT the strange quark mass changes between the $\mathcal{O}(\alpha_s^0)$ calculation and the $\mathcal{O}(\alpha_s^4)$ calculation by 81 MeV, whereas in FOPT the quark mass changes between the $\mathcal{O}(\alpha_s^0)$ calculation and the $\mathcal{O}(\alpha_s^4)$ calculation by 106 MeV. This dissertation concludes that less importance is placed on the unknown higher order terms in the peturbative QCD function $\Pi_5^0(q^2)$ within the CIPT framework.

Examining the stability of $\overline{m}_s$ as a function of s_0 from the sum rule Eq.(2.5) (FOPT), and Eq.(4.11) (CIPT), it is clear that strange quark mass behaves better within the CIPT framework compared to in the FOPT framework. The stability of $\overline{m}_s$ in the region $s_0 \simeq (3.0 - 5.0)\,\mathrm{GeV}^2$ is shown in figure (15).

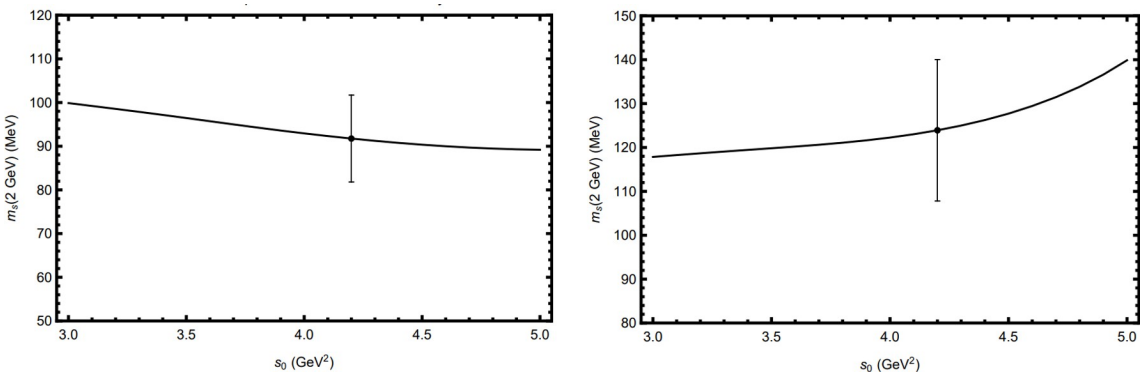

Figure 15: The quark mass $\overline{m}_s(2\ \mathrm{GeV})$ as a function of s_0 within the framework of CIPT (left) and FOPT (right). At a typical point $s_0 = 4.2\,\mathrm{GeV}^2$, $\overline{m}_s$ and its associated total uncertainty (represented as an error bar) is given.

The graphs in figure (15) each include a typical point, $s_0 = 4.2\,\mathrm{GeV}^2$, within the stability region where the error bar for $\overline{m}_s$, representing the total uncertainty, is displayed. Since FOPT places a greater importance on the unknown higher order terms in the peturbative QCD function $\Pi_5^0(q^2)$, the total uncertainty for $\overline{m}_s$ in FOPT is far larger than the total uncertainty for $\overline{m}_s$ in CIPT.

From figures (14) and (15), the conclusion based on the criteria of convergence and stability, is that CIPT is the preferred framework for determining $\overline{m}_s$.

The suitability of various integration kernels $P_5(s)$ is now investigated. Figure (16) depicts how $\overline{m}_s(2\text{ GeV})$ varies over a given energy range depending on the choice of kernel (a) Eq.(6.3), (b) Eq.(6.1), or (c) Eq.(6.2).

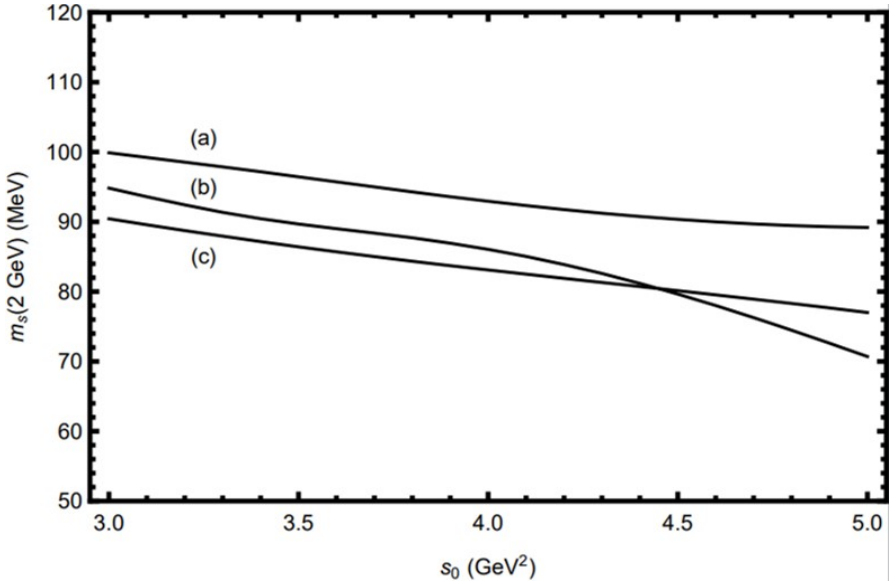

Figure 16: The quark mass $\overline{m}_s(2\text{ GeV})$ as a function of s_0 in CIPT from the FESR Eq.(4.11), where the integration kernel has the form (a) $P_{5\,3}(s) = (s - c)\,(s - s_0)$, (b) $P_{5\,1}(s) = 1 - a_0\,s - a_1\,s^2$ or (c) $P_{5\,2}(s) = (s - m_1^2)\,(s - m_2^2)\,(s - s_0)$.

From figure (16), the stability of the up and down quark mass under various different integration kernels can be examined. Kernels (a) and (c) lead to more stable $\overline{m}_s(s)$ results; however none of these kernels lead to compellingly stable results. Kernel (a) is chosen as the optimal kernel, since it does not introduce higher dimensional condensates into the FESR. The stability of $\overline{m}_s$ is taken into consideration when calculating the final uncertainty; but, it is hoped that future work built upon this determination will aim to improve the stability of the strange quark mass determination.

The final strange quark mass determination uses the hadronic kernel (a) Eq.(6.3), within the framework of CIPT. Since the sum rule (Eqs.(2.5),(4.11)) yields $(\overline{m}_s + \overline{m}_{ud})$ in the case of the strange quark, in order to disentangle the individual mass values one requires as external input the quark mass ratio m_s/m_{ud}. The recent PDG value [13] suffices

$$\frac{m_s}{m_{ud}} \,=\, 27.3 \,\pm\, 0.7\,, \tag{8.7}$$

where $m_{ud} \equiv (m_u \,+\, m_d)/2$.

This leads to

$$\overline{m}_s|_{\rm CIPT}(2\,{\rm GeV}) \,=\, (91.8 \,\pm\, 9.9)\,{\rm MeV}\,. \tag{8.8}$$

The total uncertainty for $\overline{m}_s(2\,\text{GeV})$ given in Eq.(8.8) is due to various different sources. The break down of these uncertainties is shown in table (2). A general description of each

uncertainty can be found after table (1), and specifically for the strange quark mass after figure (14).

	$\bar{m}_s(2\,\mathrm{GeV})$ (MeV)	Δ_{α_s}	$\Delta_{\langle G^2\rangle}$	Δ_{s_0}	Δ_{HAD}	$\Delta_{\text{6-loop}}$	Δ_{T}
CIPT	91.753	3.901	0.749	2.650	8.159	3.064	9.938

Table 2: Results for the various uncertainties of $\overline{m}_s(2\,\mathrm{GeV})$ within the CIPT framework, together with the total uncertainty added in quadrature, Δ_T.

The PDG average [13] $\overline{m}_s|_{\mathrm{PDG}}(2\,\mathrm{GeV}) = (95\,^{+9}_{-3})\,\mathrm{MeV}$, and the FLAG Collaboration average [2] $\overline{m}_s|_{\mathrm{FLAG}}(2\,\mathrm{GeV}) = (92.0 \pm 2.1)\,\mathrm{MeV}$ can be compared with this dissertation's result for the strange quark mass. Figure (17) gives a detailed comparison of this dissertation's result, Eq.(8.8), compared to previous numerical and analytical determinations in the field. Here, the determination in Eq.(8.8) is in good agreement with most recent results in the literature.

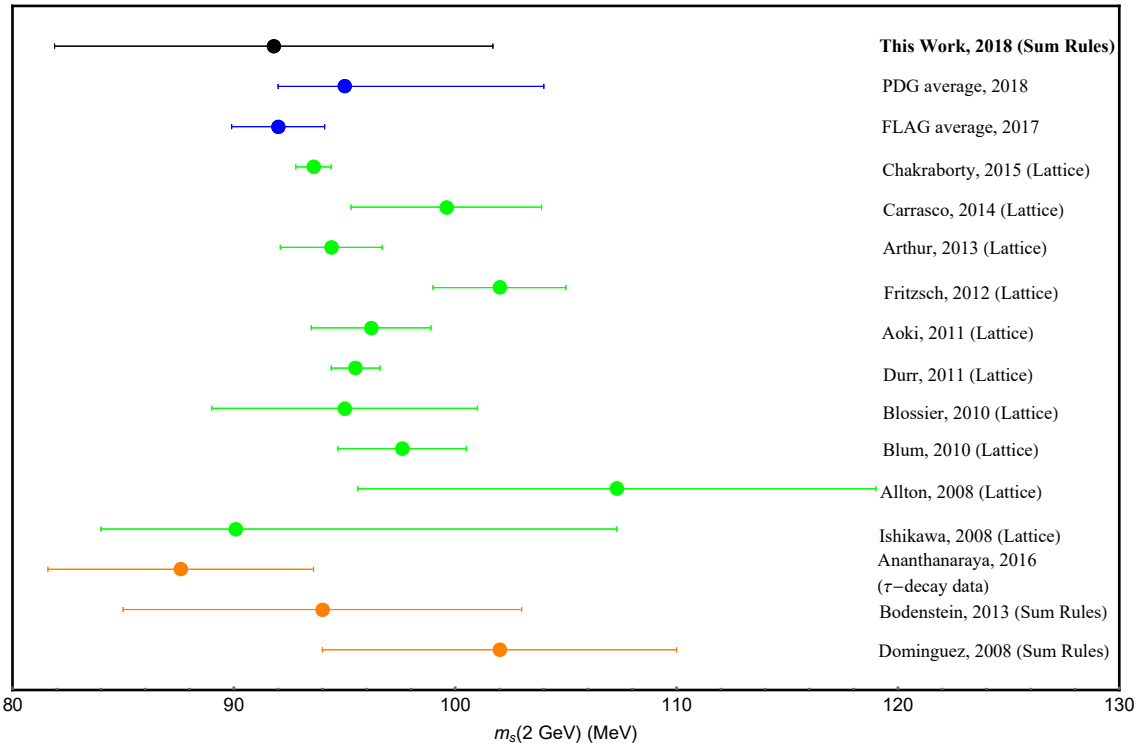

Figure 17: The strange quark mass obtained in Eq.(8.8) compared to the PDG [13] and FLAG [2] averages, as well as the most recent analytical results [16–18] (the Ananthanarayan et al. determination extracts the strange quark from τ-decay spectral moments using renormalization techniques, while the latter two are sum rule determinations) and lattice QCD results [57–61, 63–67].

Figures (10) and (11) also appear in the publication [68] that resulted from the work in this dissertation.

Part II
Regularization and Renormalization

There are two types of singularities in perturbative QCD: ultraviolet (UV) singularities and infrared (IR) singularities. The former divergences occur in the high momentum limit, while the latter occur in the low momentum limit [28]. Singularities are handled in quantum field theory through regularization and renormalization. These two related, but independent techniques are used in order to obtain finite and meaningful results from expressions containing divergences. Regularization introduces the concept of a regulator parameter to deal with divergent integrals. The regulator ϵ, the minimal space distance, is introduced in regularizing UV divergences since they are short-distance effects. The result will frequently contain terms $\propto \frac{1}{\epsilon}$ which are not well defined in the limit of the vanishing regulator ($\epsilon \to 0$). Hence, the renormalization technique follows regularization. A fundamental requirement of renormalization is that there exists observed values equal to some physical quantities that are expressed by seemingly divergent expressions (e.g. the $\frac{1}{\epsilon}$ terms). Renormalization removes these ultraviolet divergences in the theory by absorbing these divergences into the parameters of the Lagrangian. This is done through calculating subtraction terms and defining Z coefficients which multiply the terms of the Lagrangian. Regularization and renormalization enable us to calculate finite values for many quantities that appear divergent.

9 The QCD Renormalized Coupling Constant

This section outlines the method used to calculate the renormalized coupling constant of QCD (g_R) to lowest order. The $\beta(a_s)$ function is then defined as the derivative of the coupling constant with respect to some renormalization scale parameter μ and the first β coefficient β_0 (Eq.(9.25)) is derived.

There are three types of UV divergences in the QCD Feynman diagrams at one loop that contribute to the renormalization of the coupling constant. Namely:

(i) The vacuum polarization diagrams of QCD. The diagrams (A I) – (A IV) contribute to the lowest order renormalization of the coupling constant [6].

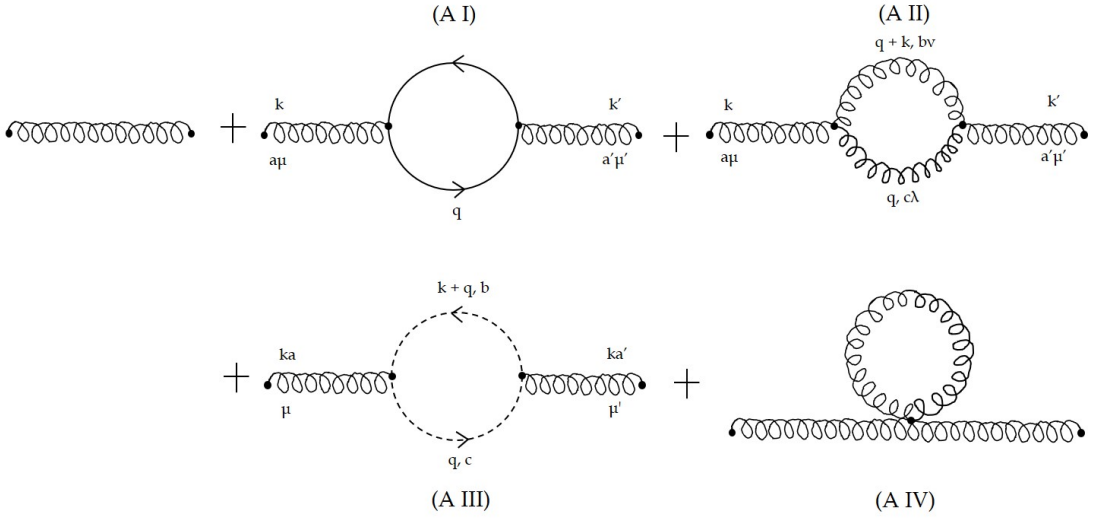

(ii) The self energy diagrams of QCD. The (B I) diagram contributes to the lowest order renormalization of the coupling constant [6].

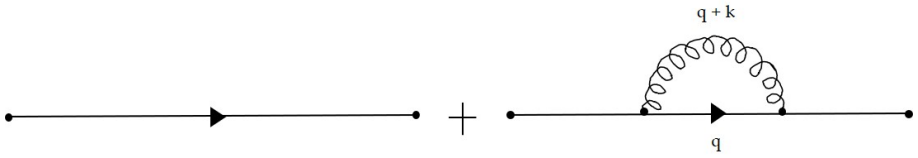

(B I)

(iii) The vertex correction diagrams of QCD. The diagrams (C I) and (C III) contribute to the lowest order renormalization of the coupling constant [6].

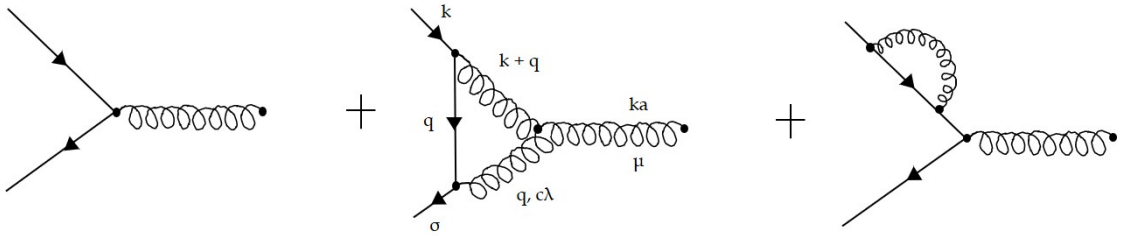

(C I)

(C II)

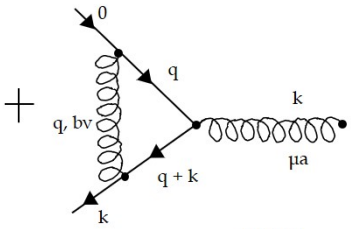

(C III)

In order to calculate the vertex correction diagrams we choose a specific configuration of the momenta, where zero momentum has been assigned to the incoming antiquark and a momentum k has been assigned to the outgoing antiquark. The particular Lorentz frame where the momenta are thus configured simplifies the calculations while the divergent terms remain unchanged, since the renormalization constants for the coupling constants, masses and wave functions are constants and thus do not depend on the momenta.

Further, note that the diagrams contributing to the one loop ghost-gluon vertex renormalization are not present. This calculation does include the lowest order ghost loop contribution, diagram (A III). These ghost fields, known as Fadeev-Popov ghost fields, are constructed to cancel the degrees of freedom of the gluon field that are unphysical, i.e. without the ghost terms gauge invariance can not be restored.

We begin by calculating the four vacuum polarization diagrams (A I) – (A IV). The method is broadly outlined below. For full details, see [6].

Diagram (A I): The Feynman rules can be used to write down the vacuum polarization tensor

$$\Pi^{aa'\,(\mathrm{A\,I})}_{\mu\mu'}(k) \;=\; \sum_{i=1}^{n_f} g_0^2 \int \frac{d^4q}{(2\pi)^4} \;\times\; \mathrm{tr}\left\{ \frac{\lambda^a}{2}\frac{\lambda^{a'}}{2}\, \frac{\not{q} \;+\; \not{k} \;+\; m_i}{(q+k)^2 \;-\; m_i^2 \;+\; i\eta}\, \gamma_\mu\, \frac{\not{q} \;+\; m_i}{q^2 \;-\; m_i^2 \;+\; i\eta}\, \gamma_{\mu'} \right\}, \tag{9.1}$$

where a and a' are colour indexes and λ are the Gell-Mann matrices [10]. The trace of their product gives rise to colour-factors C_F [13]. In Eq.(9.1)

$$\mathrm{tr}\left\{ \frac{\lambda^a}{2}\frac{\lambda^{a'}}{2} \right\} \;=\; \delta_{a\,a'}\,\frac{1}{2}\,, \tag{9.2}$$

where $C_3 \;=\; 1/2$ is the colour-factor due to a gluon splitting into a quark-antiquark pair [13].

For simplicity we work in the massless limit, setting $m_i \;=\; 0$ whenever this will not lead to infrared divergences. In order to simplify Eq.(9.1) we use a Feynman parameter integral to bring the product of two momentum-dependent denominators into a simpler form which allows us to perform the momentum integration

$$\frac{1}{(q+k)^2 \;-\; m_i^2 \;+\; i\eta}\,\frac{1}{q^2 \;-\; m_i^2 \;+\; i\eta} \;=\; \int_0^1 dz\, \frac{1}{((q+kz)^2 + k^2 z(1-z) \;-\; m_i^2 \;+\; i\eta)^2}\,. \tag{9.3}$$

Next, the linear term in the denominator is removed by performing the substitution $q_\mu \;\to\; q'_\mu = q_\mu - k_\mu z$, and the trace is taken. Terms proportional to odd powers of q are neglected, which can be seen from making the substitution $q_\nu \;\to\; -q_\nu$. By the same reasoning, only the diagonal terms will contribute when integrating over the even powers of q

$$\int d^4q\, q_\mu\, q_\nu f(q^2) \;=\; \frac{1}{4}\int d^4q\, g_{\mu\nu}\, q^2\, f(q^2)\,. \tag{9.4}$$

Finally, we continue the momentum integral to Euclidean space ($q_\mu \;\to\; \tilde{q}_\mu = (iq^0, \mathbf{q})$), and generalize to a d-dimensional integral which we perform. Notice that since the remaining expression is infrared safe the left over terms proportional to the quark mass can be neglected. This leaves us with

$$\Pi^{aa'\,(\mathrm{A\,I})}_{\mu\mu'}(k) \;=\; i\left(g_{\mu\mu'}\,k^2 \;-\; k_\mu k_{\mu'}\right)\frac{g_0^2}{16\,\pi^2}\,\frac{2\,n_f}{3}\left[\frac{1}{\epsilon} \;-\; \ln\left(\frac{-k^2}{h^2}\right) \;+\; \mathrm{const}\right], \tag{9.5}$$

where n_f is the number of active quark flavours, and the quantity h was introduced from dimensional arguments when we extended the integral to d-dimensions in order to ensure the total dimension of the expression was unchanged. Eq.(9.5) is the contribution of diagram (A I) to the vacuum polarization divergence in the QCD Feynman diagrams.

Diagram (A II): Using the three-gluon vertex Feynman rule twice, we write down the vacuum polarization tensor

$$\begin{aligned}\Pi^{aa'\,(\mathrm{A\,II})}_{\mu\mu'}(k) \;=\; g_0^2\,\frac{1}{2}\int\frac{d^4k}{(2\pi)^4}\Bigg\{ & f^{abc}\Big(g_{\mu\lambda}(k-q)_\nu \;+\; g_{\nu\mu}(-q-2k)_\lambda \;+\; g_{\lambda\nu}(q+q+k)_\mu\Big)\\ & \times\; f_{a'bc}\Big(g^\lambda_{\mu'}(-k+q)^\nu \;+\; g^\nu_{\mu'}(q+2k)^\lambda \;+\; g^{\nu\lambda}(-2q-k)_{\mu'}\Big)\\ & \times\; \frac{1}{(q+k)^2\;+\;i\eta}\,\frac{1}{q^2\;+\;i\eta}\Bigg\},\end{aligned} \tag{9.6}$$

where f^{abc} are the SU(3) group structure constants which are related to the Gell-Mann matrices, and the factor $1/2$ is the symmetry factor. The symmetry factor is calculated by counting the number of ways the components in a Feynman diagram can be interchanged without changing the diagram. The combinatorics behind the calculation of these factors is explained extensively in [6, 28].

We simplify the numerator of vacuum polarization tensor by using

$$f^{abc}f^{a'bc} \;=\; \delta_{aa'}\,C_2 \;=\; \delta_{aa'}\,N \quad \text{for SU(N)}\,, \tag{9.7}$$

where $C_2 \equiv N_c = 3$ is the colour-factor due to a gluon emission from a gluon, and N is the number of dimensions in the group.

Now, noticing that this equation is similar to Eq.(9.1), we follow the same procedure as we followed for diagram (A I). Again we make use of Feynman parametrization Eq.(9.3), and substitute $q_\mu \to q'_\mu = q_\mu - k_\mu z$. Next, we continue the integral to Euclidean space ($q_\mu \to \tilde{q}_\mu = (iq^0, \mathbf{q})$), and perform the d-dimensional integral.

Finally, this yields

$$\Pi^{aa'\,(\mathrm{A\,II})}_{\mu\mu'}(k) \;=\; i\Big(-19\,g_{\mu\mu'}\,k^2 \;+\; 22\,k_\mu k_{\mu'}\Big)\,\frac{g_0^2\,\delta_{aa'}}{16\pi^2}\,\frac{C_2}{12}\left[\frac{1}{\epsilon} \;-\; \ln\left(\frac{-k^2}{h^2}\right) \;+\; \text{const}\right], \tag{9.8}$$

which is the contribution of diagram (A II) to the vacuum polarization divergence in the QCD Feynman diagrams. It is worth noting that although the gauge is fixed in this derivation, the vacuum polarization tensor Eq.(9.6) is not gauge invariant ($k^\mu\,\Pi^{aa'\,(\mathrm{A\,II})}_{\mu\mu'}(k) \neq 0$). Gauge invariance can not be restored without the ghost fields, whose one loop contribution is calculated in the following diagram (A III).

Diagram (A III): The vacuum polarization tensor of the ghost contribution is

$$\Pi^{aa'\,(\mathrm{A\,III})}_{\mu\mu'}(k) \;=\; -\,g_0^2\,f^{abc}\,f^{a'cb}\int\frac{d^4q}{(2\pi)^4}\,q_{\mu'}\,\frac{1}{(q^2\;+\;i\eta)}\,(k+q)_\mu\,\frac{1}{((q+k)^2\;+\;i\eta)}\,, \tag{9.9}$$

where the order of the colour indices on the structure constants f^{abc} and $f^{a'cb}$ is: gluon, outgoing ghost and incoming ghost [6]; and the negative sign is due to the anticommutativity property of ghost fields.

Using the same method of introducing a Feynman parameter integral Eq.(9.3), performing the variable shift $q_\mu \rightarrow q'_\mu = q_\mu - k_\mu z$, introducing the Euclidean coordinates ($\tilde{q}_\mu = (iq^0, \mathbf{q})$), and calculating the d-dimensional integral, results in

$$\Pi^{aa'\,(\mathrm{A\,III})}_{\mu\mu'}(k) \,=\, i\Big(\,-\,g_{\mu\mu'}\,k^2\,-\,2\,k_\mu k_{\mu'}\Big)\,\frac{g_0^2\,\delta_{aa'}}{16\pi^2}\,\frac{C_2}{12}\left[\frac{1}{\epsilon}\,-\,\ln\left(\frac{-k^2}{h^2}\right)\,+\,\mathrm{const}\right], \quad (9.10)$$

which is the contribution of diagram (A III) to the vacuum polarization divergence in the QCD Feynman diagrams.

Notably the sum of the gluon and ghost vacuum polarization diagrams

$$\Pi^{aa'\,(\mathrm{A\,II})}_{\mu\mu'}(k) + \Pi^{aa'\,(\mathrm{A\,III})}_{\mu\mu'}(k) \,=\, i\left(k_\mu k_{\mu'} - g_{\mu\mu'}\,k^2\right)\frac{g_0^2\,\delta_{aa'}}{16\pi^2}\,\frac{20\,C_2}{12}\left[\frac{1}{\epsilon} - \ln\left(\frac{-k^2}{h^2}\right) + \mathrm{const}\right] \quad (9.11)$$

is transverse.

Diagram (A IV): The vacuum polarization tensor of the four gluon vertex diagram is zero

$$\Pi^{aa'\,(\mathrm{A\,IV})}_{\mu\mu'}(k) \,=\, 0\,. \quad (9.12)$$

This is because the gluon bubble is proportional to $\frac{1}{q^2}$ (since there is no external momentum), and in pure dimensional regularization

$$\int d^dq\,\frac{1}{q^2} \,=\, 0\,. \quad (9.13)$$

In theory, the vacuum polarization tensor $\Pi^{aa'\,(\mathrm{A\,IV})}_{\mu\mu'}(k)$ would have a non-zero contribution if we imposed an infrared cutoff. The vacuum polarization tensor would then diverge quadratically and logarithmically in the ultraviolet region. However for the purpose of this derivation we consider the case of pure dimensional regularization[3].

Adding up the contributions from diagrams (A I) - (A III) (Eqs. (9.5, 9.11)), we get the contribution to the renormalization of the coupling constant due to the vacuum polarization divergences

[3]First proposed by G. 't Hooft and M. Veltman in [69].

$$
\begin{aligned}
&\Pi_{\mu\mu'}^{aa'\,(\mathrm{A\,I})}(k) \,+\, \Pi_{\mu\mu'}^{aa'\,(\mathrm{A\,II})}(k) \,+\, \Pi_{\mu\mu'}^{aa'\,(\mathrm{A\,III})}(k) \\
&= i\left(k_\mu k_\nu \,-\, g_{\mu\nu}\,k^2\right)\frac{g_0^2}{16\pi^2}\left(\frac{20}{12}\,C_2 \,-\, \frac{2}{3}\,n_f\right)\left[\frac{1}{\epsilon} \,-\, \ln\left(\frac{-k^2}{h^2}\right)\right] \\
&\equiv i\left(k_\mu k_\nu \,-\, g_{\mu\nu}\,k^2\right)Z^a\,,
\end{aligned}
\tag{9.14}
$$

where Z^a is the vacuum polarization divergent factor which we will need in the renormalization process.

Diagram (B I): Next, the contribution from the self-energy diagram is calculated. From the Feynman rules we write down

$$
\Sigma^b(k) \,=\, g_0^2\,\frac{1}{3}\int\frac{d^4q}{(2\pi)^4}\,\gamma_\mu\,\frac{\not{q}}{q^2\,+\,i\eta}\,\gamma^\mu\,\frac{1}{(q+k)^2\,+\,i\eta}\,\mathrm{tr}\Big(\frac{\lambda_a}{2}\,\frac{\lambda_a}{2}\Big)\,, \tag{9.15}
$$

where the inserted factor of $1/3$ counteracts the fact that we have average over all 3 quarks.

We simplify the numerator in Eq.(9.3) using $\gamma_\mu \not{q} \gamma^\mu = \gamma_\mu q_\nu \gamma^\nu \gamma^\mu = q_\nu \gamma_\mu (\,2g^{\mu\nu} - \gamma^\mu\gamma^\nu\,)$ $= 2\not{q} - \gamma_\mu\gamma^\mu\not{q} \,=\, 2\not{q} - 4\not{q} = -2\not{q}$; and follow the increasingly familiar steps of Feynman parameterization Eq.(9.3), performing the substitution $q_\mu \,\to\, q'_\mu = q_\mu - k_\mu z$, introducing Euclidean coordinates and extending the integral to d-dimensions.

Hence, the contribution to the renormalization of the coupling constant due to the self-energy divergences is

$$
\begin{aligned}
\Sigma^b(k) \,&=\, i\not{k}\,\frac{g_0^2}{16\pi^2}\,\frac{4}{3}\left[\frac{1}{\epsilon} \,-\, \ln\left(\frac{-k^2}{h^2}\right) \,+\, \mathrm{const}\right] \\
&\equiv\, i\not{k}\,Z^b\,,
\end{aligned}
\tag{9.16}
$$

where Z^b is the divergent factor due to the self-energy graphs which we will need in the renormalization process.

Finally, we calculate the vertex correction diagrams (C I) and (C III).

Diagram (C I): Using the Feynman rules in the massless limit ($m \,\to\, 0$) we write down

$$
\begin{aligned}
\Gamma_\mu^{a\,(\mathrm{C\,I})} \,&=\, -i\,g_0^3\int\frac{d^4q}{(2\pi)^4}\left\{f^{abc}\left(g_{\mu\lambda}(k-q)_\nu \,+\, g_{\nu\mu}(-q-2k)_\lambda \,+\, g_{\lambda\nu}(2q+k)_\mu\right)\right. \\
&\left.\times\,\frac{\lambda^b}{2}\,\frac{\lambda^c}{2}\,\gamma^\nu\not{q}\gamma^\lambda\,\frac{1}{\left(q^2\,+\,i\eta\right)^2}\,\frac{1}{\left((q+k)^2\,+\,i\eta\right)}\right\},
\end{aligned}
\tag{9.17}
$$

where Γ^a_μ corrects the bare vertex $\gamma_\mu \lambda^a/2$. Remember that a Lorentz frame with a specific configuration of the momenta where zero momentum has been assigned to the incoming antiquark and a momentum k has been assigned to the outgoing antiquark, is chosen in order to simplify the vertex correction calculations.

We use $-if^{abc}\,\frac{\lambda^b}{2}\,\frac{\lambda^c}{2} = -\frac{i}{2}f^{abc}\,[\frac{\lambda^b}{2}\,,\,\frac{\lambda^c}{2}] = \frac{1}{2}f^{abc}f^{dbc}\,\frac{\lambda^d}{2} = N\frac{\delta_{ad}}{2}\frac{\lambda^d}{2} \equiv \frac{C_2}{2}\frac{\lambda^a}{2}$ to simplify Eq.(9.17); and repeat the procedure of introducing a Feynman parameter integral Eq.(9.3), shifting the variables $q_\mu \rightarrow q'_\mu = q_\mu - k_\mu z$, introducing Euclidean coordinates and performing the d-dimensional integral. This yields

$$\Gamma^{a\,(\mathrm{C\,I})}_\mu = i\,g_0\,\frac{\lambda^a}{2}\,\gamma_\mu\,\frac{g_0^2}{16\pi^2}\,\frac{3\,C_2}{2}\left[\frac{1}{\epsilon} - \ln\left(\frac{-k^2}{h^2}\right) + \text{finite terms}\right], \tag{9.18}$$

where only the divergent terms are written out explicitly (the finite terms do not affect the renormalization procedure). Eq.(9.18) is the contribution of the vertex correction diagram (C I) in calculating the renormalized quark-gluon vertex.

Diagram (C III): Again, writing down the Feynman rules in the massless limit ($m_i \rightarrow 0$) for the next vertex correction diagram, gives

$$\Gamma^{a\,(\mathrm{C\,III})}_\mu = g_0^3 \int \frac{d^4q}{(2\pi)^4}\,\frac{\lambda^b}{2}\,\gamma^\lambda\,\frac{\lambda^a}{2}\,(\not{q}+\not{k})\,\gamma_\mu\,\not{q}\,\frac{\lambda^b}{2}\,\gamma_\lambda\,\frac{1}{\left(q^2 + i\eta\right)^2}\,\frac{1}{\left((q+k)^2 + i\eta\right)}\,. \tag{9.19}$$

Choosing the same specific configuration of the momenta, and following the same integration method as in diagram (C I), yields

$$\Gamma^{a\,(\mathrm{C\,III})}_\mu = i\,g_0\,\frac{\lambda^a}{2}\,\gamma_\mu\,\frac{g_0^2}{16\pi^2}\left(\frac{4}{3} - \frac{C_2}{2}\right)\left[\frac{1}{\epsilon} - \ln\left(\frac{-k^2}{h^2}\right) + \text{finite terms}\right], \tag{9.20}$$

which is the contribution of the vertex correction diagram (C III) in calculating the renormalized quark-gluon vertex.

The sum of diagrams (C I) and (C III) is

$$\begin{aligned}\Gamma^{a\,(\mathrm{C\,I})}_\mu + \Gamma^{a\,(\mathrm{C\,III})}_\mu &= i\,g_0\,\frac{\lambda^a}{2}\,\gamma_\mu\,\frac{g_0^2}{16\pi^2}\left[\frac{1}{\epsilon} - \ln\left(\frac{-k^2}{h^2}\right) + \text{finite terms}\right]\left(\frac{4}{3} - \frac{C_2}{2} + \frac{3\,C_2}{2}\right) \\ &\equiv i\,g_0\,\frac{\lambda^a}{2}\,\gamma_\mu\,Z^c\,,\end{aligned} \tag{9.21}$$

where Z^c is the divergent factor due to the vertex correction graphs which we will need in the renormalization process.

Having calculated the renormalization constants Z^a (Eq.(9.14)), Z^b (Eq.(9.16)) and Z^c (Eq.(9.21)), we can proceed with renormalizing the coupling constant. The contributions from the vacuum polarization, self energy, and vertex corrections combine to give the renormalized quark-gluon vertex. Figure (18) demonstrates that half the correction to the gluon propagator Z^a, the full vertex correction Z^c, and two times half of the self-energy correction Z^b due to 'gluon boomerangs', is required to form the renormalized quark-gluon vertex.

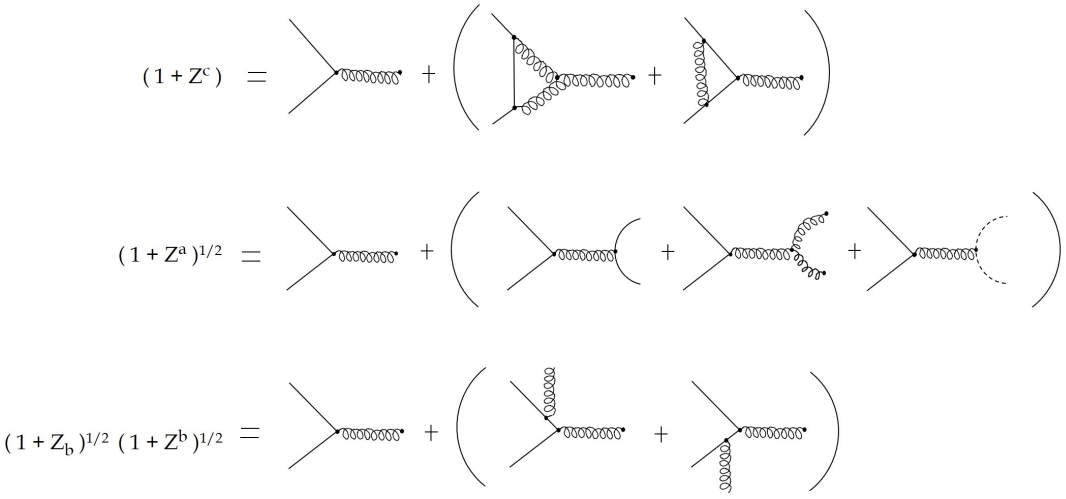

Figure 18: Diagrammatic depiction of the terms contributing to the renormalized quark-gluon vertex.

Adding up the contributions depicted in figure (18), results in the total vertex

$$\begin{aligned}
\Gamma_\mu^{a\,(\mathrm{TOTAL})} &= -\frac{\lambda^a}{2}\, g_0\, \gamma_\mu \left(1+Z_b\right)^{\frac{1}{2}} \left(1+Z^b\right)^{\frac{1}{2}} \left(1+Z^c\right) \left(1+Z^a\right)^{\frac{1}{2}} \\
&= -i\,\frac{\lambda^a}{2}\, g_0\, \gamma_\mu \left\{ 1 \,-\, \frac{g_0^2}{16\pi^2} \left[\frac{1}{2}\left(-\,2\times\frac{4}{3}\right) + \left(\frac{4}{3} - \frac{C_2}{2} + \frac{3\,C_2}{2}\right) + \frac{1}{2}\left(\frac{20}{12}C_2 - \frac{2}{3}n_f\right)\right] \right. \\
&\qquad \left. \left[\frac{1}{\epsilon} \,-\, \ln\left(\frac{-k^2}{h^2}\right) \,+\, \ldots \right] \right\} \\
&= -i\,\frac{\lambda^a}{2}\, g_0\, \gamma_\mu \left\{ 1 \,-\, \frac{g_0^2}{16\pi^2} \left(\frac{11}{6}C_2 - \frac{1}{3}n_f\right) \left[\frac{1}{\epsilon} \,-\, \ln\left(\frac{-k^2}{h^2}\right) \,+\, \text{finite terms} \right] \right\},
\end{aligned} \tag{9.22}$$

where $\gamma_\mu \lambda^a/2$ is the bare vertex, and we have made use of the binomial expansion $(1 + Z^a)^{\frac{1}{2}} \approx (1 + (1/2)Z^a)$.

The renormalized coupling constant (g_R), is now found simply by subtracting the value of the correction $\Gamma_\mu^{a\,(\mathrm{TOTAL})}$ at some renormalization scale μ^2, yielding

$$\begin{aligned} g_R &= g_0 - \frac{g_0^3}{16\pi^2}\left(\frac{11}{6}C_2 - \frac{1}{3}n_f\right)\left[\frac{1}{\epsilon} - \ln\left(\frac{-k^2}{h^2}\right) - \frac{1}{\epsilon} + \ln\left(\frac{-\mu^2}{h^2}\right)\right] \\ &= g_0 + \frac{g_0^3}{16\pi^2}\left(\frac{11}{6}C_2 - \frac{1}{3}n_f\right)\ln\left(\frac{-k^2}{\mu^2}\right). \end{aligned} \tag{9.23}$$

We have followed [6] in order to derive a relation between the coupling constant determined at scale $-k^2 = \mu^2$ (g_0), with the coupling constant determined at a different scale $-k^2$ (g_R). It should be noted that there are other ways to explain the renormalization procedure which are equivalent.

From here one calculates the QCD $\beta(g_R)$ function by taking the derivative of g_R with respect to μ

$$\begin{aligned} \beta(g_R) := \mu\left(\frac{\partial g_R}{\partial \mu}\right)\Bigg|_{-k^2=\mu^2} &= -\frac{g_0^3}{16\pi^2}\left(\frac{11}{6}C_2 - \frac{1}{3}n_f\right)\left(\frac{2\mu}{\mu^2}\right)\mu \\ &= -\frac{g_0^3}{16\pi^2}\left(\frac{11}{3}C_2 - \frac{2}{3}n_f\right) + \mathcal{O}(g_0^5). \end{aligned} \tag{9.24}$$

Using the QCD colour-factor $C_2 = 3$, we read off the first β coefficient as

$$\beta_0 = \frac{1}{4}\left(11 - \frac{2}{3}n_f\right). \tag{9.25}$$

The subsequent β coefficients are given in Eq.(10.3), and can be calculated order by order in perturbation theory. It must however be remembered that the higher β coefficients are dependent on the chosen regularization scheme.

Eq.(9.24) is a linearly separable differential equation which, to lowest loop order, can be solved analytically to find an explicit solution for $g(-k^2)$.

Linearly separating the differentials in the one-loop approximation of Eq.(9.24), gives

$$\int_{g(\mu^2)}^{g(-k^2)} \frac{dg}{g^3} = -\beta_0 \int_{\mu^2}^{(-k^2)^2} \frac{d\mu}{\mu}. \tag{9.26}$$

Integrating Eq.(9.26) leads to

$$\frac{1}{g^2(\mu^2)} - \frac{1}{g^2(-k^2)} = -\beta_0 \ln\left(\frac{-k^2}{\mu^2}\right), \tag{9.27}$$

where it is easy to solve for $\alpha_s^2(-k^2) = g^2(-k^2)/4\pi$, to find

$$\alpha_s(-k^2) = \frac{\alpha_s(\mu^2)}{1 + \frac{\alpha_s}{4\pi}\left(11 - \frac{2\,n_f}{3}\right)\ln\left(\frac{-k^2}{\mu^2}\right)}\,. \tag{9.28}$$

Eq.(9.28) is the running coupling constant in QCD to lowest loop order.

At higher loop orders, the differential equation describing the scale dependence of $\alpha_s(-k^2)$, Eq.(9.24), and the equivalent differential equation describing the scale dependence of the quark masses, become increasing difficulty to solve analytically. These equations, known as the renormalization group equations, and their solutions are discussed in detail in sections (10) and (11).

10 The Renormalization Group Equations

As was discussed in section (9), one removes the divergences present in QCD and QED through regularization and renormalization. A nonphysical renormalization scale parameter, μ, is introduced in the renormalization procedure to denote the point at which one performs the subtraction of the divergences to render the amplitudes finite. Both the renormalized coupling $\alpha_s(\mu^2)$ and the quark masses $\overline{m}_q(\mu^2)$ depend on the renormalization scheme used to define the theory and on the scale parameter, μ. If we set μ^2 approximately equal to the scale of the momentum transfer Q^2 in a particular interaction, $\alpha_s(\mu^2 \approx Q^2)$ becomes the effective strength of the strong coupling for that interaction [13].

As in Part I, we make use of the physical energy scale parameter, s (where $s = Q^2 = -q^2$). The scale dependence of $\alpha_s(s)$ and $\overline{m}_q(s)$ is governed by corresponding renormalization group equations (RG equations) which rely on QCD's anomalous dimensions as input.

The strong coupling, $\alpha_s(s)$, satisfies the differential RGE [70]

$$\frac{da_s}{d\ln s} = \beta(a_s) = -a_s^2\,(\beta_0 \,+\, a_s\,\beta_1 \,+\, a_s^2\,\beta_2 \,+\, a_s^3\,\beta_3 \,+ a_s^4\,\beta_4)\,, \tag{10.1}$$

where the $\beta(a_s)$ function is known up to $\mathcal{O}(a_s^6)$, and $a_s \equiv \frac{\alpha_s}{\pi} = \frac{g_R^2}{4\pi^2}$. The RGE given in Eq.(10.1) is equivalent to Eq.(9.24). Given the renormalization point, the $\beta(a_s)$ function describes how the strong coupling depends on the momentum transfer.

The quark masses, $\overline{m}_q(s)$, satisfy the differential RGE [70]

$$\frac{1}{\overline{m}_q}\frac{d\overline{m}_q}{d\ln s} = \gamma(a_s) = -a_s\,(\gamma_0 \,+\, a_s\,\gamma_1 \,+\, a_s^2\,\gamma_2 \,+\, a_s^3\,\gamma_3 \,+\, a_s^4\,\gamma_4)\,, \tag{10.2}$$

where the $\gamma(a_s)$ function is an anomalous dimension and is known up to $\mathcal{O}(a_s^5)$.

The s-dependence of a_s and $\overline{m}_q$ in Eqs.(10.1 – 10.2) is implicit i.e. $a_s = a_s(s)$ and $\overline{m}_q = \overline{m}_q(s)$.

The coefficients of the $\beta(a_s)$ function, which are now known to five-loop order [71–73], are given by

$$\beta_0 \,=\, \frac{1}{4}\left(11 - \frac{2}{3}\,n_f\right)$$

$$\beta_1 \,=\, \frac{1}{16}\left(102 - \frac{38}{3}\,n_f\right)$$

$$\beta_2 = \frac{1}{64}\left(\frac{2857}{2} - \frac{5033}{18}n_f + \frac{325}{54}\,n_f^2\right)$$

$$\beta_3 = \frac{1}{4^4}\Bigg\{\frac{149753}{6} + 3564\,\zeta_3 - \left(\frac{1078361}{162} + \frac{6508}{27}\,\zeta_3\right)n_f + \left(\frac{50065}{162} + \frac{6472}{81}\,\zeta_3\right)n_f^2 + \frac{1093}{729}\,n_f^3\Bigg\}$$

$$\begin{aligned}\beta_4 = \frac{1}{4^5}\Bigg\{&\frac{8157455}{16} + \frac{621885}{2}\,\zeta_3 - \frac{88209}{2}\,\zeta_4 - 288090\,\zeta_5 \\ &+ n_f\left(-\frac{336460813}{1944} - \frac{4811164}{81}\,\zeta_3 + \frac{33935}{6}\,\zeta_4 + \frac{1358995}{27}\,\zeta_5\right) \\ &+ n_f^2\left(\frac{25960913}{1944} + \frac{698531}{81}\,\zeta_3 - \frac{10526}{9}\,\zeta_4 - \frac{381760}{81}\,\zeta_5\right) \\ &+ n_f^3\left(-\frac{630559}{5832} - \frac{48722}{243}\,\zeta_3 + \frac{1618}{27}\,\zeta_4 + \frac{460}{9}\,\zeta_5\right) + n_f^4\left(\frac{1205}{2916} - \frac{152}{81}\,\zeta_3\right)\Bigg\},\end{aligned} \tag{10.3}$$

where ζ_n is the Riemann zeta-function and $n_f = 3$ for three active quark flavours.

The $\gamma(a_s)$ function coefficients, also currently known to five-loop order [74–76], are

$$\gamma_0 = 1$$

$$\gamma_1 = \frac{1}{16}\left(\frac{202}{3} - \frac{20}{9}\,n_f\right)$$

$$\gamma_2 = \frac{1}{64}\left(1249 - \left(\frac{2216}{27} + \frac{160}{3}\zeta_3\right)n_f - \frac{140}{81}n_f^2\right)$$

$$\begin{aligned}\gamma_3 = \frac{1}{256}\Bigg\{&\frac{4603055}{162} + \frac{135680}{27}\,\zeta_3 - 8800\,\zeta_5 \\ &+ \Big(-\frac{91723}{27} - \frac{34192}{9}\,\zeta_3 + 880\,\zeta_4 + \frac{18400}{9}\,\zeta_5\Big)n_f \\ &+ \Big(\frac{5242}{243} + \frac{800}{9}\,\zeta_3 - \frac{160}{3}\,\zeta_4\Big)n_f^2 + \Big(-\frac{332}{243} + \frac{64}{27}\zeta_3\Big)n_f^3\Bigg\}\end{aligned}$$

$$\gamma_4 \;=\; \frac{1}{4^5}\Bigg\{\frac{99512327}{162} + \frac{46402466}{243}\,\zeta_3 + 96800\,\zeta_3^2 - \frac{698126}{9}\,\zeta_4 - \frac{231757160}{243}\,\zeta_5$$
$$+ 242000\,\zeta_6 + 412720\,\zeta_7 + n_f\,\Big(-\frac{150736283}{1458} + \frac{12538016}{81}\,\zeta_3 - \frac{75680}{9}\,\zeta_3^2$$
$$+ \frac{2038742}{27}\,\zeta_4 + \frac{49876180}{243}\,\zeta_5 - \frac{638000}{9}\,\zeta_6 - \frac{1820000}{27}\,\zeta_7\Big)$$
$$+ n_f^2\,\Big(\frac{1320742}{729} + \frac{2010824}{243}\,\zeta_3 + \frac{46400}{27}\,\zeta_3^2 - \frac{166300}{27}\,\zeta_4 - \frac{264040}{81}\,\zeta_5 + \frac{92000}{27}\,\zeta_6\Big)$$
$$+ n_f^3\,\Big(\frac{91865}{1458} + \frac{12848}{81}\,\zeta_3 + \frac{448}{9}\,\zeta_4 - \frac{5120}{27}\,\zeta_5\Big) + n_f^4\,\Big(-\frac{260}{243} - \frac{320}{243}\,\zeta_3 + \frac{64}{27}\,\zeta_4\Big)\Bigg\}, \tag{10.4}$$

where ζ_n is the Riemann zeta-function and $n_f = 3$ for three active quark flavours.

It is important to be aware that there are consequences to crossing flavour thresholds. In the succeeding section (11), we concentrate on the perturbative expansions (in the light quark sector) of $\alpha_s(s)$ and $\overline{m}_q(s)$ resulting from Eqs.(10.1 – 10.2). If we proceed to higher energies (into the heavy quark region), the renormalization scale crosses quark mass flavour thresholds: finite threshold corrections appear [77] and the scale dependence of the mass then needs to be matched above and below the threshold. One has to specify a new initial condition for the running coupling constant at each threshold.

11 Series Expansion of the Quark Mass Renormalization Group Equation: an Application of Rubi

The recent calculation of the $\beta(a_s)$ function to five-loop order by [71–73], has ensured that the series expansion of the running quark mass can now be calculated to five-loop order. Previously this series expansion had been calculated by Chetyrkin et al. [78] to four-loop order, which built on the three-loop order calculation done by Kniehl [79]. Chrishtie et al. [80] provide a new exposition into the topic to four-loop order without the use of Computer Algebra Systems (CAS), but stop short of explicitly providing the series expansion. Recently, Kateav et al. have calculated the quark mass perturbative expansion to five-loop order in [81], which was done at roughly the same time as the work presented in this section of the dissertation [82].

In this section, we derive the perturbative expansion of the running quark mass. This series solution to Eq.(10.2) involves performing a Taylor expansion of $\overline{m}_q(s)$ at some reference scale $s = s^*$, in powers of $\eta = \ln(s/s^*)$. To third- and fourth-loop order this calculation is a fairly trivial exercise. At higher loop orders, however, this computation becomes more difficult and CAS such as Mathematica [83] and SymPy [84] (the popular open-source alternative implemented in Python) struggle to intuitively solve the RG equation without the additional use of Rubi.

Rule-based Integration (Rubi) [85] is an enhanced method of symbolic integration which allows for the integration of many difficult integrals not accomplished by other CAS. Using Rubi, many techniques involving integration become tractable. With Rubi, integrals are approached using step-wise simplification; distilling an integral (if the solution is unknown) into composite integrals which highlight yet undiscovered integration rules. The next subsection (11.1) quantitatively examines the benefits of Rubi compared with other CAS. First, an outline of the method for using Rubi to derive the perturbative expansion of the running quark mass – an original method developed in [82] by myself – is given in the following subsection (11.2). The derivation is purely symbolic.

11.1 The Power of Rubi as a Symbolic Integration Tool

Computer Algebra Systems such as Mathematica [83] and SymPy [84], have built-in symbolic integral routines. Rule-based Integration (Rubi) developed by [19] is principally a package (designed for Mathematica) that provides a method of symbolic integration organized by decision tree pattern matching, which matches the form of the integral against known integral rules. Rubi comprises 6700+ rules collated from familiar favourites [86–88] and in doing so it offers not only a means of integrating, but a growing complete reference for integration rules. These rules are in human-readable form with cross references to Rubi rule numbers and to the source. Rubi can also print the rules applied at each stage of solving the integral – a useful technique for pedagogical and diagnostic purposes.

Without proper consideration it may not be obvious why Rubi marks a significant improvement to effectively solving integrals. The effectiveness of these routines have been independently investigated by [89] with the results presented in Table 3. Comparing Rubi 4.15.2, Mathematica 11.3 and SymPy 1.1.1, Abbasi [89] divides the quality of integral's antiderivatives into four groups. *Group A* consists of integrals that were easily solved, where

the antiderivative is optimal in quality and leafsize. *Group B* is the group of integrals which were solved, but the leafsize twice that of optimal. *Group C's* integrals were solved, but the solution contains hypergeometric functions, special functions or imaginary units while the optimal antiderivative does not. Finally *Group F* are all integrals which cannot be solved by the CAS. See [89] for more details.

System	% A grade	% B grade	% C grade	% F grade
Rubi 4.15.2	99.76	0.08	0.06	0.1
Mathematica 11.3	75.37	8.46	15.81	2.67
SymPy 1.1.1	30.29	0	0	69.71

Adapted: Abbasi (2018) pg. 6 [89]

Table 3: Antiderivative Grade distribution for each CAS

Rule-based integration is the focus of much attention in development not only by [19], but by others. For example SymPy 1.1.1 currently fairs comparatively poorly in symbolic integration to other CAS (Table 3). However, the rules and implementation (pattern matching in a decision tree) behind Rubi are currently being developed into SymPy, see [90] for details. This would clearly improve the quality of this open source alternative.

Having examined how powerful Rubi is as a symbolic integration tool, we would want to explore how it can be applied in computation, and – in particular – in deriving the perturbative series expansion of the quark mass renormalization group equation, which describes the running of $\overline{m}_q(s)$. The integral of interest, Eq.(11.3), is particularly challenging for CAS.

11.2 The Perturbative Series Expansion of $\overline{m}_q(s)$

The quark mass RG equation (Eq.(10.2)) can be identified as a linearly separable differential equation. As such, we are able to exactly solve for $\overline{m}_q$ given the coefficients of the $\beta(a_s)$ and $\gamma(a_s)$ functions to a certain order. The exact solutions to leading and next-to-leading order are given in [79]. However, it is difficult to obtain the exact solution of $\overline{m}_q$ at higher orders, and this becomes a numerical procedure. Therefore, it is more lucid to solve the renormalization group equations in terms of a power expansion, since this type of solution provides insight into the renormalization scheme dependence of the running quark mass on the energy scale parameter s, at higher powers. This is important in accurately determining the light quark mass at a chosen scale. Hence, we proceed with determining a perturbative series expansion of Eq.(10.2).

This is achieved by dividing Eq.(10.2) by Eq.(10.1) and linearly separating the differentials to yield

$$\frac{d\overline{m}_q}{\overline{m}_q} = \frac{\gamma(a_s)}{\beta(a_s)}\, da_s\,, \tag{11.1}$$

where $\beta(a_s)$ and $\gamma(a_s)$ were defined in Eqs.(10.1 - 10.2).

Integrating Eq.(11.1) leads to

$$\ln\left(\frac{\overline{m}_q(s)}{\overline{m}_q(s^*)}\right) = \int_{a_s(s^*)}^{a_s(s)} da'_s \frac{\gamma(a'_s)}{\beta(a'_s)}\,, \tag{11.2}$$

which can be easily rearranged to find

$$\overline{m}_q(s) = \overline{m}_q(s^*)\,\exp\left(\int_{a_s(s^*)}^{a_s(s)} da'_s\,\frac{\gamma(a'_s)}{\beta(a'_s)}\right)\,, \tag{11.3}$$

where $\overline{m}_q(s^*)$ is the initial condition.

Both Mathematica and Rubi can be used in attempts to solve the integral in Eq.(11.3). What is of interest is how each of these CAS approach solving the chosen problem. In terms of the integral classification we introduced in subsection (11.1), we can classify the integral in Eq.(11.3) as a *Group F* integral, which means that Rubi and Mathematica are unable to solve the integral analytically. Naïvely using Mathematica's inbuilt integration function immediately yields an answer in terms of a RootSum object. Mathematica then struggles to find the definite integral (and series expansion) due to infinities arising from the logarithmic terms in this RootSum object. Mathematica's solution has a low interpretability and it's not clear what part of the integration process eventually yields the RootSum object.

Comparatively Rubi's attempt at the integral is a partial solution involving lower order integrals. The key advantage Rubi offers here is in simplification and clarity in identifying the unevaluated sections of the problem. Rubi performs the integral step-wise while printing the integration rule that it employs at each stage – which is worth emphasising. This allows the researcher to focus on what Rubi does *not* know. Should the researcher find an analytical solution for these unknown integrals it is easy to develop the appropriate rule and submit it to the Rubi GitHub project [85]. The high interpretability of Rubi's attempt means that these remaining integrals can then be added to Rubi's repository using other techniques, or suitably approximated if no exact solution can be found. Finding the series expansion from this point is straightforward.

Rubi's attempt at the indefinite version of the integral in Eq.(11.3) yields

$$\begin{aligned}
F(a'_s) \;&=\; \int da'_s\,\frac{\gamma(a'_s)}{\beta(a'_s)} \\
&=\; \frac{\gamma_0\ln(a'_s)}{\beta_0} - \frac{1}{4\,\beta_0\,\beta_4}\Bigg\{\left(\beta_4\,\gamma_0 - \beta_0\,\gamma_4\right)\,\ln\left(\beta_0 + \beta_1\,a'_s + \beta_2\,{a'_s}^2 + \beta_3\,{a'_s}^3 + \beta_4\,{a'_s}^4\right) \\
&+\; I_0\left(3\,\beta_1\,\beta_4\,\gamma_0 - 4\beta_0\,\beta_4\,\gamma_1 + \beta_0\,\beta_1\,\gamma_4\right) \;+\; 2\,I_1\left(\beta_2\,\beta_4\,\gamma_0 - 2\,\beta_0\,\beta_4\,\gamma_2 + \beta_0\,\beta_2\,\gamma_4\right) \\
&+ I_2\left(\beta_3\,\beta_4\,\gamma_0 - 4\,\beta_0\,\beta_4\,\gamma_3 + 3\,\beta_0\,\beta_3\,\gamma_4\right)\Bigg\}
\end{aligned} \tag{11.4}$$

where

$$I_n = \int da'_s \, \frac{a'^n_s}{\beta_0 \, + \, \beta_1 \, a'_s \, + \, \beta_2 \, a'^{\,2}_s \, + \, \beta_3 \, a'^{\,3}_s \, + \, \beta_4 \, a'^{\,4}_s} \tag{11.5}$$

The integrals I_n do not at present have an analytic solution in terms of algebraic functions – at least, they are unknown by Rubi. At this stage, however, Mathematica is able to re-write these integrals in terms of RootSum objects (without logarithmic divergences) that can be suitably simplified when the series expansion is performed.

The definite integral of Eq.(11.4) is found simply by using the Fundamental Theorem of Calculus[4]. The upper bound of the definite integral, the scale dependent strong coupling $a_s(s)$, is rewritten as its perturbative solution in terms of some known $a_s(s^*)$ (e.g. at the tau-lepton mass scale) up to $\mathcal{O}(a_s^6)$ [70]

$$\begin{aligned}
a_s(s) \; = \; & a_s(s^*) + a_s^2(s^*) \Big(- \beta_0 \, \eta \Big) + a_s^3(s^*) \Big(- \beta_1 \, \eta + \beta_0^2 \, \eta^2 \Big) \\
& + \, a_s^4(s^*) \Big(- \beta_2 \, \eta + \frac{5}{2} \, \beta_0 \, \beta_1 \, \eta^2 - \beta_0^3 \, \eta^3 \Big) \\
& + \, a_s^5(s^*) \Big(- \beta_3 \, \eta + \frac{3}{2} \, \beta_1^2 \, \eta^2 + 3 \, \beta_0 \, \beta_2 \, \eta^2 - \frac{13}{3} \, \beta_0^2 \, \beta_1 \, \eta^3 + \beta_0^4 \, \eta^4 \Big) \\
& + \, a_s^6(s^*) \Big(- \beta_4 \, \eta + \frac{7}{2} \, \beta_0 \, \beta_1 \, \eta^2 + \frac{7}{2} \, \beta_0 \, \beta_3 \, \eta^2 - \frac{35}{6} \, \beta_0 \, \beta_1^2 \, \eta^3 - 6 \, \beta_0^2 \, \beta_2 \, \eta^3 \\
& + \, \frac{77}{12} \, \beta_0^3 \, \beta_1 \, \eta^4 - \beta_0^5 \, \eta^5 \Big) \, ,
\end{aligned} \tag{11.6}$$

where $a_s(s)$ is defined in Eq.(3.8) and the variable η used throughout Part II is defined as

$$\eta \equiv \ln(s/s^*) \, . \tag{11.7}$$

Using Eq.(11.6) the resulting definite integral of Eq.(11.4) is quite lengthy, despite some simplification occurring between polynomial sums arising from the I_n integrals in Eq.(11.4). It can be viewed in the supplementary Mathematica notebook.

Focusing on Eq.(11.3), next is to exponentiate the definite integral, and perform a series expansion at some reference scale $s = s^*$.

Reordering the perturbative solution in terms of $a_s(s^*)$ yields

[4] An assumption of the Fundamental Theorem of Calculus is that the function to be integrated must be continuous. In the present case, the integrand is a rational function and therefore continuous up to isolated poles in the complex plane.

$$
\begin{aligned}
\overline{m}_q(s) \;=\; \overline{m}_q(s^*) \Bigg\{ & 1 - a_s(s^*)\,\gamma_0\,\eta + \frac{1}{2}\,a_s^2(s^*)\,\eta\,\Big[-2\,\gamma_1 + \gamma_0\,(\beta_0 \,+\, \gamma_0)\,\eta\Big] \\
& - \frac{1}{6}\,a_s^3(s^*)\,\eta\,\Big[6\,\gamma_2 - 3\,\Big(\beta_1\,\gamma_0 \,+ 2\,(\beta_0 \,+\, \gamma_0)\,\gamma_1\Big)\,\eta \,+\, \gamma_0\,(2\,\beta_0^2 \,+ 3\,\beta_0\,\gamma_0 \,+\, \gamma_0^2)\,\eta^2\Big] \\
& + \frac{1}{24}\,a_s^4(s^*)\,\eta\,\Big[-24\,\gamma_3 \,+\, 12(\beta_2\,\gamma_0 \,+\, 2\beta_1\,\gamma_1 \,+\, \gamma_1^2 \,+ 3\,\beta_0\,\gamma_2 \,+ 2\,\gamma_0\,\gamma_2)\,\eta \\
& - 4\,\Big(6\,\beta_0^2\,\gamma_1 \,+\, 3\,\gamma_0^2\,(\beta_1 \,+\, \gamma_1) \,+\, \beta_0\,\gamma_0\,(5\,\beta_1 \,+\, 9\,\gamma_1)\Big)\,\eta^2 \,+\, \gamma_0\,(6\,\beta_0^3 \,+\, 11\,\beta_0^2\,\gamma_0 \\
& + 6\,\beta_0\,\gamma_0^2 \,+\, \gamma_0^3)\,\eta^3\Big] \\
& + \frac{1}{120}\,a_s^5(s^*)\,\eta\,\Big[-120\,\gamma_4 \,+\, \frac{1}{\beta_0}60\,\Big(-7\,\beta_1\,\beta_2\,\gamma_0 \,+\, 4\,\beta_0^2\,\gamma_3 \,+\, \beta_0\,(7\,\beta_1\,\gamma_0 \,+\, \beta_3\,\gamma_0 \\
& + 2\,\beta_2\,\gamma_1 \,+\, 3\,\beta_1\,\gamma_2 \,+\, 2\gamma_1\,\gamma_2 \,+\, 2\,\gamma_0\,\gamma_3)\Big)\,\eta \,-\, 20\,\Big(3\beta_1^2\,\gamma_0 \,+\, \beta_1\,(14\,\beta_0 \,+\, 9\,\gamma_0)\,\gamma_1 \\
& + 3\,(2\beta_0 \,+\, \gamma_0)(\beta_2\,\gamma_0 \,+\, \gamma_1^2 \,+\, 2\,\beta_0\,\gamma_2 \,+\, \gamma_0\,\gamma_2)\Big)\,\eta^2 \,+\, 10\Big(12\,\beta_0^3\,\gamma_1 \,+\, \gamma_0^3(3\,\beta_1 \,+\, 2\,\gamma_1) \\
& + \beta_0\,\gamma_0^2\,(13\,\beta_1 \,+\, 12\,\gamma_1) \,+\, \beta_0^2\,\gamma_0\,(13\,\beta_1 \,+\, 22\,\gamma_1)\Big)\,\eta^3 \,-\, \gamma_0\,\Big(24\,\beta_0^4 \,+\, 50\,\beta_0^3\,\gamma_0 \\
& + 35\,\beta_0^2\,\gamma_0^2 \,+\, 10\,\beta_0\,\gamma_0^3 \,+\, \gamma_0^4\Big)\,\eta^4\Big] \,+\, \mathcal{O}(a_s^6(s^*))\Bigg\}\,.
\end{aligned}
\tag{11.8}
$$

This is the updated series expansion of the quark mass renormalization group equation to five-loop order. Up to three-loop order Eq.(11.8) agrees exactly with [79], and up to four-loop order with [78].

In principle, Eq.(11.8) is valid for any number of quarks n_f, between two thresholds provided the correct initial values are used. For the light quark sector this is set to $n_f = 3$.

For three active quark flavours, substituting the known values of the γ and β coefficients into Eq.(11.8) results in

$$
\begin{aligned}
\overline{m}_q(s) \;=\; \overline{m}_q(s^*) \Bigg\{ & 1 - a_s(s^*)\,\gamma_0\,\eta + a_s^2(s^*)\Big[\frac{1}{72}\Big(-303+10n_f\Big)\,\eta + \frac{1}{24}\Big(45-2n_f\Big)\,\eta^2\Big] \\
& + a_s^3(s^*)\Big[\Big(-\frac{1249}{64} + (\frac{277}{216} + \frac{5\zeta_3}{6})n_f + \frac{140}{81}n_f^2\Big)\,\eta + \Big(\frac{607}{32} - \frac{233}{144}n_f + \frac{5}{216}n_f^2\Big)\,\eta^2 \\
& + \Big(-\frac{65}{16} + \frac{7}{18}n_f + \frac{1}{108}n_f^2\Big)\,\eta^3\Big] \\
& + a_s^4(s^*)\Big[\Big(-98.943 + 19.108n_f - 0.276n_f^2 - 0.006n_f^3\Big)\,\eta + \Big(-146.861 - 23.571n_f \\
& - 8.120n_f^2 + 0.432n_f^3\Big)\,\eta^2 + \Big(-69.086 + 9.698n_f - 0.389n_f^2 + 0.004n_f^3\Big)\,\eta^3 \\
& + \Big(9.395 - 1.407n_f + 0.070n_f^2 - 0.001n_f^3\Big)\,\eta^4\Big] \\
& + a_s^5(s^*)\Big[\Big(-559.707 + 143.686n_f - 7.482n_f^2 - 0.108n_f^3 + 0.0001n_f^4\Big)\,\eta \\
& + \Big(\frac{1}{2n_f-33}(-29836.577 + 8585.863n_f + 22.617n_f^2 - 98.278n_f^3 + 4.520n_f^4 - 0.004n_f^5)\Big)\,\eta^2 \\
& + \Big(-775.076 + 164.071n_f + 26.364n_f^2 - 3.556n_f^3 + 0.096n_f^4\Big)\,\eta^3 \\
& + \Big(230.956 - 45.430n_f + 3.081n_f^2 - 0.082n_f^3 + 0.0006n_f^4\Big)\,\eta^4 \\
& + \Big(-22.547 + 4.630n_f - 0.356n_f^2 + 0.012n_f^3 - 0.0002n_f^4\Big)\,\eta^5\Big] \;+\; \mathcal{O}(a_s^6(s^*))\Bigg\},
\end{aligned}
\tag{11.9}
$$

where the coefficients of the Riemann zeta-function have been numerically evaluated and $n_f = 3$ in the light quark sector.

11.3 Evaluating the Accuracy of the Series Expansion of $\overline{m}_q(s)$

Eq.(11.8) is the perturbative series expansion of the running quark mass $\overline{m}_q(s)$ in powers of $\eta = \ln(s/s^*)$, with the initial value $\overline{m}_q(s^*)$ to five-loop order. Now of interest is the effect of the latest loop order (i.e. the $\mathcal{O}(a^5(s^*))$ term). To do this, Eq.(11.8) is compared with the four-loop series determined by [78]. Alternatively, one could directly numerically integrate Eqs.(10.1 - 10.2) to find the running coupling $a_s(s)$ and running quark mass $\overline{m}_q(s)$ (noting that discontinuities arise at flavour thresholds). This is the method employed in RunDec, a Mathematica (and C) package used for the decoupling and running of the strong coupling constant and quark masses, developed by [40] and now in its third version.

Figure (19) provides a local error analysis, by plotting the difference between the direct numerical integration of Eq.(10.2) for the running of the up and down quark mass $\overline{m}_{ud}(s)$ and i). the perturbative series solution to five-loop order (Eq.(11.8)); ii). the perturbative

series solution to four-loop order [78]. Varying the energy scale between $1\,\mathrm{GeV}^2$ and $5\,\mathrm{GeV}^2$ in increments of 0.001, describes 4001 points at which to evaluate $\overline{m}_{ud}$. The initial quark mass condition was set to be $\overline{m}_{ud}(s^* = (2\,\mathrm{GeV})^2) = (3.9 \pm 0.3)\,\mathrm{MeV}$ [68], where $\overline{m}_{ud} \equiv (\overline{m}_u + \overline{m}_d)/2$. The strong coupling constant $\alpha_s((2\,\mathrm{GeV})^2) = 0.307 \pm 0.013$ which is found using the perturbative series expansion of the strong coupling RG equation [70] with the initial condition $\alpha_s(m_\tau^2 = 3.16\,\mathrm{GeV}^2) = 0.328 \pm 0.013$ [91] was used. The uncertainty in the quark mass and strong coupling constant are not needed in the numerical analysis that follows.

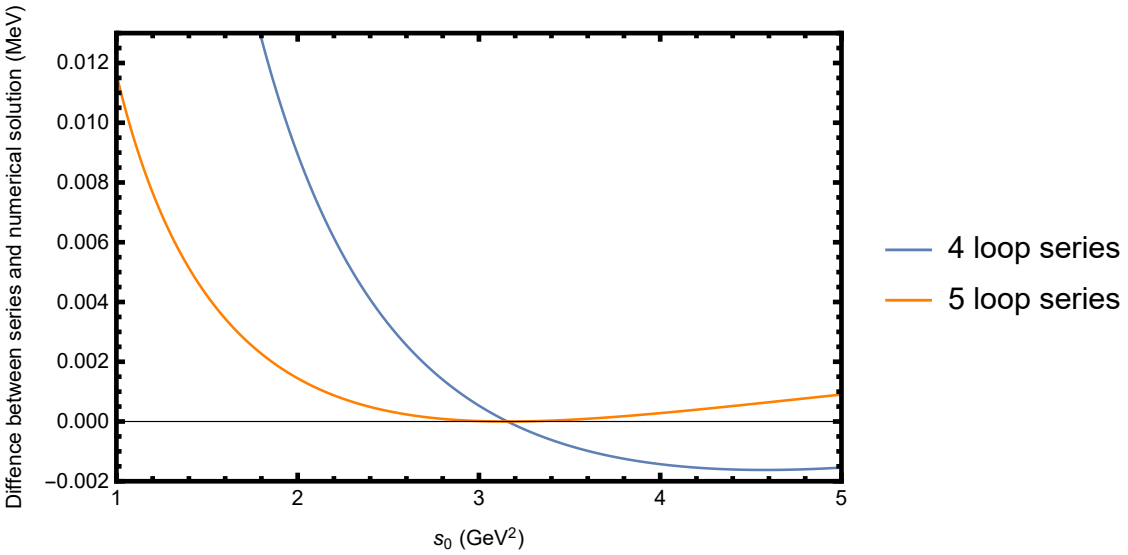

Figure 19: The local error function, $f(s_j) = r(s_j) - k(s_j)$, where $r(s_j)$ is the reference value of $\overline{m}_{ud}(s_j)$ with a scale dependence calculated by direct numerical integration of the quark mass RG equation, and $k(s_j)$ is the value of $\overline{m}_{ud}(s_j)$ with a scale dependence as either the five-loop series expansion (orange) or the four-loop series expansion (blue).

The direct numerical integration approach can be used as a reference from which statistical comparisons are drawn, indicating how well it is approximated by the four-loop [78] and by the five-loop (Eq.(11.8)) series expansion. Two common statistical evaluation criteria: Root Mean Squared Error (RMSE) and Mean Absolute Error (MAE) are used to provide a global error analysis. The Root Mean Squared Error is defined as

$$\mathrm{RMSE} = \sqrt{\frac{1}{n}\sum_{j=1}^{n}\left(\, r(s_j) - k(s_j)\,\right)^2}\,, \tag{11.10}$$

and the Mean Absolute Error is calculated as

$$\mathrm{MAE} = \frac{1}{n}\sum_{j=1}^{n}\left|\, r(s_j) - k(s_j)\,\right|\,, \tag{11.11}$$

where $r(s_j)$ is the reference i.e. $\overline{m}_{ud}(s_j)$ calculated by directly numerically integrating Eq.(10.2) at each point j in the s range described; and $k(s_j)$ is the quark mass $\overline{m}_{ud}(s_j)$ calculated using the perturbative series solution to either the four- or five-loop order at a particular point j within the s range.

The MAE can be interpreted as the average error rate, while the RMSE is more sensitive to a large deviation between the function and the reference function at a single point. The MAE and RMSE for the four- and five-loop perturbative series solution are given in table (4). The largest absolute deviation is also given, in order to provide context for the MAE and RMSE values.

Statistic	Five-loop series solution	Four-loop series solution
Mean Abs. Error	0.0015	0.0079
Root Mean Squared Error	0.0029	0.0146
Largest Abs. Deviation	0.0116	0.0578
Smallest Abs. Deviation	0	0

Table 4: Error evaluation for the forth-loop [78] and by the fifth-loop (Eq.(11.8)) series expansion, using the direct numerical integration of the quark mass RG equation as a reference

From figure (19) and the low MAE and RMSE in table (4), it is clear that the five-loop perturbative series solution for the quark mass does not deviate significantly from the direct numerical integration of the mass RG equation. Hence the $\mathcal{O}(a_s^5)$ correction to the series solution of the quark mass RG equation is a valuable addition.

11.4 Validation of Results

It has been established in subsection (11.2) that one can find the peturbative series solution of the running quark mass by focusing on the separated RG equation (Eq.(11.3)): integrating the given integral using Rubi and exponentiating the result, followed by Taylor expanding around a reference point $s = s^*$. Mathematica, in comparison, can not find the peturbative solution in this way, since it fails to evaluate the integral in Eq.(11.3) into a useful form.

This aside, one can validate the result through a different method, this time more agreeable to Mathematica. The method relies on: i). interchanging the limiting processes (performing the series expansion before integration)[5], ii). calculating the indefinite integral, followed by using the FTC to find the definite integral, iii). performing a second Taylor expansion after exponentiating the resultant integral.

[5]To be able to replace the integrand with its Taylor expansion, and then integrate term by term; a sufficient criterion is that the series expansion converges uniformly. This is indeed the case here, with the higher order terms having a decreasing contribution.

The first stage of this process is to series expand the integrand of Eq.(11.3) which yields

$$\frac{\gamma(a)}{\beta(a)} = \frac{\gamma_0}{a\,\beta_0} + \frac{\beta_0\,\gamma_1 - \beta_1\,\gamma_0}{\beta_0^2} + a\left(\frac{\left(\beta_1^2 - \beta_0\,\beta_2\right)\gamma_0}{\beta_0^3} - \frac{\beta_1\,\gamma_1}{\beta_0^2} + \frac{\gamma_2}{\beta_0}\right) + a^2\left(\frac{\left(-\beta_1^3 + 2\,\beta_0\,\beta_2\,\beta_1 - \beta_0^2\,\beta_3\right)\gamma_0}{\beta_0^4} + \frac{\left(\beta_1^2 - \beta_0\,\beta_2\right)\gamma_1}{\beta_0^3} - \frac{\beta_1\,\gamma_2}{\beta_0^2} + \frac{\gamma_3}{\beta_0}\right) + \mathcal{O}(a^3) \tag{11.12}$$

where the higher order terms are given in the supplementary Mathematica notebook.

Eq.(11.12) is now easily integrated with respect to a. After taking the definite integral and exponentiating, a second Taylor expansion is performed in order to yield the resultant series solution. See the supplementary Mathematica notebook for further details.

While the double series expansion may seem nonintuitive, it is able to reproduce the quark mass series expansion to five-loop order. Which, in turn, provides validation to the central method developed in section (11) – using Rubi.

The case for using Rubi as a tool in this situation, and in other Science, Technology, Engineering and Mathematics (STEM) research areas, is thus: it provides a lucid and intuitive approach to solving integrals, which other CAS systems are often unable to solve directly. This has been demonstrated through the derivation of the perturbative expansion of quark mass renormalization group equation, given in Eq.(11.8).

12 Conclusion

This dissertation has achieved its aim of determining the up, down and strange quark masses. The quark masses were determined from a QCD finite energy sum rule using the pseudoscalar correlator to six-loop order in perturbative QCD, with the leading vacuum condensates and higher order quark mass corrections included. The preferred calculation was done within the framework of contour improved perturbation theory. Considering the criteria of stability and convergence, this framework was favoured over fixed order perturbation theory for both the case of the correlator determining the up and down quark mass and the correlator determining the strange quark mass. Respectively, these masses were found to be $\overline{m}_u(2\,\mathrm{GeV}) = (2.6 \pm 0.4)\,\mathrm{MeV}$, $\overline{m}_d(2\,\mathrm{GeV}) = (5.3 \pm 0.4)\,\mathrm{MeV}$ and $\overline{m}_s(2\,\mathrm{GeV}) = (91.8 \pm 9.9)\,\mathrm{MeV}$ in the CIPT framework.

In this determination the systematic uncertainties stemming from the hadronic resonance sector were reduced by introducing an integration kernel in the Cauchy integral in the complex squared energy plane. Although several kernels were considered, the optimal kernel took the form of a second degree polynomial which quenches the hadronic resonance contribution at $s = s_0$, as well as halfway between the two resonances. Further, the issue of the convergence of the perturbative QCD expansion and its effect on the light quark masses was discussed.

The light quark masses presented in this dissertation are in agreement with recent sum rule and lattice QCD determinations in this field. Figures (13) and (17) show how these results compare with the current literature.

It is particularly important to realise that although these results of the up, down and strange quark masses agree with the most recent previous FESR determinations [15,17,18], the determination presented in this dissertation represents a significant improvement over past determinations and explores various original aspects in the method. The analysis of different kernels, examining the issue of the convergence of the perturbative QCD expansion, a different implementation of the running QCD coupling and a more careful error analysis are some of the considerable improvements accomplished in this determination. The calculations in this dissertation are preformed in Mathematica and represent a notable advancement in achieved numerical precision of FESR determinations of the light quark masses compared to [15, 18]. Additionally, this determination is one of the first within the field of QCD sum rules to make its code available for publication, since the author believes in the importance of modern research and open collaboration. The fully annotated Mathematica notebooks are openly accessible via the GitHub repository and in the attached supplementary material.

The second part to this dissertation focused on regularization and renormalization, particularly in regard to the quark masses. The central idea of Part II examines the renormalization group equations of the strong coupling $\alpha_s(s)$ and the quark masses $\overline{m}_q(s)$, and calculates of the updated series expansion of the quark mass renormalization group equation (RGE) to five-loop order using Rule-based Integration (Rubi), a new Mathematica package that provides a method of symbolic integration. This work has been written up into a research note [82].

To conclude, this dissertation is placed within the context of the field of QCD sum rules. An open problem in this field is the reduction of uncertainty in the method and in its inputs. The sum rule approach would benefit from more accurate determinations of the vacuum condensates, as well as updated experimental information of the resonances in the hadronic sector.

This aside, the field remains an amazingly versatile one. There are numerous application of QCD sum rules. Besides the determination of the up, down and strange quark masses described in this dissertation, further extensions from this work could consider determining the charm and bottom quark masses via a sum rule calculation. Such determinations would require experimental data on hadronic spectral densities as input, and the recently collated $e^+e^- \rightarrow$ *hadrons* data-set [92] could be used. Moreover, calculating the heavy quark masses would not be the limit to extending this work. The QCD sum rule framework can be used to calculate the vacuum condensates, the $g-2$ muon and the hadronic contributions to the running QED coupling. The author hopes to be able to further contribute to this field in the future.

In the present, the work outlined in this dissertation presents the most accurate up, down and strange quark mass determination from a QCD finite energy sum rule to date. Through a publication resulting from this dissertation [68], these results will – in all likelihood – form part of the world average for the light quark masses published by the Particle Data Group [13] in 2019.

A Appendix

A.1 FESR from Cauchy's Theorem

Consider the integration contour in the complex s-plane. Where s_{th} is the threshold energy and s_0 is the radius of the circular integration contour.

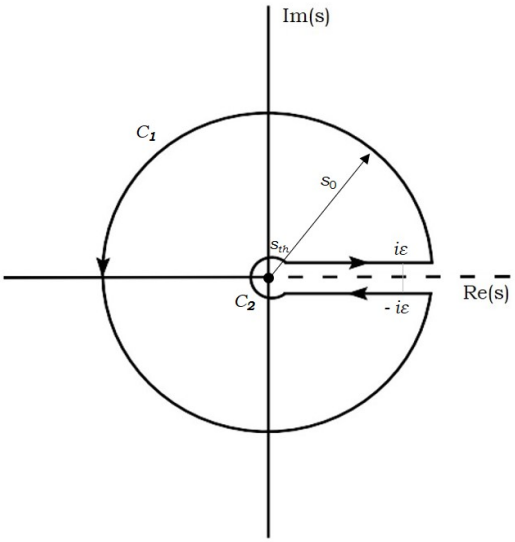

Figure 20: Integration contour in the complex s-plane.

From Cauchy's residue theorem we have

$$\oint ds\,\Pi(s) = 2\pi i\ \mathrm{Res}[\,\Pi(s), s=0\,] \tag{A.1}$$

with $\Pi(s)$ an analytic function in the complex energy plane, and $\mathrm{Res}[\,\Pi(s), s=0\,]$ the sum of the residues at the pole(s).

Using the Schwarz's Symmetry Principle inside the contour and taking the limit $\epsilon \to 0$ (Fig.(A.1)), the left hand side of Eq.(A.1) becomes

$$\oint ds\,\Pi(s) = \int_{C_1} ds\,\Pi(s) \;+\; \int_{C_2} ds\,\Pi(s) \;+\; 2i\int_{s_{th}}^{s_0} ds\ \mathrm{Im}\,\Pi(s)\,. \tag{A.2}$$

Assuming that the limit $\epsilon \to 0$ is taken, the integral about C_2 vanishes. Thereafter, substituting Eq.(A.2) into Eq.(A.1), and noting that the points on C_1 obey $|s| = s_0$, one obtains

$$\oint_{|s|=s_0} ds\,\Pi(s) + 2i\int_{s_th}^{s_0} ds\,\mathrm{Im}\,\Pi(s) \;= 2\pi i\ \mathrm{Res}[\,\Pi(s), s=0\,]\,. \tag{A.3}$$

Simply dividing each term in Eq.(A.3) by $2\pi i$ and replacing the general analytic function $\Pi(s)$ with our pseudoscalar correlator $\Psi_5(s)$ (Eq.(2.2)), one has the finite energy sum rule

$$\frac{1}{2\,\pi\,i}\oint_{C(|s_0|)} ds\,\Psi_5(s)|_{\rm QCD}\,+\,\int_{s_{th}}^{s_0} ds\,\frac{1}{\pi}\,{\rm Im}\,\Psi_5(s)|_{\rm HAD} = {\rm Res}[\,\Psi_5(s), s=0\,]\,. \qquad \text{(A.4)}$$

The integrand used in the FESR can be multiplied by a meromorphic function $P_5(s)$ designed to quench the systematic uncertainties in the resonance region on the second Riemann sheet

$$\frac{1}{2\,\pi\,i}\oint_{C(|s_0|)} ds\,\Psi_5(s)|_{\rm QCD}\,P_5(s) + \int_{s_{th}}^{s_0} ds\,\frac{1}{\pi}\,{\rm Im}\,\Psi_5(s)|_{\rm HAD}\,P_5(s) = {\rm Res}[\,\Psi_5(s)P_5(s), s=0\,]\,. \qquad \text{(A.5)}$$

Eq.(A.5) is the sum rule which forms the basis of the light quark mass determinations.

In the interest of full generality we briefly discuss the form of the sum rule most beneficial for heavy quark (charm and bottom) mass determinations. The heavy quark mass determinations make use of the vector current correlator. In the heavy quark sector ${\rm Im}\,\Psi_5(s)|_{\rm HAD}$ is not model-based as in the light quark sector; instead, hadronic data (commonly e^+e^- data) directly enters the sum rule. This is done through the use of the Optical Theorem, an important property of the two-point correlation function of the vector current $\Pi(q^2)$.

Theorem A.1 (Optical Theorem) *The imaginary part of the two-point correlation function of the vector current can be directly related to the total cross-section*

$$R_f(s) \,\equiv\, \frac{\sigma(\,e^+e^-\,\to\,\mathit{hadrons}(f\overline{f})\,)}{\sigma(\,e^+e^-\,\to\,\mu^+\mu^-\,)} \,=\, 12\,\pi\,\mathit{Im}\Pi(s)$$

where

$$\sigma(\,e^+e^-\,\to\,\mu^+\mu^-\,) \,=\, 4\,\pi\,\frac{\alpha_{em}}{3\,s}\,.$$

This theorem is a direct consequence of the unitarity of the scattering matrix (S-matrix) [28], which associates the final and initial states of a physical system that undergoes a scattering process.

Using the Optical Theorem to specify how cross-section data enters the finite energy sum rule for the vector current correlator, yields

$$\frac{1}{2\,\pi\,i}\oint_{C(|s_0|)} ds\,\Psi(s)|_{\rm QCD}\,P(s) + \frac{1}{12\,\pi^2}\int_{s_{th}}^{s_0} ds\;{\rm R}_f(s)\,P(s) = {\rm Res}[\,\Psi(s)P(s), s=0\,]\,, \quad \text{(A.6)}$$

where $P(s)$ is a meromorphic function chosen to quench uncertainties in the hadronic sector. Eq.(A.6) forms the basis of the heavy quark mass sum rule determinations.

A.2 The Pseudoscalar Correlator $\Psi_5(q^2)$ in Perturbative QCD

This section derives the lowest order perturbative contribution of the pseudoscalar correlator $\Psi_5(q^2)$. The pseudoscalar correlator is defined in momentum space as

$$\Psi_5(q^2) \;=\; i \int d^4x\, e^{iqx}\, \langle\Omega|\, T\{\partial^\mu A_\mu(x)\, \partial^\nu A^\dagger_\nu(0)\}\, |\Omega\rangle \;, \tag{A.7}$$

where Ω represents the physical vacuum, and $\partial^\mu A_\mu(x)$ is the divergence of the flavour i, j axial-vector current. In QCD, $\partial^\mu A_\mu(x)$ can be related to the corresponding pseudoscalar density by the Ward Identity

$$\partial^\mu A_\mu(x) \;=\; (\overline{m}_i + \overline{m}_j)\, \mathrm{N}\{\overline{q}_j(x)\, i\,\gamma_5\, q_i(x)\}\,, \tag{A.8}$$

where N{ } is the standard normal-ordering operator, $\overline{m}_{i,j}$ are the running quark masses in QCD, and i, j denotes the quark flavour.

Inserting Eq.(A.8) into Eq.(A.7) yields

$$\begin{aligned}
\Psi_5(q^2) \;&=\; (\overline{m}_i + \overline{m}_j)^2\; i \int d^4x\, e^{iqx}\, \langle 0|\, T\{\overline{q}_j(x)\, i\gamma_5\, q_i(x)\, (\overline{q}_j(0)\, i\gamma_5\, q_i(0))^\dagger\}\, |0\rangle \\
&=\; (\overline{m}_i + \overline{m}_j)^2\; i \int d^4x\, e^{iqx}\, \langle 0|\, T\{\overline{q}_j(x)\, i\gamma_5\, q_i(x)\, \overline{q}_i(0)\, i\gamma_5\, q_j(0)\}\, |0\rangle \\
&\equiv\; (\overline{m}_i + \overline{m}_j)^2\, \Pi_5(q^2)\,,
\end{aligned} \tag{A.9}$$

where the hermitian property of the γ_5 matrix, i.e. $\gamma_5 = \gamma_5^\dagger$ has been used.

In the final line of Eq.(A.9) notice that the two-point correlation function $\Pi_5(q^2)$ is defined to differ from $\Psi_5(q^2)$ by a normalisation factor.

To proceed consider the object

$$\tau(x) \;:=\; \langle 0|\, T\{\overline{q}_j(x)\, i\gamma_5\, q_i(x)\, \overline{q}_i(0)\, i\gamma_5\, q_j(0)\}\, |0\rangle\,. \tag{A.10}$$

The time-ordered product of these four fields can be expressed as the sum over normal-ordered products formed by considering all possible contractions between pairs of the fields. This is known as Wick's Theorem.

Theorem A.2 (Wick's Theorem) *If $\phi(x_1)\,\phi(x_2)\,...\,\phi(x_m)$ denote various fields, and T{ } and N{ } are, respectively, the standard time-ordering and normal-ordering operators, then Wick's Theorem [28] states*

$$T\{\phi(x_1)\phi(x_2)...\phi(x_m)\} \;=\; N\{\phi(x_1)\phi(x_2)...\phi(x_m) \;+\; \textit{all possible contractions}\,\}$$

As an example, for $m = 4$

$$T\{\phi(x_1)\phi(x_2)\phi(x_3)\phi(x_4)\} = N\Big\{\phi(x_1)\phi(x_2)\phi(x_3)\phi(x_4) + \phi(\overbrace{x_1)\phi(x_2}^{})\phi(x_3)\phi(x_4)$$
$$+ \phi(\overbrace{x_1)\phi(x_2)\phi(x_3}^{})\phi(x_4) + \phi(\overbrace{x_1)\phi(x_2)\phi(x_3)\phi(x_4}^{})$$
$$+ \phi(x_1)\phi(\overbrace{x_2)\phi(x_3}^{})\phi(x_4) + \phi(x_1)\phi(\overbrace{x_2)\phi(x_3)\phi(x_4}^{})$$
$$+ \phi(x_1)\phi(x_2)\phi(\overbrace{x_3)\phi(x_4}^{}) + \phi(\overbrace{x_1)\phi(x_2}^{})\phi(\overbrace{x_3)\phi(x_4}^{})$$
$$+ \phi(\overbrace{x_1)\phi(x_2}^{}\overbrace{)\phi(x_3}^{})\phi(x_4) + \phi(\overbrace{x_1)\phi(x_2}^{}\overbrace{)\phi(x_3)\phi(x_4}^{})\Big\} . \tag{A.11}$$

Further, when nonadjacent fields are contracted, the contraction is defined to yield a factor of D_F *or* S_F *(depending if the fields in question are bosonic or fermionic). For example, considering four quark fields where* $q(x_1)$ *and* $q(x_3)$ *are contracted gives*

$$N\{q(\overbrace{x_1)\,q(x_2)\,q(x_3}^{})\,q(x_4)\} = S_F(x_1 - x_3)\,N\{q(x_2)\,q(x_4)\} \tag{A.12}$$

where S_F *is the fermionic propagator*

$$S_F(x-y) := \frac{1}{(2\pi)^4}\int d^4k\, e^{ik(x-y)}\,\frac{\not{k}+m}{k^2-m^2+i\epsilon}$$

and $\not{p} \equiv \gamma^\mu\, p_\mu$.

Lastly, since $\langle 0|N(\textit{any operator})|0\rangle = 0$*, the vacuum expectation value of a term which contains uncontracted operators is equal to zero.*

Taking the vacuum expectation value of Eq.(A.11), and using Eq.(A.12) to simplify contracted terms yields

$$\langle 0|\,T\{\phi(x_1)\,\phi(x_2)\,\phi(x_3)\,\phi(x_4)\}\,|0\rangle = S_F(x_1-x_2)S_F(x_3-x_4) + S_F(x_1-x_3)S_F(x_2-x_4)$$
$$+ S_F(x_1-x_4)S_F(x_2-x_3)\ . \tag{A.13}$$

Using Wick's Theorem (specifically Eq.(A.13)) to contract alike fields simplifies $\tau(x)$, Eq.(A.10), significantly

$$\begin{aligned}\tau(x) &= (i)^2\,\langle 0|\,T\{\overline{q}_j(x)\ \gamma_5\ q_i(x)\ \ \overline{q}_i(0)\,\gamma_5\ q_j(0)\}\,|0\rangle \\ &= -\,\mathrm{S_{F,\,j}}(-x)\,\gamma_5\ \ \mathrm{S_{F,\,i}}(x)\,\gamma_5 \\ &= -\,\mathrm{N_C}\ \mathrm{tr}\Big(\mathrm{S_{F,\,j}}(-x)\,\gamma_5\ \ \mathrm{S_{F,\,i}}(x)\,\gamma_5\Big)\ .\end{aligned} \tag{A.14}$$

Notice that the colour factor $\mathrm{N_C}$ is present to account for the three quark colours. Using the definition of the fermionic propagator $\mathrm{S_F}$ in momentum k-space, τ becomes

$$\begin{aligned}
\tau(k) \;&=\; -\,\mathrm{N_C}\;\mathrm{tr}\Big(\frac{\not{k}_2 + m_j}{k_2^2 - m_j^2}\,\gamma_5\,\frac{\not{k}_1 + m_i}{k_1^2 - m_i^2}\,\gamma_5\Big) \\
&=\; -\,\mathrm{N_C}\;\mathrm{tr}\Big(\frac{\not{k}_2\,\gamma_5\,\not{k}_1\,\gamma_5 \;+\; \not{k}_2\,\gamma_5\,m_i\,\gamma_5 \;+\; m_j\,\gamma_5\,\not{k}_1\,\gamma_5 \;+\; m_j\,\gamma_5\,m_i\gamma_5}{(k_2^2 - m_j^2)\,(k_1^2 - m_i^2)}\Big) \qquad \text{(A.15)} \\
&=\; -\,\mathrm{N_C}\;\mathrm{tr}\Big(\frac{-\not{k}_2\,\not{k}_1 \;+\; m_j\,m_i}{(k_2^2 - m_j^2)\,(k_1^2 - m_i^2)}\Big),
\end{aligned}$$

where the final line follows from remembering $\not{k} \;=\; \gamma^\mu\,k_\mu$, and the properties of the gamma matrices, namely: $\{\gamma^5, \gamma^\mu\} = \gamma^5\gamma^\mu \;+\; \gamma^\mu\gamma^5 \;=\; 0$, $(\gamma^5)^2 \;=\; \mathrm{I_4}$ and $\mathrm{tr}(\gamma^\mu) \;=\; 0$.

Taking the trace of the remaining terms (using $\mathrm{tr}(\gamma^\mu\gamma^\nu) \;=\; 4\eta^{\mu\nu}$) gives

$$\tau(k) \;=\; -\,\mathrm{N_C}\;\frac{4\,(m_j\,m_i \;-\; k_2\,k_1)}{(k_2^2 - m_j^2)\,(k_1^2 - m_i^2)}\,. \qquad \text{(A.16)}$$

Fourier transforming $\tau(k)$ back into position space

$$\tau(x) \;=\; -\,\mathrm{N_C}\int\frac{d^4k_1}{(2\pi)^4}\int\frac{d^4k_2}{(2\pi)^4}\;\frac{4\,(m_j\,m_i \;-\; k_2\,k_1)}{(k_2^2 - m_j^2)\,(k_1^2 - m_i^2)}\,e^{i\,(k_2 - k_1)\,x}\,. \qquad \text{(A.17)}$$

Substituting Eq.(A.17) into Eq.(A.9), the pseudoscalar correlator $\Psi_5(q^2)$ becomes

$$\begin{aligned}
\Psi_5(q^2) \;&=\; -(\overline{m}_i + \overline{m}_j)^2\,i\int d^4x\,e^{iqx}\,\mathrm{N_C}\int\frac{d^4k_1}{(2\pi)^4}\int\frac{d^4k_2}{(2\pi)^4}\;\frac{4\,(m_j\,m_i \;-\; k_2\,k_1)}{(k_2^2 - m_j^2)(k_1^2 - m_i^2)}\;e^{i(k_2 - k_1)x} \\
&=\; -(\overline{m}_i + \overline{m}_j)^2\,i\,\mathrm{N_C}\int\frac{d^4k_1}{(2\pi)^4}\int d^4k_2\;\frac{4\,(m_j\,m_i \;-\; k_2\,k_1)}{(k_2^2 - m_j^2)(k_1^2 - m_i^2)}\;\delta^{(4)}(q + k_2 - k_1)\,.
\end{aligned} \qquad \text{(A.18)}$$

where the integration in d^4x is performed using

$$\int d^4x\,e^{iqx}\,e^{ik_2x}\,e^{-ik_1x} \;=\; (2\pi)^4\,\delta^{(4)}(q + k_2 - k_1)\,. \qquad \text{(A.19)}$$

In Eq.(A.18) we now use the delta function to integrate over k_2. Renaming $k_1 \;\equiv\; k$ gives

$$\Psi_5(q^2) \;=\; -\,4\,(\overline{m}_i + \overline{m}_j)^2\,i\,\mathrm{N_C}\int\frac{d^4k}{(2\pi)^4}\;\frac{(m_j\,m_i \;-\; k\,(k - q))}{((k - q)^2 - m_j^2)(k^2 - m_i^2)}\;. \qquad \text{(A.20)}$$

The term proportional to $m_j\, m_i$ is suppressed for the case of the light quarks and can be neglected in our derivation of the lowest order perturbative contribution of the pseudoscalar correlator $\Psi_5(q^2)$. We are therefore left with

$$\begin{aligned}\Psi_5(q^2) \;&=\; 4\,(\overline{m}_i + \overline{m}_j)^2\, i\,\mathrm{N_C} \int \frac{d^4k}{(2\pi)^4}\, \frac{k^2 - k\,q}{(k^2\,(k-q)^2)} \\ &= -\,4\,(\overline{m}_i + \overline{m}_j)^2\, i\,\mathrm{N_C}\; q^\mu \int \frac{d^4k}{(2\pi)^4}\, \frac{k_\mu}{(k^2\,(k-q)^2)}\,,\end{aligned} \tag{A.21}$$

where the simplification in the last line is due to the integral of the first term (k_2) vanishing.

Performing the final integral in d^4k leaves us with

$$\Psi_5(q^2) \;=\; -(\overline{m}_i + \overline{m}_j)^2 \left(\frac{3}{8\,\pi^2}\right) q^2\, \ln\left(\frac{-q^2}{\mu^2}\right), \tag{A.22}$$

where dimensional regularization was used and the divergence ($1/\epsilon$) was subtracted according to the $\overline{MS}$ prescription. Eq.(A.22) is the perturbative contribution of the pseudoscalar correlator to lowest order of α_s.

A.3 Mass Definitions

The quark mass is a fundamental parameter of QCD which enters the QCD Lagrangian [13] as

$$\mathcal{L} = i \sum_q \bar{\psi}_q^a \left(\nabla_\mu \gamma_\mu + i\, m_q\right) \psi_q^a - \frac{1}{4} \mathrm{G}_{\mu\nu}^n \mathrm{G}^{n\,\mu\nu}\,, \tag{A.23}$$

where

$$\begin{aligned} \nabla_\mu &= \partial_\mu - i\, g\, \frac{\lambda^n}{2}\, A_\mu^n \\ \mathrm{G}_{\mu\nu}^n &= \partial_\mu A_\mu^n - \partial_\nu A_\mu^n + g\, f^{nml}\, A_\mu^m\, A_\nu^l \end{aligned} \tag{A.24}$$

and repeated indices are summed over. γ_μ are the Dirac γ-matrices, g is the gauge coupling constant in QCD, f^{nml} are the SU(3) group structure constants, A_μ^n are the gluon fields with a colour-index $n = 1, 2 \ldots 8$ representing the 8 types of gluons, and ψ_q^a are the quark-field spinors for a q flavour quark with a colour-index $a = 1, 2, 3$ and mass m_q.

The quark masses can be defined in various ways. The definitions relevant in light quark mass determinations – the $\overline{MS}$-mass and the scale invariant mass – are described below. There are other ways to define particle masses (for example, the on-shell mass scheme which is common in QED, electroweak interactions and in QCD to define the heavy quarks) but they do not pertain directly to this dissertation.

A.3.1 $\overline{\mathrm{MS}}$ - mass

All parameters of the Lagrangian that are related to a physical observable depend on the scale used to define the theory. The quark masses $\overline{m}_q$, depend on some scale parameter μ, as well as the chosen renormalization scheme. The minimal subtraction (MS-scheme) is a particular renormalization scheme in Quantum Field Theory, developed separately by 't Hooft [69] and Weinberg [93] in 1973. In the MS-scheme, the infinities beyond leading order in perturbative QCD are dealt with by absorbing the divergent parts of the radiative corrections into the counterterms. Throughout this dissertation we work in the modified minimal subtraction scheme ($\overline{\mathrm{MS}}$-scheme) [69, 94]. Similar to the MS-scheme, in the $\overline{\mathrm{MS}}$-scheme the divergent parts of the radiative corrections are also absorbed into the counterterms. In addition, a universal constant that arises with the divergences in pQCD calculations is absorbed concurrently in the $\overline{\mathrm{MS}}$-scheme. This renormalization scheme is the most commonly used scheme in QCD perturbation theory. The renormalization group equation Eq.(10.2) describes the running of the quark masses in the $\overline{\mathrm{MS}}$-scheme, $\overline{m}_q(\mu)$. The current convention is to report the quark masses at a scale of $\mu = 2\,\mathrm{GeV}$.

A.3.2 Scale Invariant Mass

The scale invariant mass is defined recursively from $\overline{m}_q(\mu)$, as the $\overline{\mathrm{MS}}$-mass at the scale $\mu = m_q$. It is denoted by $\overline{m}_q(\overline{m}_q)$. To calculate the scale invariant mass, we start with the quark mass defined at an initial scale, $\overline{m}_q(\mu_0)$. Eq.(11.3) is then used to run the mass to a new scale[6] $\mu_1 = \overline{m}_q(\mu_0)$. Next, we repeat the process by running the mass to the scale $\mu_2 = \overline{m}_q(\mu_1)$. In theory, after an infinite number of recursions, $\overline{m}_q(\overline{m}_q)$ is obtained. In practice an acceptable level of precision is reached after approximately 10 recursions.

[6] The running of the quark mass can be calculated by solving the integral Eq.(11.3) numerically in Mathematica, using the series expansion of the quark mass renormalization group equation to five-loop order developed in section (11), or by using the Mathematica package RunDec [40].

A.4 Accessing the Mathematica Code

The Mathematica code used in the numerical calculations to generate all the results of this dissertation and the subsequent publications is provided as supplementary material.

The code is organized into three comprehensively annotated Mathematica notebooks: (a) `Up-down-quark masses sum rules calculations`, (b) `Strange quark mass sum rules calculations`, and (c) `Series solution of quark mass RGE`.

All publications resulting from this dissertation (listed on page (iii)) have the corresponding Mathematica notebook attached. It is still uncommon in the field of theoretical physics to make the code available with a published paper. Historically, this was not possible as it made publications unreadable and too expensive to print. However, these reasons are no longer applicable in the present day, and the author has made the code available with the publications resulting from this dissertation, since she believes in the importance of modern research and open collaboration.

For readers please always check for the latest versions of the notebooks in the GitHub repository:
`https://github.com/AlexesMes/light-quark-masses`.
This repository holds the work of A. Mes in Quantum Chromodynamic finite energy sum rules and contains additional resources which would be of interest.

References

[1] F. Knechtli, M. Günther, and M. Peardon. *Lattice Quantum Chromodynamics: Practical Essentials.* Springer, (2017).

[2] S. Aoki *et al.*, FLAG Coll. *Review of Lattice Results Concerning Low-energy Particle Physics. Eur. Phys. J.* ***C***, 77(2):112, (2017).

[3] C. Dominguez. *Analytical Determination of the QCD Quark Masses.* In *50 Years Of Quarks, pp.287-313.* World Scientific Publishing Co., Singapore, (2015).

[4] P. Colangelo and A. Khodjamirian. *QCD Sum Rules, a Modern Perspective.* In *At The Frontier of Particle Physics: Handbook of QCD (in 3 Volumes), pp.1495-1576.* World Scientific Publishing Co., (2001).

[5] C. Dominguez. *Quantum Chromodynamics Sum Rules.* Springer, (2018).

[6] W. Greiner, S. Schramm, and E. Stein. *Quantum Chromodynamics.* Springer, (2007).

[7] M.A. Shifman, A.I. Vainshtein and V.I. Zakharov. *QCD and Resonance Physics: Theoretical Foundations. Nucl. Phys.* ***B***, 147:385, (1979).

[8] R. Shankar. *Determination of the Quark-Gluon Coupling Constant. Physical Review* ***D***, 15(3):755, (1977).

[9] J.P. Carlomagno and M. Loewe. *Comparison between the Continuum Threshold and the Polyakov Loop as Deconfinement Order Parameters. Physical Review* ***D***, 95(3):036003, (2017).

[10] M. Thomson. *Modern Particle Physics.* Cambridge University Press, (2013).

[11] E. de Rafael. *An Introduction to Sum Rules in QCD.* Les Houches Summer School: Lectures, (1998).

[12] A. Radyushkin. *Introduction to QCD Sum Rule Approach.* World Scientific Publishing Co., (2001).

[13] M. Tanabashi et al. *Particle Data Group Review. Physical Review* ***D***, 98:030001, (2018).

[14] J. Yuan, Z. Zhang, T. Steele, H. Jin, and Z. Huang. *Constraint on the Light Quark Mass m_q from QCD Sum Rules in the I= 0 Scalar Channel. Physical Review* ***D***, 96(1):014034, (2017).

[15] C. Dominguez, N.F Nasrallah, R. Röntsch, and K. Schilcher. *Up-and Down-quark Masses from Finite-Energy QCD Sum Rules to Five Loops. Physical Review* ***D***, 79(1):014009, (2009).

[16] B. Ananthanarayan and D. Das. *Optimal Renormalization and the Extraction of the Strange Quark Mass from Moments of the τ-decay Spectral Function. Physical Review* ***D***, 94(11):116014, (2016).

[17] S. Bodenstein, C. Dominguez, and K. Schilcher. *Strange Quark Mass from Sum Rules with Improved Perturbative QCD Convergence. Journal of High Energy Physics*, 2013(7):138, (2013).

[18] C. Dominguez, N.F Nasrallah, R. Röntsch, and K. Schilcher. *Strange Quark Mass from Finite Energy QCD Sum Rules to Five Loops. Journal of High Energy Physics*, 05:020, (2008).

[19] A.D. Rich and P. Scheibe. *Rule-based Integration (Rubi): An Extensive System of Symbolic Integration Rules.* `https://rulebasedintegration.org/`, (2018).

[20] M. Shifman. *Quark-hadron Duality.* In *At The Frontier of Particle Physics: Handbook of QCD*, pages 1447–1494. World Scientific, (2001).

[21] E.C. Poggio, H.R. Quinn, and S. Weinberg. *Smearing Method in the Quark Model. Physical Review* ***D***, 13(7):1958, (1976).

[22] K.G. Chetyrkin, C. Dominguez, D. Pirjol, and K. Schilcher. *Mass Singularities in Light Quark Correlators: The Strange Quark Case. Physical Review* ***D***, 51:5090–5100, (1995).

[23] L.J. Reinders, S. Yazaki, and H.R. Rubinstein. *Hadron Properties from QCD Sum Rules. Phys. Rep.*, 127(CERN-TH-4079):1–97, (1984).

[24] N.N. Bogolyubov and D.V. Shirkov. *Introduction to the Theory of Quantized Fields. Intersci. Monogr. Phys. Astron.*, 3:1–720, (1980).

[25] R. Oehme. *Analytic Structure of Amplitudes in Gauge Theories with Confinement. International Journal of Modern Physics* ***A***, 10(14):1995–2014, (1995).

[26] K.G. Wilson. *Non-Lagrangian Models of Current Algebra. Physical Review*, 179(5):1499, (1969).

[27] K.G. Wilson. *Renormalization Group and Strong Interactions. Physical Review* ***D***, 3(8):1818, (1971).

[28] M. Peskin and D. Schroeder. *An Introduction to Quantum Field Theory.* Addison-Wesley Publishing Company, (1995).

[29] H Reinhardt and H Weigel. *Vacuum Nature of the QCD Condensates. Physical Review* ***D***, 85(7):074029, (2012).

[30] C. Dominguez and K. Schilcher. *QCD Vacuum Condensates from τ-lepton Decay Data. Journal of High Energy Physics*, 2007(01):093, (2007).

[31] M. Gell-Mann, R.J. Oakes, and B. Renner. *Behavior of Current Divergences under SU(3) X SU(3). Physical Review*, 175:2195, (1968).

[32] J. Bordes, C. Dominguez, P. Moodley, J. Penarrocha, and K. Schilcher. *Chiral Corrections to the SU(2) $\bigotimes$ SU(2) Gell-Mann-Oakes-Renner Relation. Journal of High Energy Physics*, 2010(5):64, (2010).

[33] J. Bordes, C. Dominguez, P. Moodley, J. Penarrocha, and K. Schilcher. *Corrections to the SU(3) $\bigotimes$ SU (3) Gell-Mann-Oakes-Renner Relation and Chiral Couplings L_8^r and H_2^r. Journal of High Energy Physics*, 2012(10):102, (2012).

[34] S.G. Gorishny, A.L. Kataev, S.A. Larin, and L.R. Surgaladze. *Three-loop QCD Correction to the Correlator of the Quark Scalar Currents and $\Gamma_t ot$ ($H^0 \to$ hadrons). Modern Physics Letters* ***A***, 5(32):2703–2711, (1990).

[35] K.G. Chetyrkin and A. Khodjamirian. *Strange Quark Mass from Pseudoscalar Sum Rule with $\mathcal{O}(\alpha_s^4)$ Accuracy. The European Physical Journal C-Particles and Fields*, 46(3):721–728, (2006).

[36] M. Jamin and M. Münz. *The Strange Quark Mass from QCD Sum Rules. Zeitschrift für Physik* ***C*** *Particles and Fields*, 66(4):633–645, (1995).

[37] F. Le Diberder and A. Pich. *The Perturbative QCD Prediction to R_τ Revisited. Physics Letters* ***B***, 286(1-2):147–152, (1992).

[38] A. Pivovarov. *Renormalization Group Analysis of the τ-lepton Decay within QCD. Zeitschrift für Physik* ***C*** *Particles and Fields*, 53(3):461–463, (1992).

[39] M. Jamin. *Contour-Improved versus Fixed-Order Perturbation Theory in Hadronic τ Decays. Journal of High Energy Physics*, 2005(09):058, (2005).

[40] K.G. Chetyrkin, J.H. Kühn, and M. Steinhauser. *RunDec: A Mathematica Package for Running and Decoupling of the Strong Coupling and Quark masses. arXiv preprint hep-ph/0004189*, (2000).

[41] K.G. Chetyrkin, D. Pirjol, and K. Schilcher. *Order-α_s^3 Determination of the Strange Quark Mass. Physics Letters* ***B***, 404(3-4):337–344, (1997).

[42] H. Pagels and A. Zepeda. *Where are the Corrections to the Goldberger-Treiman Relation? Physical Review* ***D***, 5(12):3262, (1972).

[43] J. Bijnens, J. Prades, and E. de Rafael. *Light Quark Masses in QCD. Physics Letters* ***B***, 348(1-2):226–238, (1995).

[44] V.A. Schegelsky, A.V. Sarantsev, A.V. Anisovich, and M.P. Levchenko. *Partial Wave Analysis of $\pi^+\pi^-\pi^0$ Production in Two-photon Collisions at LEP. The European Physical Journal* ***A*** *- Hadrons and Nuclei*, 27(2):199–205, (2006).

[45] M. Jamin, J.A. Oller, and A. Pich. *Light Quark Masses from Scalar Sum Rules. The European Physical Journal* ***C*** *– Particles and Fields*, 24(2):237–243, (2002).

[46] P. Colangelo, F. De Fazio, G. Nardulli, and N. Paver. *On the QCD Sum Rule Determination of the Strange Quark Mass. Physics Letters* ***B***, 408(1-4):340–346, (1997).

[47] C. Dominguez, L. Pirovano, and K. Schilcher. *The Strange-Quark Mass from QCD sum Rules in the Pseudoscalar Channel. Physics Letters* ***B***, 425(1-2):193–198, (1998).

[48] G.W. Brandenburg, R.K. Carnegie, R.J. Cashmore, M. Davier, et al. *Evidence for a New Strangeness-one Pseudoscalar Meson. Physical Review Letters*, 36(21):1239, (1976).

[49] C. Daum, J.G. Loken, J. Turnau, B. Alper, et al. *Diffractive Production of Strange Mesons at 63 GeV. Nuclear Physics* ***B***, 187(CERN-EP-81-04):1–41, (1981).

[50] T. Armstrong, M. Baubillier, W. Beusch, I.J. Bloodworth, M. Bonesini, et al. *A Partial-Wave Analysis of the K - Φ System Produced in the Reaction $K^-p \to K^+K^-K^-p$ at 18.5 GeV/c. Nuclear Physics* ***B***, 221(1):1–15, (1983).

[51] R. Aaij, B. Adeva, M. Adinolfi, Z. Ajaltouni, S. Akar, et al. *Observation of $J/\psi\phi$ Structures Consistent with Exotic States from Amplitude Analysis of $B^+ \to J/\psi\phi K^+$ decays. Physical Review Letters*, 118(2):022003, (2017).

[52] K. Maltman and J. Kambor. *Decay Constants, Light Quark Masses, and Quark Mass Bounds from Light Quark Pseudoscalar Sum Rules. Physical Review* ***D***, 65(7):074013, (2002).

[53] M. González-Alonso, A. Pich, and J. Prades. *Pinched Weights and Duality Violation in QCD Sum Rules: a Critical Analysis. Physical Review* ***D***, 82(1):014019, (2010).

[54] A. Pich and A. Rodríguez-Sánchez. *Updated Determination of* $\alpha_s(m_\tau^2)$ *from* τ *Decays. Modern Physics Letters* ***A***, 31(30):1630032, (2016).

[55] C. Dominguez, L.A. Hernandez, and K. Schilcher. *Determination of the Gluon Condensate from Data in the Charm-Quark Region. Journal of High Energy Physics*, (2015)(7):110, (2015).

[56] B.L. Ioffe. *QCD (Quantum Chromodynamics) at Low Energies. Progress in Particle and Nuclear Physics*, 56(1):232–277, (2006).

[57] N. Carrasco, A. Deuzeman, P. Dimopoulos, R. Frezzotti, V. Giménez, et al. *Up, Down, Strange and Charm Quark Masses with* $N_f = 2 + 1 + 1$ *Twisted Mass Lattice QCD. Nuclear Physics* ***B***, 887:19–68, (2014).

[58] R. Arthur, T. Blum, P.A. Boyle, N.H. Christ, N. Garron, et al. *Domain Wall QCD with Near-Physical Pions. Physical Review* ***D***, 87(9):094514, (2013).

[59] Y. Aoki, R. Arthur, T. Blum, P.A. Boyle, D. Brömmel, et al. *Continuum Limit Physics from* $2 + 1$ *Flavor Domain Wall QCD. Physical Review* ***D***, 83(7):074508, (2011).

[60] S. Durr, Z. Fodor, C. Hoelbling, S.D. Katz, S. Krieg, et al. *Lattice QCD at the Physical Point: Light Quark Masses. Physics Letters* ***B***, 701(2):265–268, (2011).

[61] B. Blossier, P. Dimopoulos, R. Frezzotti, V. Lubicz, M. Petschlies, et al. *Average Up/Down, Strange, and Charm Quark Masses with* $N_f = 2$ *Twisted-Mass Lattice QCD. Physical Review* ***D***, 82(11):114513, (2010).

[62] C. McNeile, C.T. Davies, E. Follana, K. Hornbostel, G.P. Lepage, et al. *High-Precision c and b Masses, and QCD Coupling from Current-Current Correlators in Lattice and Continuum QCD. Physical Review* ***D***, 82(3):034512, (2010).

[63] C. Allton, D.J. Antonio, Y. Aoki, T. Blum, P.A. Boyle, et al. *Physical Results from* $2 + 1$ *Flavor Domain Wall QCD and SU(2) Chiral Perturbation Theory. Physical Review* ***D***, 78(11):114509, (2008).

[64] T. Ishikawa, S. Aoki, M. Fukugita, S. Hashimoto, K.I. Ishikawa, et al. *Light-Quark Masses from Unquenched Lattice QCD. Physical Review* ***D***, 78(1):011502, (2008).

[65] B. Chakraborty, C.T.H. Davies, B. Galloway, P. Knecht, J. Koponen, et al. *High-Precision Quark Masses and QCD Coupling from* $n_f = 4$ *Lattice QCD. Physical Review* ***D***, 91(5):054508, (2015).

[66] P. Fritzsch, F. Knechtli, B. Leder, M. Marinkovic, S. Schaefer, et al. *The Strange Quark Mass and Lambda Parameter of Two Flavor QCD. Nuclear Physics* ***B***, 865(3):397–429, (2012).

[67] T. Blum, R. Zhou, T. Doi, M. Hayakawa, T. Izubuchi, et al. *Electromagnetic Mass Splittings of the Low Lying Hadrons and Quark Masses from* $2+1$ *Flavor Lattice QCD + QED. Physical Review* ***D***, 82(9):094508, (2010).

[68] C. Dominguez, A. Mes, and K. Schilcher. *Up-and Down-quark Masses from QCD Sum Rules. Journal of High Energy Physics*, 2019(2):57, (2019).

[69] G. 't Hooft and M. Veltman. *Regularization and Renormalization of Gauge Fields. Nuclear Physics* ***B***, 44(1):189–213, (1972).

[70] M. Davier, A. Höcker, and Z. Zhang. *The Physics of Hadronic Tau Decays. Reviews of modern physics*, 78(4):1043, (2006).

[71] P.A. Baikov, K.G. Chetyrkin, and J.H. Kühn. *Five-Loop Running of the QCD Coupling Constant. Physical review letters*, 118(8):082002, (2017).

[72] T. Luthe, A. Maier, P. Marquard, and Y. Schröder. *Complete Renormalization of QCD at Five Loops. Journal of High Energy Physics*, 2017(3):20, (2017).

[73] F. Herzog, B. Ruijl, T. Ueda, J.A.M. Vermaseren, and A. Vogt. *The Five-loop Beta Function of Yang-Mills Theory with Fermions. Journal of High Energy Physics*, 2017(2):90, (2017).

[74] P.A. Baikov, K.G. Chetyrkin, and J.H. Kühn. *Quark Mass and Field Anomalous Dimensions to* $\mathcal{O}(\alpha_s^5)$. *Journal of High Energy Physics*, 2014(10):76, (2014).

[75] K.G. Chetyrkin. *Quark Mass Anomalous Dimension to* $\mathcal{O}(\alpha_s^4)$. *Physics Letters* ***B***, 404:161–165, (1997).

[76] J.A.M. Vermaseren, S.A. Larin, and T. Van Ritbergen. *The 4-loop Quark Mass Anomalous Dimension and the Invariant Quark Mass. Physics Letters* ***B***, 405(3-4):327–333, (1997).

[77] K.G. Chetyrkin, B.A. Kniehl, and M. Steinhauser. *Decoupling Relations to* $\mathcal{O}(\alpha_s^3)$ *and their connection to Low-energy Theorems. Nuclear Physics* ***B***, 510(1-2):61–87, (1998).

[78] K.G. Chetyrkin, B.A. Kniehl, and A. Sirlin. *Estimations of Order* α_s^3 *and* α_s^4 *Corrections to Mass-dependent Observables. Physics Letters* ***B***, 402(3-4):359–366, (1997).

[79] B.A. Kniehl. *Dependence of Electroweak Parameters on the Definition of the Top-Quark Mass. Zeitschrift für Physik* ***C****: Particles and Fields*, 72(3):437, (1996).

[80] F.A. Chishtie, D.G.C. McKeon, and T.N. Sherry. *A Systematic Expansion of Running Couplings and Masses. arXiv preprint arXiv:1806.02534*, (2018).

[81] A.L. Kataev and V.S. Molokoedov. *Multiloop Contributions to the* $\overline{MS}$*-on-shell Mass Relation for Heavy Quarks in QCD and Charged Leptons in QED and the Asymptotic Structure of the Perturbative QCD Series. arXiv preprint arXiv:1807.05406*, (2018).

[82] A. Mes and J. Stephens. *An Application of Rubi: Series Expansion of the Quark Mass Renormalization Group Equation. arXiv preprint arXiv:1811.04892*, (2018).

[83] *Wolfram Research, Inc.* Mathematica, Version 11.3, (2018). Champaign, IL.

[84] A. Meurer, C. Smith, M. Paprocki, O. Čertík, S. Kirpichev, M. Rocklin, A. Kumar, S. Ivanov, J. Moore, and S. Singh. *SymPy: Symbolic Computing in Python. Peer* ***J*** *Computer Science*, 3:e103, (2017).

[85] A. Rich, P. Scheibe, and N. Abbasi. *Rule-based Integration: An Extensive System of Symbolic Integration Rules. Journal of Open Source Software*, 3(32):1073, (2018).

[86] M. Abramowitz and I.A. Stegun. *Handbook of Mathematical Functions: with Formulas, Graphs, and Mathematical Tables*. United States National Bureau of Standards, (1964).

[87] W.H Beyer. *CRC Standard Mathematical Tables and Formulae*. CRC Press, Boca Raton [u.a.], 29. ed. edition, (1991).

[88] I.S. Gradstejn and I.M. Ryzik. *Table of Integrals, Series, and Products*. Academic Press, New York [u.a.], 5th ed. edition, (1994).

[89] N.M. Abbasi. *Computer Algebra Independent Integration Tests*. `https://www.12000.org/my_notes/CAS_integration_tests/reports/rubi_4_15_2/index.pdf`, (2018).

[90] SymPy and Collaborators. *Rubi Integrator*. `https://github.com/sympy/sympy/issues/12233`, (2017).

[91] A. Pich. *Precision Physics with QCD*. In *EPJ Web of Conferences*, volume 137, page 01016. EDP Sciences, (2017).

[92] A. Keshavarzi, D. Nomura, and T. Teubner. *Muon $g-2$ and $\alpha(M_Z^2)$: A New Data-based Analysis*. *Physical Review* ***D***, 97:114025, (2018).

[93] Steven Weinberg. *New Approach to the Renormalization Group*. *Physical Review* ***D***, 8(10):3497, (1973).

[94] W.A Bardeen, A.J. Buras, D.W. Duke, and T. Muta. *Deep-inelastic Scattering beyond the Leading Order in Asymptotically Free Gauge Theories*. *Physical Review* ***D***, 18(11):3998, (1978).